

Derivation of the core mass – halo mass relation of fermionic and bosonic dark matter halos from an effective thermodynamical model

Pierre-Henri Chavanis

Laboratoire de Physique Théorique, Université de Toulouse, CNRS, UPS, France

We consider the possibility that dark matter halos are made of quantum particles such as fermions or bosons in the form of Bose-Einstein condensates. In that case, they generically have a “core-halo” structure with a quantum core that depends on the type of particle considered and a halo that is relatively independent of the dark matter particle and that is similar to the NFW profile of cold dark matter. The quantum core is equivalent to a polytrope of index $n = 3/2$ for fermions, $n = 2$ for noninteracting bosons, and $n = 1$ for bosons with a repulsive self-interaction in the Thomas-Fermi limit. We model the halo by an isothermal gas with an effective temperature T . We then derive the core mass – halo mass relation $M_c(M_v)$ of dark matter halos from an effective thermodynamical model by maximizing the entropy $S(M_c)$ with respect to the core mass M_c at fixed total mass and total energy. We obtain a general relation, valid for an arbitrary polytropic core, that is equivalent to the “velocity dispersion tracing” relation according to which the velocity dispersion in the core $v_c^2 \sim GM_c/R_c$ is of the same order as the velocity dispersion in the halo $v_v^2 \sim GM_v/r_v$. We provide therefore a justification of this relation from thermodynamical arguments. In the case of fermions, we obtain a relation $M_c \propto M_v^{1/2}$ that agrees with the relation found numerically by Ruffini *et al.* [Mon. Not. R. Astron. Soc. **451**, 622 (2015)]. In the case of noninteracting bosons, we obtain a relation $M_c \propto M_v^{1/3}$ that agrees with the relation found numerically by Schive *et al.* [Phys. Rev. Lett **113**, 261302 (2014)]. In the case of bosons with a repulsive self-interaction in the Thomas-Fermi limit, we predict a relation $M_c \propto M_v^{2/3}$ that still has to be confirmed numerically. Using a Gaussian ansatz, we obtain a general approximate core mass – halo mass relation $M_c(M_v)$ that is valid for bosons with arbitrary repulsive or attractive self-interaction. For an attractive self-interaction, we determine the maximum halo mass $(M_v)_{\max}$ that can harbor a stable quantum core (dilute axion “star”). Above that mass, the quantum core collapses. Finally, we argue that the fundamental mass scale of the bosonic dark matter particle is $m_\Lambda = \hbar\sqrt{\Lambda}/c^2 = 2.08 \times 10^{-33} \text{ eV}/c^2$ and that the fundamental mass scale of the fermionic dark matter particle is $m_\Lambda^* = (\Lambda\hbar^3/Gc^3)^{1/4} = \sqrt{m_\Lambda M_P} = 5.04 \times 10^{-3} \text{ eV}/c^2$, where Λ is the cosmological constant and M_P is the Planck mass. Their ratio is $m_\Lambda^*/m_\Lambda = (c^5/G\hbar\Lambda)^{1/4} = 2.42 \times 10^{30}$ which explains the difference of mass between fermions and bosons in dark matter models. The actual value of the dark matter particle mass is equal to these mass scales multiplied by a large factor that we obtain from our model.

PACS numbers: 95.30.Sf, 95.35.+d, 98.62.Gq

I. INTRODUCTION

The nature of dark matter (DM) is still unknown and remains one of the greatest mysteries of modern cosmology. The standard cold dark matter (CDM) model works remarkably well at large (cosmological) scales and is consistent with ever improving measurements of the cosmic microwave background (CMB) from WMAP and Planck missions [1, 2]. However, it encounters serious problems at small (galactic) scales. In particular, it predicts that DM halos should be cuspy [3], with a density diverging as r^{-1} for $r \rightarrow 0$, while observations reveal that they have a flat core density [4]. On the other hand, the CDM model predicts an over-abundance of small-scale structures (subhalos/satellites), much more than what is observed around the Milky Way [5]. These problems are referred to as the “cusp problem” and “missing satellite problem”. The expression “small-scale crisis of CDM” has been coined.

In order to solve these problems, some authors have proposed to take the quantum nature of the DM particle

into account.¹ Indeed, quantum mechanics creates an effective pressure even at zero thermodynamic temperature ($T_{\text{th}} = 0$) that may balance the gravitational attraction at small scales and lead to cores instead of cusps. The DM particle could be a fermion, like a massive neutrino, with a mass $\sim 170 \text{ eV}/c^2$ (see Appendix D of [14]). It could also be a boson in the form of a Bose-Einstein condensate (BEC), like an ultralight axion, with a mass in the range $2.19 \times 10^{-22} \text{ eV}/c^2 < m < 1.10 \times 10^{-3} \text{ eV}/c^2$ depending whether the bosons are noninteracting or self-interacting (see Appendix D of [14]).

In these quantum models, DM halos have a “core-halo” structure which results from a process of violent collisionless relaxation [15] and gravitational cooling [16–18]. The core stems from the equilibrium between quantum pressure and gravitational attraction. For fermions, the quantum pressure arises from the Pauli exclusion principle like in the case of white dwarfs and neutron stars.

¹ See our previous papers [6, 7] for an exhaustive list of references (more than 200) on the subject. See also the reviews [8–13].

For bosons, the quantum pressure arises from the Heisenberg uncertainty principle or from the repulsive self-interaction of the bosons like in the case of boson stars. Quantum mechanics stabilizes the halo against gravitational collapse,² leading to a flat core instead of a cusp. The quantum core is equivalent to a polytrope of index $n = 3/2$ for fermions, $n = 2$ for noninteracting bosons, and $n = 1$ for bosons with a repulsive self-interaction in the Thomas-Fermi (TF) limit. It is responsible for the finite density of the DM halos at the center. The core mass-radius relation is $M_c R_c^3 = 1.49 \times 10^{-3} h^6 / G^3 m^8$ for fermions, $M_c R_c = 5.25 \hbar^2 / G m^2$ for noninteracting bosons, and $R_c = \pi (a_s \hbar^2 / G m^3)^{1/2}$ for self-interacting bosons in the TF limit. On the other hand, the halo is relatively independent of quantum effects and is similar to the Navarro-Frenk-White (NFW) profile [3] produced in CDM simulations or to the empirical Burkert profile [4] deduced from the observations. It is responsible for the flat rotation curves of the galaxies at large distances. We shall approximate this halo by an isothermal atmosphere with an effective temperature T .³ In that case, the density decreases at large distance as $\rho \propto r^{-2}$ [29], instead of r^{-3} for the NFW and Burkert profiles, leading exactly to flat rotation curves for $r \rightarrow +\infty$. For sufficiently large halos, the halo mass-radius relation is $M_h = 1.76 \Sigma_0 r_h^2$ [7] where

$$\Sigma_0 = \rho_0 r_h = 141 M_\odot / \text{pc}^2 \quad (1)$$

is the universal surface density of DM halos deduced from the observations [30–32]. Ultracompact halos like dSphs ($r_h \sim 1$ kpc and $M_h \sim 10^8 M_\odot$) are dominated by the quantum core and have almost no atmosphere. Large halos like the Medium Spiral ($r_h \sim 10$ kpc and $M_h \sim 10^{11} M_\odot$) are dominated by the isothermal atmosphere.

² This is true for the nonrelativistic systems that we consider here. For general relativistic systems, there is a maximum mass $M_{\text{max}}^{\text{GR}}$ [19–24] above which the system collapses towards a black hole. In our case, we will find that $M_c \ll M_{\text{max}}^{\text{GR}}$ so that a Newtonian approach is sufficient. On the other hand, if the bosons have an attractive self-interaction, like in the case of the axion [11], there exists a maximum mass M_{max} [6] for the quantum core even in the Newtonian regime. Above that limit, the quantum core (dilute axion star) undergoes gravitational collapse.

³ We approximate the atmosphere by an isothermal sphere but we stress that the temperature is effective and does not correspond to the true thermodynamic temperature (which is almost equal to zero). In particular, the atmosphere does not correspond to a statistical equilibrium state resulting from a “collisional” evolution of the quantum particles of mass m which would be much too long (much larger than the age of the Universe) [7]. It may rather correspond to an out-of-equilibrium thermodynamical state - or quasistationary state - resulting from a collisionless free fall evolution (independent of m) like in Lynden-Bell’s theory of violent relaxation [15]. In the case of fuzzy DM, the approximately isothermal atmosphere (due to quantum interferences of excited states) may result either from a collisionless relaxation or from the “collisional” evolution of quasiparticles (granules) of the size of the solitonic core and of mass $m_* \gg m$ as argued in [25–28].

In a recent paper [7], we have developed of model of DM halos made of bosons with a repulsive self-interaction in the TF limit. We have obtained a generic phase diagram (see Fig. 49 of [7]) determining the structure of the DM halos (measured by the core mass M_c) as a function of their mass M_h . There is a minimum halo mass $(M_h)_{\text{min}}$ corresponding to the ground state of the boson gas ($T = 0$) at which the DM halo is a purely quantum object without isothermal atmosphere ($M_c \simeq M_h$). We will call it the “minimum halo”. Larger halos have a “core-halo” structure with a quantum core, representing a “nucleus” or a “bulge”, and an isothermal atmosphere. We found a branch along which the core mass M_c decreases as the halo mass M_h increases. Rapidly, the core mass becomes negligible and the halos behave as purely isothermal halos without quantum core. However, we found a critical point $(M_h)_{\text{CCP}}$, that we interpreted as a canonical critical point, at which a bifurcation occurs. On the new branch, the core mass M_c increases as the halo mass M_h increases. On that branch, we found another critical point at a higher mass $(M_h)_{\text{MCP}}$, that we interpreted as a microcanonical critical point, above which the quantum core becomes unstable and is replaced by a supermassive black hole resulting from a gravothermal catastrophe [33] followed by a dynamical instability of general relativistic origin [34]. Considering the bifurcated branch with the “core-halo” structure, we developed an effective thermodynamical model to analytically predict the core mass – halo mass relation $M_c(M_h)$.⁴ We showed that this relation is equivalent to the “velocity dispersion tracing” relation according to which the velocity dispersion in the core $v_c^2 \sim GM_c/R_c$ is of the same order as the velocity dispersion in the halo $v_h^2 \sim GM_h/r_h$ [7, 36, 37]. We could provide therefore a justification of this relation from thermodynamical arguments.

In the present paper, we extend this thermodynamical model to the case of DM halos made of fermions and to the case of DM halos made of noninteracting bosons. To unify the formalism, we model the quantum core as a polytrope of arbitrary index n (with $n = 3/2$ for fermions, $n = 2$ for noninteracting bosons, and $n = 1$ for self-interacting bosons in the TF limit) and we model the atmosphere as an isothermal gas with a uniform density confined within a “box” of radius R . The radius of the box is identified with the halo radius r_h and the total mass of the system contained within the box (core + halo) is identified with the halo mass M_h . They are related by $M_h = 1.76 \Sigma_0 r_h^2$ [7]. We analytically compute the entropy $S(M_c)$ of the system. By maximizing $S(M_c)$ as a function of M_c for a given value of the mass M_h , radius r_h and energy E_h , we obtain the core mass M_c as a function of the halo mass M_h . We find this relation to be always (for any value of n) equivalent to

⁴ This thermodynamical model was originally introduced in [35] to analytically obtain the caloric curves of self-gravitating fermions.

the velocity dispersion tracing relation, thereby generalizing our previous result [7]. Using a Gaussian ansatz, we obtain a general approximate relation $M_c(M_h)$ that is valid for bosons with arbitrary repulsive or attractive self-interaction. For an attractive self-interaction, we determine the maximum halo mass $(M_h)_{\max}$ that can harbor a stable quantum core (dilute axion “star”). Finally, we use our results to predict the fundamental mass scale of the bosonic or fermionic DM particle in terms of the fundamental constants of physics.

The paper is organized as follows. In Sec. II we consider models of DM halos with a quantum (fermionic or bosonic) core and an isothermal atmosphere. In Sec. III we show that these models can be obtained in a unified manner from a generalized wave equation introduced in [7, 38, 39]. In Sec. IV we obtain the core mass – halo mass relation of DM halos from an analytical thermodynamical model. This relation is valid for a general polytropic core. In Sec. V we show that this relation is equivalent to the velocity dispersion tracing relation. In Secs. VI and VII we specifically apply these results to DM halos made of fermions, noninteracting bosons and self-interacting bosons.

II. QUANTUM MODELS OF DM HALOS

In this section, we review quantum models of DM halos made of fermions or bosons. If DM halos are quantum objects, there must be a minimum halo radius R and a minimum halo mass M in the Universe corresponding to the ground state ($T = 0$) of the self-gravitating quantum gas. This result is in agreement with the observations. Indeed, there are apparently no DM halos with a radius smaller than $R \sim 1$ kpc and a mass smaller than $M \sim 10^8 M_\odot$, the typical values of the radius and mass of dSphs like Fornax. This observational result cannot be explained by the CDM model which predicts the existence of DM halos at all scales.

Ultracompact dwarf DM halos just have a quantum core without atmosphere (ground state). Larger DM halos have a core-halo structure with a quantum core corresponding to the ground state ($T = 0$) of the quantum gas and an “atmosphere” resulting from violent relaxation and gravitational cooling. The atmosphere has a density profile that can be fitted by the empirical Burkert profile or by NFW profile. In this paper, we shall approximate this density profile by an isothermal profile of effective temperature T . It is the atmosphere that fixes the size of large halos and explains why their radius r_h increases with their mass as $M_h \propto r_h^2$ (since Σ_0 is constant). By contrast, the radius R_c of the quantum core usually decreases or remains constant as its mass M_c increases (see below).

To determine the parameters of the DM particle, we

proceed as follows (see Appendix D of [14]).⁵ We assume that the smallest halo that has been observed, with a typical radius and a typical mass

$$R \sim 1 \text{ kpc}, \quad M \sim 10^8 M_\odot, \quad (\text{Fornax}), \quad (2)$$

corresponds to the ground state of a self-gravitating quantum gas. Using the mass-radius relation $M(R)$ of the self-gravitating quantum gas at $T = 0$, we can obtain the parameters of the DM particle. We can then check that the nonrelativistic treatment used in this paper is valid by showing that $M_c \ll M_{\max}^{\text{GR}}$.

A. Fermionic DM

The equation of state of a nonrelativistic Fermi gas at $T = 0$ is [40]

$$P = \frac{1}{20} \left(\frac{3}{\pi} \right)^{2/3} \frac{h^2}{m^{8/3}} \rho^{5/3}. \quad (3)$$

This is a polytropic equation of state of index $\gamma = 5/3$ (i.e. $n = 3/2$) and polytropic constant

$$K = \frac{1}{20} \left(\frac{3}{\pi} \right)^{2/3} \frac{h^2}{m^{8/3}}. \quad (4)$$

In the TF approximation, which amounts to neglecting the quantum potential, the fundamental differential equation of hydrostatic equilibrium determining the density profile of a nonrelativistic fermion star⁶ at $T = 0$ with the equation of state (3) writes (see Appendix A)

$$\frac{1}{8} \left(\frac{3}{\pi} \right)^{2/3} \frac{h^2}{m^{8/3}} \Delta \rho^{2/3} = -4\pi G \rho. \quad (5)$$

It can be reduced to the Lane-Emden equation (A8) of index $n = 3/2$. This profile has a compact support (see Fig. 1) and the fermion star is stable. The mass-radius relation is

$$M_c R_c^3 = \frac{9\omega_{3/2}}{8192\pi^4} \frac{h^6}{G^3 m^8}, \quad (6)$$

where $\omega_{3/2} = 132.3843$. On the other hand, from Eqs. (B7) and (B9) which reduce to⁷

$$E_c = U_c + W_c, \quad (7)$$

⁵ Our aim here is not to make an accurate model of DM halos. Therefore, an order of magnitude of the DM particle parameters is sufficient.

⁶ In this paper, the name “fermion star” refers to ultracompact DM halos made of fermions or to the fermionic core of larger DM halos (the same comment applies to the names “boson stars”, “BEC stars” and “axion stars” used below).

⁷ In the main text, we denote by E_c , U_c and W_c what are called E_{tot} , U and W in the Appendices.

$$2U_c + W_c = 0, \quad (8)$$

and from the Betti-Ritter formula (C5), we obtain

$$E_c = -U_c = \frac{1}{2}W_c = -\frac{3}{7}\frac{GM_c^2}{R_c}. \quad (9)$$

Combined with Eq. (6), we find that the energy of a nonrelativistic fermion star at $T = 0$ (ground state) is

$$E_c = -\frac{3}{7}\left(\frac{8192\pi^4}{9\omega_{3/2}}\right)^{1/3}\frac{G^2m^{8/3}M_c^{7/3}}{h^2}. \quad (10)$$

Let us assume that the smallest DM halo that we know, with mass M and radius R , corresponds to the ground state of a nonrelativistic self-gravitating Fermi gas. From the mass-radius relation (6), we get

$$\frac{m}{\text{eV}/c^2} = 2.27 \times 10^4 \left(\frac{\text{pc}}{R}\right)^{3/8} \left(\frac{M_\odot}{M}\right)^{1/8}. \quad (11)$$

Using the reference values of M and R corresponding to Fornax [see Eq. (2)], we find a fermion mass (see Appendix D of [14]):

$$m = 170 \text{ eV}/c^2. \quad (12)$$

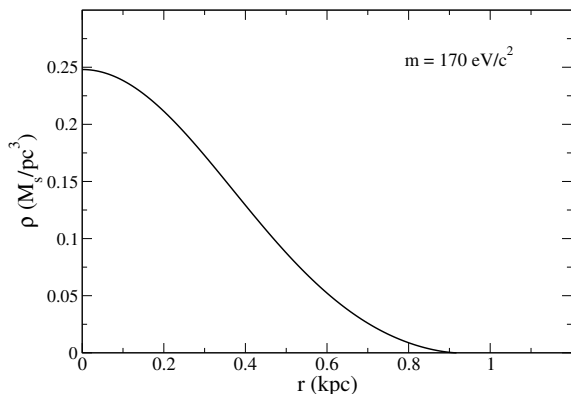


FIG. 1: Density profile of the “minimum halo” (ground state) of surface density $\Sigma_0 = \rho_0 r_h = 141 M_\odot/\text{pc}^2$ made of fermions of mass $m = 170 \text{ eV}/c^2$.

Alternatively, using the results of Appendix G and taking $m = 170 \text{ eV}/c^2$ in the numerical applications, we find that the minimum halo radius, the minimum halo mass and the maximum central density are

$$(r_h)_{\min} = 1.50 \left(\frac{\hbar^6}{G^3 m^8 \Sigma_0}\right)^{1/5} = 570 \text{ pc}, \quad (13)$$

$$(M_h)_{\min} = 4.47 \left(\frac{\hbar^{12} \Sigma_0^3}{G^6 m^{16}}\right)^{1/5} = 9.09 \times 10^7 M_\odot. \quad (14)$$

$$(\rho_0)_{\max} = 0.667 \left(\frac{\Sigma_0 m^{4/3} G^{1/2}}{\hbar}\right)^{6/5} = 0.248 M_\odot/\text{pc}^3, \quad (15)$$

where Σ_0 is the universal density of DM halos given by Eq. (1). These values can be improved if we have a more reliable expression of the fermion mass m , but they are sufficient for our purposes (the same comment applies to the bosonic models considered below).

The maximum mass of a fermion star at $T = 0$ set by general relativity is $M_{\max} = 0.384 (\hbar c/G)^{3/2}/m^2$ and its minimum radius is $R_{\min} = 8.73 GM_{\max}/c^2$ [19]. They can be written as

$$\frac{M_{\max}}{M_\odot} = 6.26 \times 10^{17} \left(\frac{\text{eV}/c^2}{m}\right)^2, \quad \frac{R_{\min}}{\text{km}} = 12.9 \frac{M_{\max}}{M_\odot}. \quad (16)$$

For a fermion of mass $m = 170 \text{ eV}/c^2$, we obtain $M_{\max} = 2.17 \times 10^{13} M_\odot$ and $R_{\min} = 8.85 \text{ pc}$. The maximum mass is much larger than the typical core mass of a DM halo. Assuming that a fermion star at $T = 0$ describes the quantum core of a DM halo, we conclude that such cores are nonrelativistic since $M_c \ll M_{\max}$ in general. Since the maximum mass is much larger than the core mass, gravity can be treated within a Newtonian framework.

B. Noninteracting bosonic DM

We consider a gas of noninteracting bosons at $T = 0$ forming a BEC. The wavefunction of a self-gravitating BEC without self-interaction is governed by the Schrödinger-Poisson equation [6]. Using Madelung’s hydrodynamic representation of the Schrödinger equation [41], we find that the fundamental differential equation of quantum hydrostatic equilibrium determining the density profile of the BEC is [6]

$$\frac{\hbar^2}{2m^2} \Delta \left(\frac{\Delta \sqrt{\rho}}{\sqrt{\rho}}\right) = 4\pi G \rho. \quad (17)$$

This equation can be solved numerically [17, 18, 21, 25–27, 42–44]. The density profile of a noninteracting BEC star at $T = 0$ (ground state) extends to infinity (see Fig. 2) and the BEC star is stable. The mass-radius relation is

$$M_c(R_c)_{99} = 9.95 \frac{\hbar^2}{Gm^2}, \quad (18)$$

where $(R_c)_{99}$ is the radius enclosing 99% of the mass. From Eqs. (B1) and (B6) which reduce to

$$E_c = \Theta_Q^c + W_c, \quad (19)$$

$$2\Theta_Q^c + W_c = 0, \quad (20)$$

we obtain

$$E_c = -\Theta_Q^c = \frac{1}{2}W_c. \quad (21)$$

From numerical computations [21, 42, 43], we find that the total energy of a noninteracting BEC star at $T = 0$ (ground state) is

$$E_c = -0.0543 \frac{G^2 M_c^3 m^2}{\hbar^2}. \quad (22)$$

Actually, we find in Appendix E that there exists another solution of Eq. (17). It has a compact support (see Fig. 2) and its profile corresponds to a polytrope of index $\gamma = 3/2$ (i.e. $n = 2$). Its energy is lower than the energy of the solution considered here, suggesting that it is more stable, even if comparing the energies of stable states may not be decisive in view of the very long lifetime of metastable states in systems with long-range interactions. In the following, in order to develop a unified description of fermions and bosons based on polytropic equations of state, we will use the solution from Appendix E. However, as far as scalings and orders of magnitude are concerned, we would get similar results by using the more conventional (but maybe less stable) solution of this section.

Let us assume that the smallest DM halo that we know, with mass M and radius R , corresponds to the ground state of a noninteracting BEC star. From the mass-radius relation (18), we get

$$\frac{m}{\text{eV}/c^2} = 9.22 \times 10^{-17} \left(\frac{\text{pc}}{R}\right)^{1/2} \left(\frac{M_\odot}{M}\right)^{1/2}. \quad (23)$$

Using the reference values of M and R corresponding to Fornax [see Eq. (2)], we find a boson mass (see Appendix D of [14]):

$$m = 2.92 \times 10^{-22} \text{ eV}/c^2. \quad (24)$$

Alternatively, using the results of Appendix G and taking $m = 2.92 \times 10^{-22} \text{ eV}/c^2$ in the numerical applications, we find that the minimum halo radius, the minimum halo mass and the maximum central density are (computed from the polytropic solution of Appendix E)

$$(r_h)_{\min} = 0.913 \left(\frac{\hbar^2}{Gm^2\Sigma_0}\right)^{1/3} = 378 \text{ pc}, \quad (25)$$

$$(M_h)_{\min} = 1.61 \left(\frac{\hbar^4\Sigma_0}{G^2m^4}\right)^{1/3} = 3.89 \times 10^7 M_\odot. \quad (26)$$

$$(\rho_0)_{\max} = 1.09 \frac{G^{1/3}m^{2/3}\Sigma_0^{4/3}}{\hbar^{2/3}} = 0.371 M_\odot/\text{pc}^3, \quad (27)$$

where Σ_0 is the universal density of DM halos given by Eq. (1).

The maximum mass of a noninteracting boson star at $T = 0$ set by general relativity is $M_{\max} = 0.633 \hbar c/Gm$ and its minimum radius is $R_{\min} = 9.53 GM_{\max}/c^2$ [20, 21]. They can be written as

$$\frac{M_{\max}}{M_\odot} = 8.48 \times 10^{-11} \frac{\text{eV}/c^2}{m}, \quad \frac{R_{\min}}{\text{km}} = 14.1 \frac{M_{\max}}{M_\odot}. \quad (28)$$

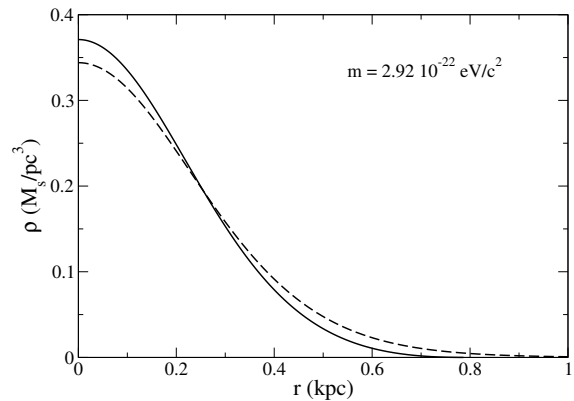


FIG. 2: Density profile of the “minimum halo” (ground state) of surface density $\Sigma_0 = \rho_0 r_h = 141 M_\odot/\text{pc}^2$ made of non-interacting bosons of mass $m = 2.92 \times 10^{-22} \text{ eV}/c^2$. We have plotted the polytropic profile with a compact support obtained in Appendix E (solid line) and the more conventional profile computed in [17, 18, 21, 25–27, 42–44] for which $(r_h)_{\min} = 410 \text{ pc}$, $(M_h)_{\min} = 4.52 \times 10^7 M_\odot$ and $(\rho_0)_{\max} = 0.344 M_\odot/\text{pc}^3$ (dashed line taken from [7, 43]).

For a boson of mass $m = 2.92 \times 10^{-22} \text{ eV}/c^2$, we obtain $M_{\max} = 2.90 \times 10^{11} M_\odot$ and $R_{\min} = 0.133 \text{ pc}$. The maximum mass is much larger than the typical core mass of a DM halo. Assuming that a BEC star at $T = 0$ (soliton) describes the quantum core of a DM halo, we conclude that such cores are nonrelativistic since $M_c \ll M_{\max}$ in general. Since the maximum mass is much larger than the core mass, gravity can be treated within a Newtonian framework.

C. Bosonic DM with a repulsive self-interaction in the TF limit

We consider a gas of self-interacting bosons at $T = 0$ forming a BEC. The wavefunction of a self-gravitating BEC with a quartic self-interaction is governed by the GPP equations [6]. The equation of state of a self-interacting BEC is [6]

$$P = \frac{2\pi a_s \hbar^2}{m^3} \rho^2, \quad (29)$$

where a_s is the scattering length of the bosons. This is a polytropic equation of state of index $\gamma = 2$ (i.e. $n = 1$) and polytropic constant

$$K = \frac{2\pi a_s \hbar^2}{m^3}. \quad (30)$$

We assume that the self-interaction is repulsive ($a_s > 0$). Using Madelung’s hydrodynamic representation of the GPP equations, and taking the quantum potential into account, we find that the fundamental differential equation of quantum hydrostatic equilibrium determining the

density profile of the BEC is [6]

$$-\frac{\hbar^2}{2m^2}\Delta\left(\frac{\Delta\sqrt{\rho}}{\sqrt{\rho}}\right)+\frac{4\pi a_s\hbar^2}{m^3}\Delta\rho=-4\pi G\rho. \quad (31)$$

This equation can be solved numerically [43]. The density profile of a noninteracting BEC star at $T = 0$ (ground state) extends to infinity. The mass-radius relation has been obtained in [6, 43].

In the TF approximation, which amounts to neglecting the quantum potential, the fundamental differential equation of hydrostatic equilibrium determining the density profile of a self-interacting BEC star at $T = 0$ with the equation of state (29) writes (see Appendix A)

$$\frac{4\pi a_s\hbar^2}{m^3}\Delta\rho=-4\pi G\rho. \quad (32)$$

It can be reduced to the Lane-Emden equation (A8) of index $n = 1$ which has a simple analytical solution [40]. This profile has a compact support (see Fig. 3) and the self-interacting BEC star is stable. A self-gravitating BEC with a repulsive self-interaction in the TF approximation has a unique radius [6, 23, 45–49],

$$R_c=\pi\left(\frac{a_s\hbar^2}{Gm^3}\right)^{1/2}, \quad (33)$$

that is independent of its mass. From Eqs. (B7) and (B9) which reduce to

$$E_c=U_c+W_c, \quad (34)$$

$$3U_c+W_c=0, \quad (35)$$

and from the Betti-Ritter formula (C5), we obtain

$$E_c=-2U_c=\frac{2}{3}W_c=-\frac{1}{2}\frac{GM_c^2}{R_c}. \quad (36)$$

Combined with Eq. (33), we find that the energy of a self-interacting BEC star at $T = 0$ (ground state) in the TF limit is

$$E_c=-\frac{1}{2\pi}\frac{G^{3/2}m^{3/2}M_c^2}{a_s^{1/2}\hbar}. \quad (37)$$

Let us assume that the smallest DM halo that we know, with mass M and radius R , corresponds to the ground state of a self-interacting BEC star. From Eq. (33), we get

$$\frac{a_s}{\text{fm}}\left(\frac{\text{eV}/c^2}{m}\right)^3=3.28\times 10^{-3}\left(\frac{R}{\text{pc}}\right)^2. \quad (38)$$

This formula depends only on R . Using the reference value of R corresponding to Fornax [see Eq. (2)], we find that the ratio a_s/m^3 of the boson parameters a_s and m is given by (see Appendix D of [14]):

$$\frac{a_s}{\text{fm}}\left(\frac{\text{eV}/c^2}{m}\right)^3=3.28\times 10^3. \quad (39)$$

In order to determine the mass of the boson, we need another relation. In this respect, we note that m and a_s must satisfy the constraint $\sigma/m < 1.25 \text{ cm}^2/\text{g}$ set by the Bullet Cluster [50], where $\sigma = 4\pi a_s^2$ is the self-interaction cross section. In Appendix D of [14] we have considered two extreme cases corresponding to an upper boson mass

$$m=1.10\times 10^{-3}\text{ eV}/c^2, \quad a_s=4.41\times 10^{-6}\text{ fm}, \quad (40)$$

and a lower boson mass

$$m=2.92\times 10^{-22}\text{ eV}/c^2, \quad a_s=8.13\times 10^{-62}\text{ fm}. \quad (41)$$

The upper boson mass (40) corresponds to the bound $\sigma/m = 1.25 \text{ cm}^2/\text{g}$. The lower boson mass (41) corresponds to the transition between the TF regime and the noninteracting regime. We note that when a self-interaction between the bosons is allowed, a large mass window is open. In particular, a repulsive self-interaction allows one to have a larger boson mass than in the noninteracting case. As discussed in Appendix D.4 of [14] this may be interesting in view of the fact that the mass of a noninteracting boson ($m \sim 1 - 10 \times 10^{-22} \text{ eV}/c^2$) is in tension with observations of the Lyman- α forest [27]. *This tension could reflect the fact that bosons have a repulsive self-interaction.*

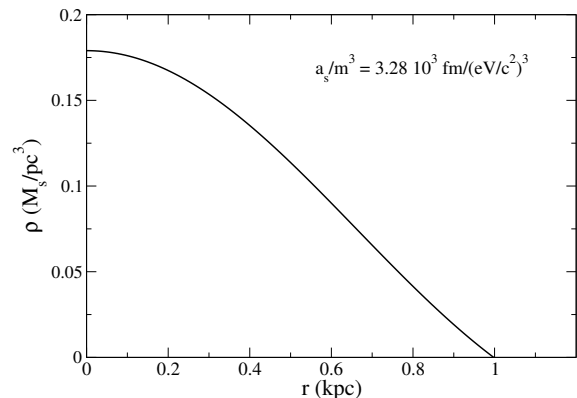


FIG. 3: Density profile $\rho = \rho_0 \sin(\pi r/R_c)/(\pi r/R_c)$ of the “minimum halo” (ground state) of surface density $\Sigma_0 = \rho_0 r_h = 141 M_\odot/\text{pc}^2$ made of self-interacting bosons in the TF limit with $a_s/m^3 = 3.28 \times 10^3 \text{ fm}/(\text{eV}/c^2)^3$.

Alternatively, using the results of Appendix G and taking $a_s/m^3 = 3.28 \times 10^3 \text{ fm}/(\text{eV}/c^2)^3$ in the numerical applications, we find that the minimum halo radius, the minimum halo mass and the maximum central density are

$$(r_h)_{\min}=2.47\left(\frac{a_s\hbar^2}{Gm^3}\right)^{1/2}=786\text{ pc}, \quad (42)$$

$$(M_h)_{\min}=13.0\frac{a_s\hbar^2\Sigma_0}{Gm^3}=1.86\times 10^8 M_\odot. \quad (43)$$

$$(\rho_0)_{\max} = 0.404 \left(\frac{Gm^3 \Sigma_0^2}{a_s \hbar^2} \right)^{1/2} = 0.179 M_\odot / \text{pc}^3, \quad (44)$$

where Σ_0 is the universal density of DM halos given by Eq. (1).

The maximum mass of a self-interacting boson star set by general relativity is $M_{\max} = 0.307 \hbar c^2 \sqrt{a_s} / (Gm)^{3/2}$ and its minimum radius is $R_{\min} = 6.25 GM_{\max} / c^2$ [22–24]. They can be written as

$$\frac{M_{\max}}{M_\odot} = 1.12 \left(\frac{a_s}{\text{fm}} \right)^{1/2} \left(\frac{\text{GeV}/c^2}{m} \right)^{3/2}, \quad (45)$$

$$\frac{R_{\min}}{\text{km}} = 9.27 \frac{M_{\max}}{M_\odot}. \quad (46)$$

We note that these results do not depend on the specific mass m and scattering length a_s of the bosons, but only on the ratio a_s/m^3 . For a ratio $(a_s/\text{fm})(\text{eV}/mc^2)^3 = 3.28 \times 10^3$, we obtain $M_{\max} = 2.03 \times 10^{15} M_\odot$ and $R_{\min} = 609 \text{ pc}$. The maximum mass is much larger than the typical core mass of a DM halo. Assuming that a self-interacting BEC star at $T = 0$ describes the quantum core of a DM halo, we conclude that such cores are nonrelativistic since $M_c \ll M_{\max}$ in general. Since the maximum mass is much larger than the core mass, gravity can be treated within a Newtonian framework.

D. Bosonic DM with an attractive self-interaction

We consider a gas of self-interacting bosons at $T = 0$ forming a BEC. The wavefunction of a self-gravitating BEC with a quartic self-interaction is governed by the GPP equations [6]. The equation of state of a self-interacting BEC is given by Eq. (29). We assume that the self-interaction is attractive ($a_s < 0$). This is the case for the axion [11]. Using Madelung’s hydrodynamic representation of the GPP equations, and taking the quantum potential into account, we find that the fundamental differential equation of quantum hydrostatic equilibrium determining the density profile of the BEC is given by Eq. (31) [6]. This equation can be solved numerically [43]. The density profile of a noninteracting BEC star at $T = 0$ (ground state) extends to infinity. The mass-radius relation has been obtained in [6, 43]. There is a maximum mass [6]

$$M_{\max}^{\text{exact}} = 1.012 \frac{\hbar}{\sqrt{Gm|a_s|}} \quad (47)$$

corresponding to a minimum stable radius

$$(R_{99}^*)^{\text{exact}} = 5.5 \left(\frac{|a_s| \hbar^2}{Gm^3} \right)^{1/2}. \quad (48)$$

When $M_c > M_{\max}$ the axion star is expected to collapse and form a dense axion star, a black hole or a bosonova as discussed in [51–59].

E. Mass-radius relation of isothermal DM halos

In the previous subsections, we have focused on the quantum core of DM halos. Ultracompact dwarf DM halos just have a quantum core (ground state). Larger DM halos have a “core-halo” structure with a quantum core surrounded by an atmosphere. We have seen that the structure of the quantum core strongly depends on the nature of the DM particle. By contrast, the structure of the atmosphere is relatively independent of the DM particle. We assume that it has an isothermal equation of state

$$P = \rho \frac{k_B T}{m} \quad (49)$$

with an effective temperature T . For sufficiently large DM halos, the isothermal atmosphere dominates the core. Indeed, the DM halo mass M_h is much larger than the core mass M_c and it is a good approximation to assume that the DM halo is purely isothermal.⁸ Therefore, from the “outside”, large DM halos behave as classical isothermal spheres. If M_h represents the halo mass and r_h the halo radius as defined in Appendix G, then the mass-radius and temperature-radius relations of isothermal DM halos are [7]

$$M_h = 1.76 \Sigma_0 r_h^2, \quad \frac{k_B T}{m} = 0.954 G \Sigma_0 r_h, \quad (50)$$

where Σ_0 is the universal surface density of DM halos given by Eq. (1). On the other hand, the circular velocity at the halo radius is

$$v_h^2 = \frac{GM_h}{r_h} = 1.76 \Sigma_0 G r_h = 1.33 G \Sigma_0^{1/2} M_h^{1/2}. \quad (51)$$

III. A GENERALIZED WAVE EQUATION

A. Coarse-grained dynamics

The previous results can be obtained in a unified manner from the generalized GPP equations [7, 38, 39]

$$i\hbar \frac{\partial \psi}{\partial t} = -\frac{\hbar^2}{2m} \Delta \psi + m\Phi \psi + \frac{K\gamma m}{\gamma-1} |\psi|^{2(\gamma-1)} \psi + 2k_B T \ln |\psi| \psi - i\frac{\hbar}{2} \xi \left[\ln \left(\frac{\psi}{\psi^*} \right) - \left\langle \ln \left(\frac{\psi}{\psi^*} \right) \right\rangle \right] \psi, \quad (52)$$

$$\Delta \Phi = 4\pi G |\psi|^2. \quad (53)$$

As discussed in more detail in [7, 38], the thermal (T) and dissipative (ξ) terms present in the generalized GPP

⁸ We have in mind, for example, the Medium Spiral ($R \sim 10 \text{ kpc}$ and $M \sim 10^{11} M_\odot$).

equations (52) and (53) parametrize the complicated processes of violent relaxation [15] and gravitational cooling [16] experienced by a collisionless system of self-gravitating fermions or bosons. As a result, the generalized GPP equations (52) and (53) describe the evolution of the system on a “coarse-grained” scale.

B. Madelung transformation

Making the Madelung transformation

$$\psi(\mathbf{r}, t) = \sqrt{\rho(\mathbf{r}, t)} e^{iS(\mathbf{r}, t)/\hbar}, \quad (54)$$

$$\rho = |\psi|^2, \quad \mathbf{u} = \frac{\nabla S}{m}, \quad (55)$$

we can show that the generalized GPP equations (52) and (53) are equivalent to the fluid equations

$$\frac{\partial \rho}{\partial t} + \nabla \cdot (\rho \mathbf{u}) = 0, \quad (56)$$

$$\frac{\partial \mathbf{u}}{\partial t} + (\mathbf{u} \cdot \nabla) \mathbf{u} = -\frac{1}{\rho} \nabla P - \nabla \Phi - \frac{1}{m} \nabla Q - \xi \mathbf{u}, \quad (57)$$

$$\Delta \Phi = 4\pi G \rho, \quad (58)$$

where

$$Q = -\frac{\hbar^2}{2m} \frac{\Delta \sqrt{\rho}}{\sqrt{\rho}} \quad (59)$$

is the quantum potential and P is the pressure determined by the equation of state

$$P = K \rho^\gamma + \rho \frac{k_B T}{m} \quad (\gamma = 1 + 1/n). \quad (60)$$

This equation of state has a linear part and a polytropic part. The linear (isothermal) equation of state accounts for effective thermal effects. The polytropic equation of state takes into account the self-interaction of the bosons or the quantum pressure arising from the Pauli exclusion principle for fermions. The equation of state (60) defines a composite model of DM halos with a core-halo structure. The polytropic equation of state dominates in the core where the density is high and the isothermal equation of state dominates in the halo where the density is low (we assume that $\gamma > 1$). As a result, the corresponding DM halos present a quantum (fermionic/bosonic) core surrounded by an isothermal envelope. The quantum core solves the cusp problem and the isothermal envelope leads to flat rotation curves. This model has been studied in detail in [7] for self-interacting BECs. Its extension to noninteracting BECs and fermions will be presented in a forthcoming paper.

C. Condition of quantum hydrostatic equilibrium

The equilibrium state of the hydrodynamic equations (56) and (57) satisfies the condition of quantum hydrostatic equilibrium [38]

$$\frac{\rho}{m} \nabla Q + \nabla P + \rho \nabla \Phi = \mathbf{0}. \quad (61)$$

It describes the balance between the quantum potential arising from the Heisenberg uncertainty principle, the quantum pressure (due to the Pauli exclusion principle for fermions or due to the self-interaction of the bosons), the pressure due to the effective temperature, and the gravitational attraction. Combining Eq. (61) with the Poisson equation (58), we obtain the fundamental differential equation of quantum hydrostatic equilibrium [38]

$$\frac{\hbar^2}{2m^2} \Delta \left(\frac{\Delta \sqrt{\rho}}{\sqrt{\rho}} \right) - \nabla \cdot \left(\frac{\nabla P}{\rho} \right) = 4\pi G \rho. \quad (62)$$

For the equation of state (60), it takes the form

$$\frac{\hbar^2}{2m^2} \Delta \left(\frac{\Delta \sqrt{\rho}}{\sqrt{\rho}} \right) - \frac{K\gamma}{\gamma-1} \Delta \rho^{\gamma-1} - \frac{k_B T}{m} \Delta \ln \rho = 4\pi G \rho. \quad (63)$$

This differential equation determines the general equilibrium density profile $\rho(\mathbf{r})$ of a quantum DM halo in our model [7, 38]. This profile generically has a core-halo structure with a polytropic core and an isothermal halo.

In the core, the differential equation (63) reduces to

$$\frac{\hbar^2}{2m^2} \Delta \left(\frac{\Delta \sqrt{\rho}}{\sqrt{\rho}} \right) - \frac{K\gamma}{\gamma-1} \Delta \rho^{\gamma-1} = 4\pi G \rho. \quad (64)$$

It determines the structure of the quantum core as described in Secs. II A-II D.

In the halo, the differential equation reduces to

$$-\frac{k_B T}{m} \Delta \ln \rho = 4\pi G \rho. \quad (65)$$

It is equivalent to the Emden equation [40]. It determines the structure of the isothermal atmosphere of large DM halos as described in Sec. II E.

D. Free energy

The free energy associated with the generalized GPP equations (52) and (53) or equivalently with the hydrodynamic equations (56) and (57) is

$$F = E_* - TS = \Theta_c + \Theta_Q + U + W - TS. \quad (66)$$

The energy E_* is the sum of the classical kinetic energy

$$\Theta_c = \int \rho \frac{\mathbf{u}^2}{2} d\mathbf{r}, \quad (67)$$

the quantum kinetic energy

$$\Theta_Q = \frac{\hbar^2}{8m^2} \int \frac{(\nabla\rho)^2}{\rho} d\mathbf{r}, \quad (68)$$

the internal energy associated with the polytropic equation of state

$$U = \frac{K}{\gamma-1} \int \rho^\gamma d\mathbf{r}, \quad (69)$$

and the gravitational energy

$$W = \frac{1}{2} \int \rho\Phi d\mathbf{r}. \quad (70)$$

On the other hand,

$$S = -k_B \int \frac{\rho}{m} (\ln \rho - 1) d\mathbf{r} \quad (71)$$

is the Boltzmann entropy associated with the isothermal equation of state.

The generalized GPP equations (52) and (53) or equivalently the hydrodynamic equations (56) and (57) satisfy an H -theorem [38]

$$\dot{F} = -\xi \int \rho \mathbf{u}^2 d\mathbf{r} = -2\xi\Theta_c \leq 0. \quad (72)$$

The free energy decreases monotonically when $\xi > 0$ (or is constant when $\xi = 0$). At equilibrium, we have $\dot{F} = 0$ implying $\mathbf{u} = \mathbf{0}$. Then, Eq. (57) leads to the condition of quantum hydrostatic equilibrium (61). When $\xi > 0$, using Lyapunov's direct method, one can show that the system relaxes, for $t \rightarrow +\infty$, towards a stable equilibrium state which is a (local) minimum of free energy at fixed mass.

The extremization of the free energy at fixed mass, corresponding to the variational principle $\delta F - \frac{\mu}{m} \delta M = 0$ where μ is a Lagrange multiplier, returns the condition of quantum hydrostatic equilibrium (61). Furthermore, (local) minima of free energy are stable while maxima or saddle points are unstable.

The generalized GPP equations (52) and (53) are associated with a canonical description in which the temperature T is fixed. It is possible to modify these equations so that the temperature $T(t)$ evolves in time in order to conserve the energy E (see Appendix I of [38]). This corresponds to a microcanonical description. As is well-known [60], the equilibrium states are the same in the microcanonical and canonical ensembles. However, their stability may be different in case of ensembles inequivalence. In particular, equilibrium states that are unstable in the canonical ensemble may be stable in the microcanonical (this is because the microcanonical ensemble is more constrained than the canonical ensemble). For example, equilibrium states with a negative specific heat are always unstable in the canonical ensemble while they may be stable in the microcanonical ensemble. This property will play a fundamental role in the following analysis.

IV. ANALYTICAL MODEL OF DM HALOS WITH A POLYTROPIC CORE AND AN ISOTHERMAL ATMOSPHERE

In this section, we develop an approximate analytical model of DM halos with a quantum core surrounded by an isothermal atmosphere. For simplicity, we assume that the density of the isothermal atmosphere is uniform. In all the DM models discussed in Sec. II the quantum core can be described by a polytropic equation of state. Therefore, by considering a polytropic core with an arbitrary index n , we can account for a wide diversity of situations and, in particular, unify the treatment of fermionic and bosonic DM halos. We shall enclose the system within a box of radius R . The box is necessary to have a finite mass M . In order to connect this model with real DM halos, we shall identify the box radius R with the halo radius r_h and the mass M with the halo mass M_h . Therefore, we set

$$M = M_h, \quad R = r_h. \quad (73)$$

The mass and the radius of sufficiently large DM halos are related to each other by the first relation of Eq. (50).

A. Polytropic core

We modelize the core of a DM halo by a pure polytrope of index n . Its mass M_c and its radius R_c satisfy the mass-radius relation (see Appendix A) [40]

$$M_c^{(n-1)/n} R_c^{(3-n)/n} = \frac{K(n+1)}{G(4\pi)^{1/n} \omega_n^{(n-1)/n}}. \quad (74)$$

The internal energy and the gravitational energy of the polytropic core are given by (see Appendices B and C)

$$U_c = \frac{n}{5-n} \frac{GM_c^2}{R_c}, \quad W_c = -\frac{3}{5-n} \frac{GM_c^2}{R_c}. \quad (75)$$

Therefore, its total energy $E_c = U_c + W_c$ is

$$E_c = -\frac{3-n}{n} U_c = \frac{3-n}{3} W_c = -\frac{3-n}{5-n} \frac{GM_c^2}{R_c}. \quad (76)$$

Combined with Eq. (74), we obtain

$$E_c = -\frac{3-n}{5-n} \left[\frac{(4\pi)^{1/n}}{n+1} \right]^{n/(3-n)} \frac{1}{\omega_n^{(n-1)/(3-n)}} \times \frac{G^{3/(3-n)} M_c^{(5-n)/(3-n)}}{K^{n/(3-n)}}. \quad (77)$$

B. Isothermal atmosphere of uniform density

We modelize the halo by an isothermal atmosphere of mass $M_a = M - M_c$ contained between the spheres of

radius R_c and R . The internal energy of a gas with the isothermal equation of state (49) is [38]

$$U = \frac{k_B T}{m} \int \rho \ln \rho \, d\mathbf{r} - \frac{3}{2} N k_B T \ln \left(\frac{2\pi k_B T}{m} \right) - N k_B T - N k_B T \ln \left(\frac{2m^4}{h^3} \right). \quad (78)$$

It can be rewritten as

$$U = k_B T \int \frac{\rho}{m} \left[\ln \left(\frac{\lambda^3 \rho}{2m} \right) - 1 \right] d\mathbf{r}, \quad (79)$$

where $\lambda = h/(2\pi m k_B T)^{1/2}$ is the de Broglie wavelength. Treating the atmosphere as a gas with a uniform density, we obtain

$$U_a = \frac{k_B T}{m} (M - M_c) \left[\ln \left(\frac{M - M_c}{V} \right) - \frac{3}{2} \ln \left(\frac{2\pi k_B T}{m} \right) - 1 - \ln \left(\frac{2m^4}{h^3} \right) \right], \quad (80)$$

where $V = (4/3)\pi R^3$ is the total volume of the system. On the other hand, the gravitational energy of the uniform atmosphere in the presence of the ‘‘external’’ polytropic core is given by (see Appendix F)

$$W_a = -\frac{3GM_c(M - M_c)}{2R} - \frac{3G(M - M_c)^2}{5R}. \quad (81)$$

To obtain these results, we have assumed that $R_c \ll R$ which is a very good approximation in all cases of physical interest.

C. Free energy

Using the foregoing results, the total free energy of the system (core + halo) is

$$F = -\frac{3-n}{5-n} \frac{GM_c^2}{R_c} + \frac{k_B T}{m} (M - M_c) \left[\ln \left(\frac{M - M_c}{V} \right) - \frac{3}{2} \ln \left(\frac{2\pi k_B T}{m} \right) - 1 - \ln \left(\frac{2m^4}{h^3} \right) \right] - \frac{3GM_c(M - M_c)}{2R} - \frac{3G(M - M_c)^2}{5R}. \quad (82)$$

For a given value of M , R and T , the free energy is a function $F(M_c)$ of the core mass. The extrema of this function determine the possible equilibrium states of the system. More precisely, they determine the possible equilibrium core masses $M_c^{(i)}$ as a function of M , R and T . We recall that the equilibrium states are the same in the canonical and in the microcanonical ensembles. Indeed,

the extrema of $F(M_c)$ at fixed mass coincide with the extrema of $S(M_c)$ at fixed mass and energy. However, their stability may be different in the canonical and in the microcanonical ensembles. This is the important notion of ensembles inequivalence for systems with long-range interactions [60]. In the canonical ensemble, a minimum of $F(M_c)$ at fixed mass corresponds to a stable equilibrium state (most probable state) while a maximum of $F(M_c)$ at fixed mass corresponds to an unstable equilibrium state (less probable state). In the microcanonical ensemble, a maximum of $S(M_c)$ at fixed mass and energy corresponds to a stable equilibrium state (most probable state) while a minimum of $S(M_c)$ at fixed mass and energy corresponds to an unstable equilibrium state (less probable state). We first consider the canonical ensemble. The microcanonical ensemble is treated in Sec. IV H.

It is convenient to introduce the dimensionless variables

$$x = \frac{M_c}{M}, \quad \eta = \frac{\beta GMm}{R}, \quad (83)$$

$$f(x) = \frac{F(M_c)R}{GM^2}, \quad (84)$$

$$\nu = \left[\frac{G}{K(n+1)} \right]^{n/(3-n)} (4\pi)^{1/(3-n)} \frac{1}{\omega_n^{(n-1)/(3-n)}} \times RM^{(n-1)/(3-n)}, \quad (85)$$

$$\mu = \frac{2m^4}{h^3} \sqrt{512\pi^4 G^3 MR^3}, \quad (86)$$

and

$$C(\eta, \mu) = \frac{3}{2} \ln \eta - \ln \mu + \ln \left(\frac{6}{\sqrt{\pi}} \right), \quad (87)$$

so that Eq. (82) can be rewritten as

$$f(x) = -\frac{3-n}{5-n} \nu x^{(5-n)/(3-n)} + \frac{1}{\eta} (1-x) [\ln(1-x) + C(\eta, \mu) - 1] - \frac{3}{2} x(1-x) - \frac{3}{5} (1-x)^2 \quad (88)$$

with $0 \leq x \leq 1$. On the other hand, introducing

$$y = \frac{R_c}{R}, \quad (89)$$

the core mass-radius relation (74) can be written as

$$y x^{\frac{n-1}{3-n}} = \frac{1}{\nu}. \quad (90)$$

The condition that $y \leq 1$ ($R_c \leq R$) when $x = 1$ ($M_c = M$) implies $\nu \geq 1$.

D. Connection to DM halos

Before going further, let us connect the dimensionless variables introduced previously to the parameters of the DM halos. The variable x represents the normalized core mass. Using Eq. (73) it can be written as

$$x = \frac{M_c}{M_h}. \quad (91)$$

The variable η represents the normalized inverse temperature. For DM halos, using Eqs. (50) and (73), we get

$$\eta = \frac{\beta G M_h m}{r_h} = 1.84. \quad (92)$$

We see that the normalized inverse temperature is of order $1 - 2$. This is essentially a consequence of the virial theorem. Since our approach is approximate, we will allow η to vary slightly around this value. To fix the ideas we take $\eta = 1$. Finally, the variable ν characterizes the mass M_h of the DM halos. For fermionic DM halos, we have⁹

$$\nu_F = 8 \left(\frac{4\pi^2}{3} \right)^{2/3} \frac{1}{\omega_{3/2}^{1/3}} \frac{Gm^{8/3}}{h^2} R M^{1/3}. \quad (94)$$

Using Eqs. (50) and (73), we get

$$\nu_F = 8 \left(\frac{4\pi^2}{3} \right)^{2/3} \frac{1}{\omega_{3/2}^{1/3}} \frac{Gm^{8/3}}{h^2} \frac{1}{\sqrt{1.76 \Sigma_0}} M_h^{5/6}. \quad (95)$$

Normalizing the halo mass by the minimum halo mass from Eq. (14) we obtain

$$\nu_F = 0.582 \left(\frac{M_h}{(M_h)_{\min}} \right)^{5/6}. \quad (96)$$

For noninteracting BECDM halos, we have

$$\nu_B = \frac{2}{\omega_2} \frac{Gm^2}{h^2} R M. \quad (97)$$

Using Eqs. (50) and (73), we get

$$\nu_B = \frac{2}{\omega_2} \frac{Gm^2}{h^2} \frac{1}{\sqrt{1.76 \Sigma_0}} M_h^{3/2}. \quad (98)$$

Normalizing the halo mass by the minimum halo mass from Eq. (26) we obtain

$$\nu_B = 0.293 \left(\frac{M_h}{(M_h)_{\min}} \right)^{3/2}. \quad (99)$$

⁹ This parameter is related to the “degeneracy parameter” μ introduced in [60] and given by Eq. (86). We have

$$\nu_F = \left(\frac{4}{9\omega_{3/2}} \right)^{1/3} \mu^{2/3} = 0.149737 \mu^{2/3} = \lambda \mu^{2/3}. \quad (93)$$

For self-interacting BECDM halos in the TF limit, we have¹⁰

$$\nu_{\text{TF}} = \left(\frac{Gm^3}{a_s \hbar^2} \right)^{1/2} R. \quad (100)$$

Using Eqs. (50) and (73), we get

$$\nu_{\text{TF}} = \left(\frac{Gm^3}{a_s \hbar^2} \right)^{1/2} \frac{1}{\sqrt{1.76 \Sigma_0}} M_h^{1/2}. \quad (101)$$

Normalizing the halo mass by the minimum halo mass from Eq. (43) we obtain

$$\nu_{\text{TF}} = 2.72 \left(\frac{M_h}{(M_h)_{\min}} \right)^{1/2}. \quad (102)$$

E. Equilibrium states

The equilibrium states of DM halos, corresponding to $f'(x) = 0$, are the solutions of the equation

$$\ln(1-x) - \frac{9}{5}x\eta + \frac{3}{10}\eta + C(\eta, \mu) + \nu\eta x^{2/(3-n)} = 0. \quad (103)$$

This equation determines the normalized core mass $x = M_c/M$ as a function of η , ν and μ . It is convenient to introduce the notation

$$\eta_0 = -\frac{10}{3}C(\eta, \mu), \quad (104)$$

so we can rewrite Eq. (103) as

$$\ln(1-x) + \nu\eta x^{2/(3-n)} - \frac{9}{5}x\eta + \frac{3}{10}(\eta - \eta_0) = 0. \quad (105)$$

We note that η_0 depends weakly (logarithmically) on η and μ so, in a first approximation, it can be treated as a constant. The solutions of Eq. (103) can be easily found by studying the inverse function

$$\eta(x) = \frac{\eta_0 - \frac{10}{3} \ln(1-x)}{1 + \frac{10}{3} [\nu x^{2/(3-n)} - \frac{9}{5}x]} \quad (106)$$

for a given value of ν and μ (see Fig. 4). Our analytical model is valid for sufficiently large values of ν and μ (corresponding to large DM halos). On the other hand, the results depend on the value of the polytropic index n . In the following, we assume $1 < n < 3$.¹¹ For $x \rightarrow 0$, we get

$$\eta(x) = \eta_0 + \left(6\eta_0 + \frac{10}{3} \right) x + \dots \quad (107)$$

¹⁰ This parameter is related to the parameter $\mu_{\text{TF}} = Gm^3 R^2 / a_s \hbar^2$ introduced in [7]. We have $\nu_{\text{TF}} = \mu_{\text{TF}}^{1/2}$.

¹¹ The index $n = 1$ is special and has been treated in [7]. The condition $n < 3$ is required in order to have a stable core [40].

Close to $x = 0$, the curve $\eta(x)$ is always increasing. For $x \rightarrow 1$, we get

$$\eta \sim \frac{-\ln(1-x)}{\nu - \frac{3}{2}} \rightarrow +\infty, \quad (108)$$

where we have assumed $\nu > 3/2$ in order to avoid unphysical results due to the invalidity of our model for small values of ν .

We note that the inverse temperature $\eta(x)$ becomes infinite at some $x_i \neq 1$ when the denominator in Eq. (106) vanishes, i.e., when

$$1 + \frac{10}{3} \left[\nu x_i^{2/(3-n)} - \frac{9}{5} x_i \right] = 0. \quad (109)$$

Instead of solving Eq. (109) for x_i as a function of ν , it is simpler to study the inverse function

$$\nu(x_i) = \frac{\frac{9}{5} x_i - \frac{3}{10}}{x_i^{2/(3-n)}}. \quad (110)$$

This function (not represented) has the following properties: (i) $\nu(x_i)$ is positive provided that $x_i \geq 1/6$; (ii) $\nu(1) = 3/2$; (iii) there is a maximum

$$\nu_{\text{CCP}}^{\text{app}} = \frac{3(3-n)}{10(n-1)} [3(n-1)]^{2/(3-n)} \quad (111)$$

at $(x_i)_* = 1/[3(n-1)]$. In order to avoid unphysical results related to the divergence of the inverse temperature at some $x_i \neq 1$, we assume that $\nu > \nu_{\text{CCP}}^{\text{app}}$. We find $\nu_{\text{CCP}}^{\text{app}} = 2.7$ for $n = 2$ and $\nu_{\text{CCP}}^{\text{app}} = 1.545$ for $n = 3/2$. In a sense, this critical value $\nu_{\text{CCP}}^{\text{app}}$ is the counterpart of the canonical critical point that appears in the exact caloric curve of self-gravitating fermions and bosons (see Fig. 32 of [60] for fermions) although it manifests itself in a singular manner in our simple analytical model. Its exact value for fermions is $\nu_{\text{CCP}}^{\text{E}} = 2.85$ corresponding to $\mu_{\text{CCP}} = 83$ [60]. When $\nu > \nu_{\text{CCP}}$ several equilibrium states exist for the same value of the temperature leading to canonical phase transitions (see below).

When $\nu > \nu_{\text{CCP}}^{\text{app}}$ the curve $\eta(x)$ presents a maximum at $(x_c^{\text{artifact}}(\nu), \eta_c^{\text{artifact}}(\nu))$ and a minimum at $(x_*(\nu), \eta_*(\nu))$. They are determined by Eq. (103) and by the equation

$$\frac{2}{3-n} \nu \eta x_e^{(n-1)/(3-n)} - \frac{1}{1-x_e} - \frac{9}{5} \eta = 0 \quad (112)$$

obtained by differentiating Eq. (103) with respect to x and writing $d\eta/dx = 0$.

For $\nu, \mu \rightarrow +\infty$, we find that

$$x_c^{\text{artifact}} \sim \left[\frac{9}{10} (3-n) \frac{1}{\nu} \right]^{(3-n)/(n-1)} \rightarrow 0 \quad (113)$$

and

$$\eta_c^{\text{artifact}} \sim \frac{10}{3} \ln \mu \rightarrow +\infty. \quad (114)$$

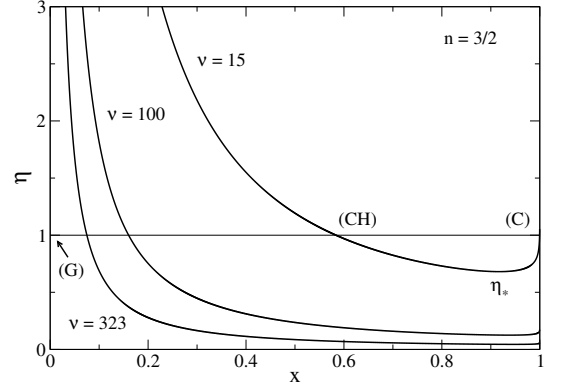


FIG. 4: The function $\eta(x)$ for different values of $\nu > \nu_{\text{CCP}}$ and for $n = 3/2$ (the figure for $n = 2$ is similar). We have indicated the gaseous phase (G), the condensed phase (C) and the core-halo phase (CH) on the curve corresponding to $\nu = 15$ (for $\eta = 1$, the core-halo solution corresponds to $x_{\text{CH}} = 0.583$). We have not represented the region $x \rightarrow 0$ and $\eta > \eta_c \sim 2.52$ which is unphysical as explained in the text.

We know that the maximum inverse temperature of a classical isothermal self-gravitating gas confined within a box is $\eta_c^{\text{class}} = 2.52$ [61]. For self-gravitating fermions and bosons, the maximum inverse temperature $\eta_c(\nu, \mu)$ of the gaseous phase is close to η_c^{class} and tends to this value when $\nu, \mu \rightarrow +\infty$ (see Fig. 14 of [60] for fermions). Therefore, the above results indicate that our simple analytical model is not valid for $x \rightarrow 0$ and $\eta > \eta_c \sim 2.52$. In particular, the maximum at $(x_c^{\text{artifact}}(\nu), \eta_c^{\text{artifact}}(\nu))$ is an artifact of our model. The true maximum is at $(x_c(\nu), \eta_c(\nu)) \sim (0, 2.52)$.

On the other hand, for $\nu, \mu \rightarrow +\infty$, we find that

$$\frac{1}{1-x_*} \sim \frac{2}{3-n} \left[\frac{3}{2} \ln \nu + \ln \mu + \ln \left(\frac{2}{3-n} \right) - \ln \left(\frac{6}{\sqrt{\pi}} \right) \right] \rightarrow 0 \quad (115)$$

and

$$\eta_* \sim \left[\frac{3}{2} \ln \nu + \ln \mu + \ln \left(\frac{2}{3-n} \right) - \ln \left(\frac{6}{\sqrt{\pi}} \right) \right] \frac{1}{\nu} \rightarrow 0. \quad (116)$$

For fermions ($n = 3/2$), using Eq. (93), we obtain at leading order $1/(1-x_*) \sim (8/3) \ln \mu$ and $\eta_* \sim (2/\lambda) (\ln \mu / \mu^{2/3})$ [35]. We note that $\eta_*(\nu)$ decreases as ν increases. This is consistent with the properties of the exact caloric curve of self-gravitating fermions (see Fig. 34 in [60]).

F. Stability of the equilibrium states

Let us now consider more specifically the function $f(x)$ giving the free energy of the system as a function of the

core mass x for a given value of ν , μ and η . Using Eq. (104), we can rewrite Eq. (88) as

$$f(x) = -\frac{3-n}{5-n}\nu x^{(5-n)/(3-n)} + \frac{1}{\eta}(1-x) \left[-\frac{3}{10}\eta_0 + \ln(1-x) - 1 \right] - \frac{3}{2}x(1-x) - \frac{3}{5}(1-x)^2. \quad (117)$$

Its first derivative is

$$f'(x) = -\nu x^{2/(3-n)} + \frac{3}{10}\frac{\eta_0}{\eta} - \frac{1}{\eta}\ln(1-x) - \frac{3}{10} + \frac{9}{5}x. \quad (118)$$

The condition $f'(x) = 0$ determines the possible equilibrium states of the system as we have just seen. The stability of these equilibrium states in the canonical ensemble is then determined by the sign of the second derivative of the free energy:

$$f''(x) = -\nu \frac{2}{3-n} x^{(n-1)/(3-n)} + \frac{1}{\eta(1-x)} + \frac{9}{5}. \quad (119)$$

In the canonical ensemble an equilibrium state is stable when $f''(x) > 0$, corresponding to a minimum of free energy, and unstable when $f''(x) < 0$, corresponding to a maximum of free energy. In Fig. 5 we have plotted the curve $f(x)$ in the case $\nu > \nu_{\text{CCP}}$ and $\eta_* < \eta < \eta_c$ where the system has three equilibrium states as detailed in the following section.

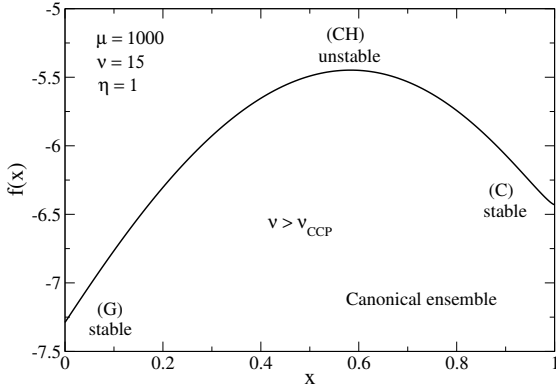


FIG. 5: Free energy $f(x)$ as a function of the core mass x for self-gravitating fermions ($n = 3/2$) with $\nu = 15$ (corresponding to $\mu = 10^3$) at $\eta = 1$. The core-halo solution (CH) at $x_* = 0.583$ is a maximum of free energy at fixed mass. Therefore, it is unstable in the canonical ensemble.

The values of the function $f(x)$ at $x = 0$ and $x = 1$ are

$$f(0) = -\frac{1}{\eta} \left(\frac{3}{10}\eta_0 + 1 \right) - \frac{3}{5} \quad (120)$$

and

$$f(1) = -\frac{3-n}{5-n}\nu. \quad (121)$$

For $x \rightarrow 0$, we find that

$$f(x) = f(0) + \frac{3}{10} \left(\frac{\eta_0}{\eta} - 1 \right) x + \dots \quad (122)$$

In practice $\eta < \eta_c < \eta_0$ so the term in parenthesis is positive. Since the function $f(x)$ is defined for $x \geq 0$, and since the slope of the function $f(x)$ at $x = 0$ is positive, the solution $x = 0$ (gaseous phase) is a local minimum of $f(x)$ even though $f'(0) \neq 0$. We shall therefore consider that the solution $x = 0$ is a stable equilibrium state.

G. The different equilibrium states

After these mathematical preliminaries, we are now ready to perform the complete analysis of the equilibrium states of our simple analytical model. As explained previously we assume $\nu > \nu_{\text{CCP}}$.

The curve $\eta(x)$ is made of a vertical branch at $x = 0$ up to $\eta = \eta_c$, then it decreases, reaches a minimum η_* at x_* , and finally increases up to infinity when $x \rightarrow 1$ (see Fig. 4). When $\eta < \eta_*$, there is a unique equilibrium state ($x = 0$). It corresponds to the gaseous phase (G). It is stable (minimum of free energy). When $\eta > \eta_c$, there is a unique equilibrium state ($x \simeq 1$). It corresponds to the condensed phase (C). It is stable (minimum of free energy). When $\eta_* < \eta < \eta_c$ there are three equilibrium states (see Figs. 4 and 5): (i) a gaseous phase (G); (ii) a core-halo phase (CH); (iii) a condensed phase (C). Let us analyze these solutions in more detail in the limit $\nu, \mu \rightarrow +\infty$:

(i) The gaseous solution (G) corresponds to a purely isothermal halo without core. The core mass is equal to zero: $x_G = 0$. This solution is stable, being a minimum of free energy, although the derivative of $f(x)$ does not vanish at $x = 0$ as explained above.

(ii) The core-halo solution (CH) corresponds to an isothermal halo harboring a core with a small mass ($x_{\text{CH}} \ll 1$). From Eq. (105), we find that the normalized core mass scales as

$$x_{\text{CH}} \sim \left[\frac{3}{10} \frac{\eta_0 - \eta}{\eta} \frac{1}{\nu} \right]^{(3-n)/2}. \quad (123)$$

For fermions, using Eq. (93), we obtain at leading order $x_{\text{CH}} \sim (\ln \mu / \lambda \eta)^{3/4} \mu^{-1/2}$ [35]. This asymptotic formula is compared with the exact value of x_{CH} in Fig. 6. Substituting Eq. (123) into Eq. (119) we find that

$$f''(x_{\text{CH}}) \sim -\frac{2}{3-n} \left[\frac{3}{10} \frac{\eta_0 - \eta}{\eta} \right]^{(n-1)/2} \nu^{(3-n)/2} \rightarrow -\infty. \quad (124)$$

Therefore, the core-halo solution is unstable in the canonical ensemble being a maximum of free energy.

(iii) The condensed solution (C) corresponds to a quantum core surrounded by a tenuous atmosphere ($x_C \sim 1$). From Eq. (105), we find that the normalized core mass

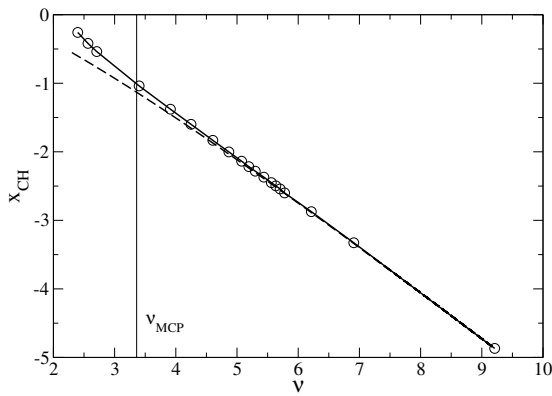


FIG. 6: Core mass (x) as a function of the halo mass (ν) for self-gravitating fermions ($n = 3/2$). The bullets are obtained by solving Eq. (103) exactly (including all the terms) for $\eta = 1$. The dashed line corresponds to Eq. (123) taking into account the fact that η_0 depends on μ hence on ν . For ν large we find an effective exponent 0.667 instead of $(3 - n)/2 = 3/4$ because of logarithmic corrections in η_0 . Coincidentally, in the region of interest $\nu < \nu_{\text{MCP}}$ (see Sec. IV H) we find an effective exponent very close to $3/4$.

scales as

$$1 - x_C \sim \frac{\sqrt{\pi}}{6} \mu \frac{e^{3\eta/2}}{\eta^{3/2}} e^{-\eta\nu}, \quad (125)$$

showing that the quantum core contains almost all the mass. Substituting Eq. (125) into Eq. (119) we find that

$$f''(x_C) \sim \frac{6}{\sqrt{\pi}} \frac{1}{\mu} \frac{\eta^{1/2}}{e^{3\eta/2}} e^{\eta\nu} \rightarrow +\infty. \quad (126)$$

Therefore, the condensed solution is stable, being a minimum of free energy.

The occurrence of three equilibrium states at the same temperature reveals the existence of a canonical phase transition associated with an isothermal collapse [62]. Such gravitational phase transitions are analyzed in detail in [60]. The gaseous (G) and condensed (C) solutions are stable while the core-halo (CH) solution is unstable. It has a negative specific heat (see Sec. IV H) which is forbidden in the canonical ensemble. It plays the role of a “germ” or a “critical droplet” in the language of phase transitions and nucleation (the quantum core is the analogue of the droplet). It creates a barrier of free energy (see Fig. 5) that the system must cross to pass from the gaseous phase to the condensed phase (or the converse). Depending on the value of the temperature T with respect to a temperature of transition T_t [60], the gaseous and the condensed states may be either fully stable (global minimum of free energy) or metastable (local minimum of free energy). However, for systems with long-range interactions, metastable states have very long lifetimes scaling as e^N where $N \gg 1$ is the number of particles in the system [63], so they are strongly stable

in practice.¹² By contrast, the core-halo state (CH) is unstable in the canonical ensemble, being a maximum (not a minimum) of free energy at fixed mass. This looks like a bad news since this core-halo structure is the most interesting structure from a physical point of view. Fortunately, we show in the next section that this core-halo structure is stable in the microcanonical ensemble (if the halo mass is not too large), being a maximum of entropy at fixed mass and energy. This is a manifestation of ensembles inequivalence for systems with long-range interactions [60]. Since the core-halo structure seems to appear in observations and numerical simulations we suggest, following our previous paper [7], that the microcanonical ensemble is more relevant than the canonical ensemble in the physics of DM halos.

H. Microcanonical ensemble

In the microcanonical ensemble, a stable equilibrium state is obtained by maximizing the entropy S at fixed mass M and energy E . Let us first compute the energy and the entropy of the system (quantum core + isothermal atmosphere) by using the same analytical model as in the previous sections.

The energy of the quantum core is given by Eq. (76). On the other hand, the energy of an isothermal self-gravitating gas is

$$E = \frac{3}{2} N k_B T + W, \quad (127)$$

where the first term is the kinetic (thermal) energy and the second term is the gravitational energy. Treating the atmosphere as a gas with a uniform density, we get

$$E_a = \frac{3}{2} (M - M_c) \frac{k_B T}{m} + W_a, \quad (128)$$

where W_a is the gravitational energy of the atmosphere in the presence of the core. It is given by Eq. (81). Therefore, the total energy of the system (core + atmosphere) is

$$E = -\frac{3-n}{5-n} \frac{GM_c^2}{R_c} + \frac{3}{2} (M - M_c) \frac{k_B T}{m} - \frac{3GM_c(M - M_c)}{2R} - \frac{3G(M - M_c)^2}{5R}. \quad (129)$$

In the microcanonical ensemble, the total energy E is fixed. Therefore, Eq. (129) determines the temperature $T(M_c)$ of the halo as a function of the core mass M_c .

¹² The system initially in the metastable gaseous phase (G) must spontaneously form a quantum core of mass $(M_c)_{\text{CH}}$ to overcome the barrier of free energy and collapse in the condensed phase (C). The probability to spontaneously form such a core, thanks to energy fluctuations, is extremely weak, scaling as e^{-N} . This is a such a rare event that the metastable gaseous phase is stable in practice.

The entropy of an isothermal self-gravitating gas is

$$S = -k_B \int \frac{\rho}{m} \ln \rho \, d\mathbf{r} + \frac{3}{2} N k_B \ln \left(\frac{2\pi k_B T}{m} \right) + \frac{5}{2} N k_B + N k_B \ln \left(\frac{2m^4}{h^3} \right). \quad (130)$$

Treating the atmosphere as a gas with a uniform density, we get

$$S = -\frac{k_B}{m} (M - M_c) \ln \left(\frac{M - M_c}{V} \right) + \frac{3}{2} \frac{k_B}{m} (M - M_c) \ln \left(\frac{2\pi k_B T}{m} \right) + \frac{5}{2} \frac{k_B}{m} (M - M_c) + \frac{k_B}{m} (M - M_c) \ln \left(\frac{2m^4}{h^3} \right). \quad (131)$$

Since the entropy of the core is equal to zero, Eq. (131) represents the total entropy of the system.

From the above expressions, we note that the free energy $F = E - TS$ of an isothermal self-gravitating gas (which is the relevant thermodynamic potential in the canonical ensemble) is

$$F = k_B T \int \frac{\rho}{m} \ln \rho \, d\mathbf{r} - \frac{3}{2} N k_B T \ln \left(\frac{2\pi k_B T}{m} \right) - N k_B T - N k_B T \ln \left(\frac{2m^4}{h^3} \right) + W. \quad (132)$$

This justifies the expression of the internal energy $U = F - W$ given by Eq. (78). On the other hand, the free energy $F = E - TS$ calculated with Eqs. (129) and (131) returns Eq. (82) of our analytical model.

Introducing the dimensionless variables

$$\Lambda = -\frac{ER}{GM^2}, \quad s(x) = \frac{S}{Nk_B}, \quad (133)$$

we get

$$\Lambda = \frac{3-n}{5-n} \nu x^{(5-n)/(3-n)} - \frac{3}{2\eta} (1-x) + \frac{3}{2} x(1-x) + \frac{3}{5} (1-x)^2 \quad (134)$$

and

$$s(x) = -(1-x) \left[\ln(1-x) + C(\eta, \mu) - \frac{5}{2} \right]. \quad (135)$$

The first equation determines the inverse temperature $\eta(x)$ as a function of the core mass x for a fixed value of the energy Λ . Then, the maximization of the entropy $s(x)$ (at fixed energy Λ) determines the equilibrium state(s) in the microcanonical ensemble. From the above expressions, we note that the dimensionless free energy (relevant in the canonical ensemble) is given by

$$f(x) = -\Lambda(x) - \frac{s(x)}{\eta}, \quad (136)$$

where now the inverse temperature η is fixed and the energy $\Lambda(x)$ depends on the core mass x . This returns Eq. (88).

One can easily check that the condition $s'(x) = 0$ for a fixed value of Λ yields Eq. (103) which was previously obtained from the condition $f'(x) = 0$ for a fixed value of η . As a result, the equilibrium states (extrema of entropy at fixed mass and energy and extrema of free energy at fixed mass) are the same in the microcanonical and canonical ensembles. However, their stability may be different in the microcanonical and canonical ensembles. This is the notion of ensembles inequivalence for systems with long-range interactions [60].

Let us first consider all the possible equilibrium states determined by Eq. (103). For each of them, we can compute the inverse temperature $\eta(x)$ and the energy $\Lambda(x)$ and plot the caloric curve $\eta(\Lambda)$, relating the temperature to the energy, parametrized by the core mass x . The minimum energy, corresponding to $x = 1$, is $\Lambda_{\max} = [(3-n)/(5-n)]\nu$. We can also add the caloric curve of the gaseous phase ($x = 0$) which is simply given by $\Lambda = 3/5 - 3/(2\eta)$. The complete caloric curve for $n = 3/2$ (fermions) and $\nu = 15$ (corresponding to $\mu = 1000$) is represented in Fig. 7. For $\eta = 1$, we recover the three solutions (G), (CH) and (C) studied in Sec. IV G. We note for future reference that the core-halo solution has an energy $\Lambda_{\text{CH}} = 1.67$ and a core mass $x_{\text{CH}} = 0.583$. We clearly see that the core-halo phase has a negative specific heat $C = dE/dT < 0$ implying that it is unstable in the canonical ensemble as we have found. However, it is known that negative specific heats are allowed in the microcanonical ensemble for systems with long-range interactions [60]. In the present case, the core-halo solution (CH) turns out to be stable in the microcanonical ensemble. This is confirmed in Fig. 8 by plotting the entropy $s(x)$ versus the core mass at the energy $\Lambda = 1.67$. We see that the core-halo solution at $x_{\text{CH}} = 0.583$ is a maximum of entropy at fixed energy. *Therefore, the core-halo solution (CH), with a negative specific heat, is unstable in the canonical ensemble while it is stable in the microcanonical ensemble.* This makes the core-halo solution extremely important since it is now justified as being the ‘‘most probable’’ configuration of the system (maximum entropy state).

This result is valid only when $\nu < \nu_{\text{MCP}}$, where ν_{MCP} is the microcanonical critical point (its exact value for fermions is $\nu_{\text{MCP}}^{\text{F}} = 28.8$ corresponding to $\mu_{\text{MCP}} = 2670$ [60]). When $\nu > \nu_{\text{MCP}}$ the caloric curve $\eta(\Lambda)$ becomes multivalued (see Fig. 9) leading to microcanonical phase transitions associated with the gravothermal catastrophe [33, 60]. In that case, we can have a microcanonical phase transition from the gaseous phase (G') to the condensed phase (C') that we do not analyze in detail here (see [60] for a detailed discussion). We just point out that the core-halo solution (CH) is now both canonically and microcanonically unstable (for $\eta = 1$ we have $\Lambda_{\text{CH}} = -0.443$ and $x_{\text{CH}} = 0.0750$). This is confirmed in Fig. 10 by plotting the entropy $s(x)$ versus the core mass at the

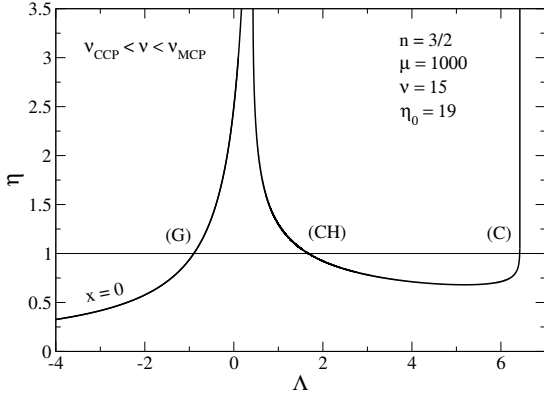


FIG. 7: Caloric curve of self-gravitating fermions $n = 3/2$ with $\nu = 15$ (corresponding to $\mu = 1000$) in the framework of our analytical model. It is in good agreement with the exact caloric curve represented in Fig. 10 of [35].

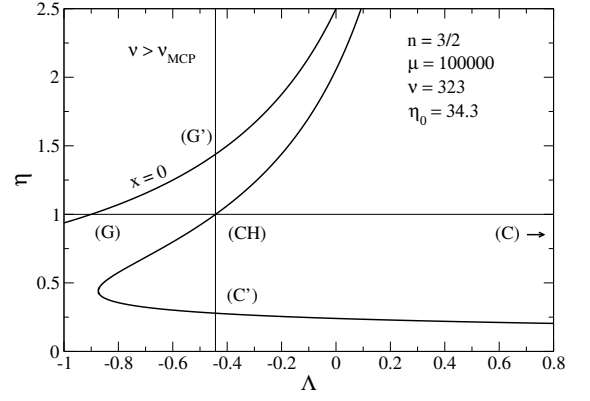


FIG. 9: Caloric curve of self-gravitating fermions $n = 3/2$ with $\nu = 323$ (corresponding to $\mu = 10^5$) in the framework of our analytical model. It is in good agreement with the exact caloric curve represented in Fig. 7 of [35].

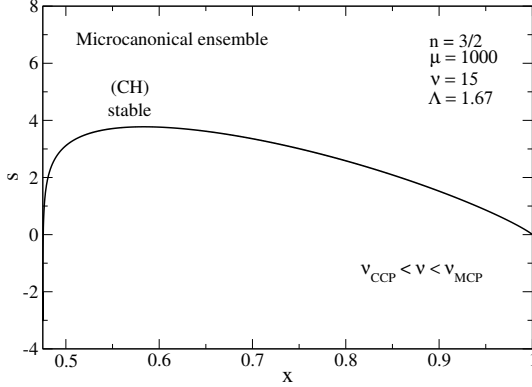


FIG. 8: Entropy $s(x)$ as a function of the core mass x for self-gravitating fermions $n = 3/2$ with $\nu = 15$ (corresponding to $\mu = 1000$) at $\Lambda = 1.67$. The core-halo solution (CH) at $x_* = 0.583$ is a maximum of entropy at fixed mass and energy. Therefore, it is stable in the microcanonical ensemble.

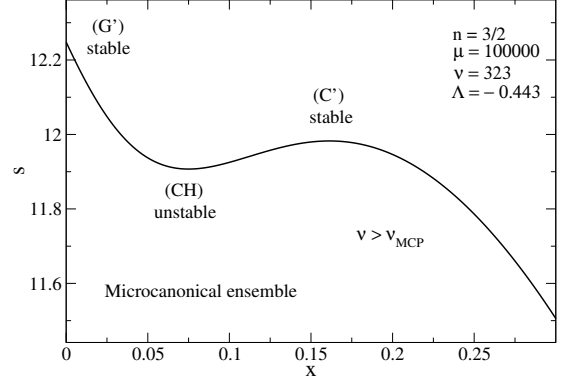


FIG. 10: Entropy $s(x)$ as a function of the core mass x for self-gravitating fermions $n = 3/2$ with $\nu = 323$ (corresponding to $\mu = 10^5$) at $\Lambda = -0.443$. The solution (CH) at $x_{\text{CH}} = 0.0750$ is a minimum of entropy at fixed mass and energy. Therefore, it is unstable in the microcanonical ensemble.

energy $\Lambda = -0.443$. We see that the core-halo solution is a minimum of entropy at fixed energy. *Therefore, the core-halo solution (CH) is unstable in the canonical and in the microcanonical ensembles.*

I. General scenario of DM halos

Recalling that ν is a measure of the size of a DM halo (see Sec. IVD), and that the virial theorem fixes the value of the normalized temperature to $\eta \sim 1$ [see Eq. (92)], the preceding results confirm and refine the scenario developed in [7]:

(i) There is a “minimum halo” of mass $(M_h)_{\text{min}} \sim 10^8 M_\odot$ (value obtained from the observations) corresponding to a purely quantum core without isothermal atmosphere (ground state).

(ii) For $(M_h)_{\text{min}} < M_h < (M_h)_{\text{CCP}}$, the caloric curve $\eta(\Lambda)$ is monotonic. As a result, the virial condition $\eta \sim 1$ determines a unique solution: a quantum phase (Q). It corresponds to a DM halo with a quantum core and a tenuous isothermal atmosphere.

(iii) For $(M_h)_{\text{CCP}} < M_h < (M_h)_{\text{MCP}}$, the caloric curve $\eta(\Lambda)$ has an N-shape structure (see Fig. 7 of this paper and Fig. 10 of [35]). As a result, the virial condition $\eta \sim 1$ determines three solutions: a gaseous phase (G), a core-halo phase (CH) and a condensed phase (C). Among these three solutions, the core-halo state (CH) corresponding to a DM halo with a quantum core and an isothermal atmosphere is the most relevant. This solution is unstable in the canonical ensemble but it is stable in the microcanonical ensemble. It has a negative specific heat. The quantum core may mimic a large bulge (not a black hole) as argued in [7]. The core mass – halo mass relation $M_c(M_h)$, which is of prime interest, is studied in

the following sections.

(iv) For $M_h > (M_h)_{\text{MCP}}$, the caloric curve $\eta(\Lambda)$ has a Z-shape structure (see Fig. 9 of this paper and Fig. 7 of [35]). As before, the virial condition $\eta \sim 1$ determines three solutions: (G), (CH) and (C). However, the core-halo solution (CH) is now unstable in both canonical and microcanonical ensembles. In that case, the system collapses and undergoes a gravothermal catastrophe [33]. A possibility is that it collapses from the gaseous phase (G') to the condensed phase (C') by forming a quantum core of mass $M_c \sim (1/3)M_h$ [64] and expelling a hot atmosphere at large distances.¹³ Alternatively, the core of the system may become relativistic during the gravothermal catastrophe and finally undergo a dynamical instability of general relativistic origin leading ultimately to a supermassive black hole (this is the scenario of Balberg *et al.* [34] advocated in [7, 65]). We stress that the process of gravothermal catastrophe is generally very long (secular) but it may be relevant in galactic nuclei or if the DM particle has a self-interaction [34].

In conclusion, we predict that DM halos with a mass $10^8 M_\odot < M_h < (M_h)_{\text{MCP}}$ harbor a quantum core (bosonic soliton or fermion ball) while DM halos with a mass $M_h > (M_h)_{\text{MCP}}$ harbor a supermassive black hole. This result is connected to the fundamental existence of a microcanonical critical point in the statistical mechanics of self-gravitating systems [60]. If our scenario turns out to be correct, it would provide a beautiful illustration of the curious thermodynamics of self-gravitating systems in a cosmological context. The value of $(M_h)_{\text{MCP}}$ depends on the type of particles that compose DM. For self-interacting bosons in TF limit we found $(M_h)_{\text{MCP}}^{\text{TF}} \sim 2 \times 10^{12} M_\odot$ (corresponding to $\mu_{\text{MCP}}^{\text{TF}} \sim 10^5$ and $\nu_{\text{MCP}}^{\text{TF}} \sim 316$) and for fermions we found $(M_h)_{\text{MCP}}^{\text{TF}} = 9.81 \times 10^9 M_\odot$ (corresponding to $\mu_{\text{MCP}}^{\text{F}} = 2670$ and $\nu_{\text{MCP}}^{\text{F}} = 28.8$). The case of noninteracting bosons is under investigation [7].¹⁴ Presently, the obtained value of $(M_h)_{\text{MCP}}$ is a rough estimate which should be improved in the future if our scenario is relevant. On the other hand, we do not preclude the presence of supermassive black holes in DM halos of mass $M_h < (M_h)_{\text{MCP}}$ if they are formed by a mechanism different from the one [34] that we have advocated.

Remark: The gaseous solutions (G) constitute the lower branch of the generic phase diagram $M_c(M_h)$ reported in Fig. 49 of [7]. The core-halo solutions (CH) constitute the upper branch of this phase diagram that appears above the canonical critical point (bifurcation

point) $(M_h)_{\text{CCP}}$. This is the branch of most physical interest in the physics of DM halos. The core mass – halo mass relation on the core-halo branch (CH) is studied in detail in the following sections. This branch becomes unstable above $(M_h)_{\text{MCP}}$ where the quantum core (bulge) is replaced by a supermassive black hole.

V. JUSTIFICATION OF THE VELOCITY DISPERSION TRACING RELATION AND DETERMINATION OF THE $M_c(M_h)$ RELATION

A. The velocity dispersion tracing relation

We consider the core-halo solution (CH) of Sec. IV G. The normalized core mass is given by Eq. (123). We first show that this result is equivalent to the “velocity dispersion tracing” relation [7, 36, 37]

$$v_c^2 \sim v_h^2 \quad \text{or} \quad M_c \sim \frac{R_c}{r_h} M_h, \quad (137)$$

stating that the velocity dispersion in the core $v_c^2 \sim GM_c/R_c$ is of the same order as the velocity dispersion in the halo $v_h^2 \sim GM_h/r_h$. Using Eq. (74), this relation can be rewritten as

$$M_c \sim \left[\frac{K(n+1)}{G} \right]^{n/2} \frac{\omega_n^{(n-1)/2}}{(4\pi)^{1/2}} \left(\frac{M_h}{r_h} \right)^{(3-n)/2}. \quad (138)$$

On the other hand, using Eqs. (83) and (85), we find that Eq. (123) is equivalent to

$$M_c \sim \left[\frac{3}{10} \frac{\eta_0 - \eta}{\eta} \right]^{(3-n)/2} \left[\frac{K(n+1)}{G} \right]^{n/2} \frac{\omega_n^{(n-1)/2}}{(4\pi)^{1/2}} \times \left(\frac{M_h}{r_h} \right)^{(3-n)/2} \quad (139)$$

The formulae (138) and (139) are consistent with each other up to a multiplicative factor of order unity containing a logarithmic correction. As a result, Eq. (123) is equivalent to the “velocity dispersion tracing” relation from Eq. (137). Our study provides therefore a justification of this relation from (effective) thermodynamical arguments.

B. The $M_c(M_h)$ relation

If we now substitute the relation $M_h = 1.76 \Sigma_0 r_h^2$ from Eq. (50) into Eq. (138) we obtain

$$M_c \sim \left[\frac{K(n+1)}{G} \right]^{n/2} \frac{\omega_n^{(n-1)/2}}{(4\pi)^{1/2}} (1.76 \Sigma_0 M_h)^{(3-n)/4}. \quad (140)$$

This equation gives the relation between the core mass M_c and the halo mass M_h . It displays the fundamental scaling

$$M_c \propto M_h^{(3-n)/4}. \quad (141)$$

¹³ As argued in [7, 65], this scenario may not be relevant for DM halos. However, in another context, it may be relevant to explain the supernova phenomenon of massive stars [64, 66].

¹⁴ In comparison, the canonical critical point is $(M_h)_{\text{CCP}}^{\text{TF}} = 3.27 \times 10^9 M_\odot$ (corresponding to $\mu_{\text{CCP}}^{\text{TF}} = 130$ and $\nu_{\text{CCP}}^{\text{TF}} = 11.4$) for self-interacting bosons in TF limit and $(M_h)_{\text{CCP}}^{\text{F}} = 6.12 \times 10^8 M_\odot$ (corresponding to $\mu_{\text{CCP}}^{\text{F}} = 83$ and $\nu_{\text{CCP}}^{\text{F}} = 2.85$) for fermions

Combining Eq. (140) with the minimum halo mass from Eq. (G6), we get

$$\frac{M_c}{(M_h)_{\min}} \sim A_n \left[\frac{M_h}{(M_h)_{\min}} \right]^{(3-n)/4}, \quad (142)$$

where

$$A_n = \left(\frac{1.76}{4\pi} \right)^{(3-n)/4} \frac{\xi_1^{(n+1)/2} (-\theta'_1)^{(n-1)/2}}{\xi_h^{(3n-1)/4} (-\theta'_h)^{(n+1)/4}} \quad (143)$$

is a constant that depends on the polytropic index n . We find below that the prefactor A_n in Eq. (142) is of order unity. Therefore, the ratio between the core mass and the halo mass is $M_c/M_h \sim [M_h/(M_h)_{\min}]^{-(n+1)/4}$. Accordingly, the core mass becomes negligible in front of the halo mass when $M_h \gtrsim 10 - 100 (M_h)_{\min}$ with $(M_h)_{\min} \sim 10^8 M_\odot$.

C. The $M_c(M_v)$ relation

Following our previous work [7], we have defined the halo mass M_h and the halo radius r_h such that r_h represents the distance at which the central density is divided by 4 (see Appendix G). However, Schive *et al.* [26] use another definition of the halo mass M_v and halo radius r_v . They are connected by

$$M_v = \frac{4}{3} \pi r_v^3 \zeta(0) \rho_{m,0} \quad (144)$$

where $\rho_{m,0} = \Omega_{m,0} \epsilon_0 / c^2$ is the present background matter density in the Universe and $\zeta(0)$ is a prefactor of order ~ 350 . For the numerical applications, we shall take $\Omega_{m,0} = 0.3089$ and $\epsilon_0 / c^2 = 8.62 \times 10^{-24} \text{ g m}^{-3}$ giving $\rho_{m,0} = 2.66 \times 10^{-24} \text{ g m}^{-3}$ [2]. Using

$$\frac{GM_v}{r_v} \sim \frac{GM_h}{r_h}, \quad (145)$$

in consistency with Eq. (137), and Eqs. (50) and (144), we obtain

$$M_h \sim \frac{1}{1.76 \Sigma_0} \left[\frac{4}{3} \pi \zeta(0) \rho_{m,0} \right]^{2/3} M_v^{4/3}. \quad (146)$$

The scaling $M_h \propto M_v^{4/3}$ was previously noted in [7]. Normalizing the halo mass by the minimum halo mass, we get

$$\frac{M_h}{(M_h)_{\min}} \sim B_n \left[\frac{M_v}{(M_h)_{\min}} \right]^{4/3} \quad (147)$$

with

$$B_n = \frac{1}{1.76 \Sigma_0} \left[\frac{4}{3} \pi \zeta(0) \rho_{m,0} \right]^{2/3} (M_h)_{\min}^{1/3}. \quad (148)$$

Combining Eqs. (142) and (147), we finally obtain the core mass – halo mass relation

$$\frac{M_c}{(M_h)_{\min}} \sim A_n B_n^{(3-n)/4} \left[\frac{M_v}{(M_h)_{\min}} \right]^{(3-n)/3}. \quad (149)$$

It exhibits the fundamental scaling $M_c \sim M_v^{(3-n)/3}$.

Remark: Since B_n is a dimensionless constant of order 10^{-3} (see below), Eq. (148) provides a relation between the DM particle parameters (m, a_s) [via $(M_h)_{\min}$], the universal DM surface density Σ_0 and the present density of matter in the Universe $\rho_{m,0}$. Expressing Σ_0 and $\rho_{m,0}$ in terms of the cosmological constant Λ , we will be able (see Sec. VI) to obtain the DM particle parameters (m, a_s) in terms of the fundamental constants of physics.

VI. APPLICATION TO QUANTUM MODELS OF DM HALOS

We now apply these results to quantum models of DM halos made of fermions, noninteracting bosons, and self-interacting bosons as described in Sec. II. For reasons that will become clear below, we treat the case of noninteracting bosons first.

A. Noninteracting bosons

A noninteracting self-gravitating BEC ($a_s = 0$) is equivalent to a polytrope of index $n = 2$ with a polytropic constant given by Eq. (E3) (see Sec. IIB and Appendix E). Using Eqs. (142), (143) and the results of Appendix G, we get

$$\frac{M_c}{(M_h)_{\min}} \sim 1.84 \left[\frac{M_h}{(M_h)_{\min}} \right]^{1/4}. \quad (150)$$

On the other hand, using Eqs. (26) and (148), we find that

$$\begin{aligned} B_2 &= \frac{1}{1.76 \Sigma_0} \left[\frac{4}{3} \pi \zeta(0) \rho_{m,0} \right]^{2/3} (1.61)^{1/3} \left(\frac{\hbar^4 \Sigma_0}{G^2 m^4} \right)^{1/9} \\ &= 2.04 \times 10^{-3}. \end{aligned} \quad (151)$$

Therefore, Eq. (147) takes the form

$$\frac{M_h}{(M_h)_{\min}} \sim 2.04 \times 10^{-3} \left[\frac{M_v}{(M_h)_{\min}} \right]^{4/3}. \quad (152)$$

Combining Eqs. (150) and (152), we obtain the core mass – halo mass relation

$$\frac{M_c}{(M_h)_{\min}} \sim 0.391 \left[\frac{M_v}{(M_h)_{\min}} \right]^{1/3}. \quad (153)$$

It exhibits the fundamental scaling $M_c \propto M_v^{1/3}$. This theoretical scaling is consistent with the scaling found

numerically by Schive *et al.* [26] (see also [67]). These authors also presented an heuristic argument to justify this relation. As discussed in Refs. [7, 36, 37], their argument is equivalent to assuming the velocity dispersion tracing relation (137). We stress, however, that this relation is not obvious *a priori* and that other relations, such as the energy tracing relation corresponding to $GM_c^2/R_c \sim GM_h^2/r_h$, could be contemplated as well [36]. They would lead to different results. The fact that the velocity dispersion tracing relation (137) can be justified from a maximum entropy principle (most probable state), as shown in the present paper, may provide a physical basis for it.

On the other hand, reversing Eq. (151) following the remark at the end of Sec. VC, we get

$$m = \frac{(1.61)^{3/4}}{(1.76)^{9/4}} \left[\frac{4}{3} \pi \zeta(0) \rho_{m,0} \right]^{3/2} \frac{\hbar}{\Sigma_0^2 G^{1/2}} \frac{1}{B_2^{9/4}}. \quad (154)$$

The present matter density in the Universe is given by $\rho_{m,0} = \Omega_{m,0} \epsilon_0 / c^2$ and the density of dark energy is given by $\rho_\Lambda = \Lambda / 8\pi G = \Omega_{de,0} \epsilon_0 / c^2$ where $\Omega_{de,0} \simeq 1 - \Omega_{m,0} = 0.6911$ is the present fraction of dark energy and $\Lambda = 1.00 \times 10^{-35} \text{ s}^{-2}$ is the cosmological constant. Therefore, we can write the present DM density in terms of the cosmological constant as

$$\rho_{m,0} = \frac{\Omega_{m,0}}{\Omega_{de,0}} \frac{\Lambda}{8\pi G} = 0.0178 \frac{\Lambda}{G}. \quad (155)$$

On the other hand, in the framework of the logotropic model [68–70], we have theoretically predicted that the surface density of the DM halos is constant and that its universal value is given in terms of an effective cosmological constant (whose value is the same as Einstein's cosmological constant) by¹⁵

$$\Sigma_0 = 0.0207 \frac{c\sqrt{\Lambda}}{G}. \quad (156)$$

Now that this formula has been isolated, we can use it independently from the theory developed in [68–70]. Combining Eqs. (154), (155) and (156) we find that the mass of the noninteracting bosonic particle is given by

$$m = 1.41 \times 10^{11} m_\Lambda, \quad (157)$$

where

$$m_\Lambda = \frac{\hbar\sqrt{\Lambda}}{c^2} = 2.08 \times 10^{-33} \text{ eV}/c^2. \quad (158)$$

This mass scale is often interpreted as the smallest mass of the bosons predicted by string theory [71] or as the

upper bound on the mass of the graviton [72].¹⁶ This is also the mass of an hypothetical particle called the cosmon [70]. We see that it fixes the mass scale of the DM particle in the case where it is a noninteracting boson. Nevertheless, there is a huge proportionality factor between them, of the order of 10^{11} . We have also found this result in Appendix F of [70] from considerations based on the Jeans instability. These considerations are further developed in Appendix I and generalized to the case of self-interacting bosons and fermions.

Remark: Returning to original variables, and using Eqs. (50), (137) and (E5), the core mass – halo mass relation of DM halos made of noninteracting bosons can be written as

$$M_c \sim 2.29 \left(\frac{\hbar^2 M_h}{G m^2 r_h} \right)^{1/2} \sim 2.64 \left(\frac{\hbar^4 \Sigma_0 M_h}{G^2 m^4} \right)^{1/4} \quad (159)$$

leading to $M_c \propto M_h^{1/4} \propto M_v^{1/3}$.

B. Self-interacting bosons

A self-gravitating BEC with a repulsive self-interaction in the TF limit ($\hbar = 0$) is equivalent to a polytrope of index $n = 1$ with a polytropic constant given by Eq. (30) (see Sec. IIC). Using Eqs. (142), (143) and the results of Appendix G, we get

$$\frac{M_c}{(M_h)_{\min}} \sim 1.16 \left[\frac{M_h}{(M_h)_{\min}} \right]^{1/2}. \quad (160)$$

On the other hand, using Eqs. (43) and (148), we find that

$$\begin{aligned} B_1 &= \frac{1}{1.76 \Sigma_0} \left[\frac{4}{3} \pi \zeta(0) \rho_{m,0} \right]^{2/3} (13.0)^{1/3} \left(\frac{a_s \hbar^2 \Sigma_0}{G m^3} \right)^{1/3} \\ &= 3.43 \times 10^{-3}. \end{aligned} \quad (161)$$

Therefore, Eq. (147) takes the form

$$\frac{M_h}{(M_h)_{\min}} \sim 3.43 \times 10^{-3} \left[\frac{M_v}{(M_h)_{\min}} \right]^{4/3}. \quad (162)$$

Combining Eqs. (160) and (162), we obtain the core mass – halo mass relation

$$\frac{M_c}{(M_h)_{\min}} \sim 6.79 \times 10^{-2} \left[\frac{M_v}{(M_h)_{\min}} \right]^{2/3}. \quad (163)$$

¹⁵ We emphasize that there is no free parameter in the logotropic model [68–70]. In particular, the prefactor 0.0207 in Eq. (156) is predicted by our model.

¹⁶ It is simply obtained by equating the Compton wavelength of the particle $\lambda_C = \hbar/mc$ with the Hubble radius $R_\Lambda = c/H_0 \sim c/\sqrt{\Lambda}$ (the typical size of the visible Universe) giving $m_\Lambda = \hbar H_0 / c^2 \sim \hbar\sqrt{\Lambda}/c^2$. By comparison, if we identify the Compton wavelength $\lambda_C = \hbar/mc$ with the Schwarzschild radius $r_S \sim Gm/c^2$ we get the Planck mass $M_P = (\hbar c/G)^{1/2}$.

It exhibits the fundamental scaling $M_c \propto M_v^{2/3}$. This is a new theoretical prediction [7] that still has to be tested with direct numerical simulations of self-interacting bosons.

On the other hand, reversing Eq. (161) following the remark at the end of Sec. V C, we get

$$\frac{m^3}{a_s} = \frac{13.0}{(1.76)^3} \left[\frac{4}{3} \pi \zeta(0) \rho_{m,0} \right]^2 \frac{\hbar^2}{G \Sigma_0^2} \frac{1}{B_1^3}. \quad (164)$$

Using Eqs. (155) and (156) we obtain

$$\frac{a_s}{m^3} = 5.34 \times 10^{-15} \frac{r_\Lambda}{m_\Lambda^3}, \quad (165)$$

where

$$\frac{r_\Lambda}{m_\Lambda^3} = \frac{2Gc^2}{\Lambda \hbar^2} = 6.11 \times 10^{17} \text{ fm (eV/c}^2\text{)}^{-3}. \quad (166)$$

In this expression, m_Λ is the mass of the cosmon given by Eq. (158) and

$$r_\Lambda = \frac{2Gm_\Lambda}{c^2} = 5.51 \times 10^{-96} \text{ m} \quad (167)$$

is the gravitational radius of the cosmon [70].

Remark: Returning to original variables, and using Eqs. (33), (50) and (137), the core mass – halo mass relation of DM halos made of self-interacting bosons in the TF limit can be written as

$$M_c \sim \pi \left(\frac{a_s \hbar^2 M_h^2}{G m^3 r_h^2} \right)^{1/2} \sim 4.17 \left(\frac{a_s \hbar^2 \Sigma_0 M_h}{G m^3} \right)^{1/2} \quad (168)$$

leading to $M_c \propto M_h^{1/2} \propto M_v^{2/3}$.

C. Fermions

A fermionic core is equivalent to a polytrope of index $n = 3/2$ with a polytropic constant given by Eq. (4) (see Sec. II A). Using Eqs. (142), (143) and the results of Appendix G, we get

$$\frac{M_c}{(M_h)_{\min}} \sim 1.50 \left[\frac{M_h}{(M_h)_{\min}} \right]^{3/8}. \quad (169)$$

On the other hand, using Eqs. (14) and (148), we find that

$$\begin{aligned} B_{3/2} &= \frac{1}{1.76 \Sigma_0} \left[\frac{4}{3} \pi \zeta(0) \rho_{m,0} \right]^{2/3} (4.47)^{1/3} \left(\frac{\hbar^{12} \Sigma_0^3}{G^6 m^{16}} \right)^{1/15} \\ &= 2.70 \times 10^{-3}. \end{aligned} \quad (170)$$

Therefore, Eq. (147) takes the form

$$\frac{M_h}{(M_h)_{\min}} \sim 2.70 \times 10^{-3} \left[\frac{M_v}{(M_h)_{\min}} \right]^{4/3}. \quad (171)$$

Combining Eqs. (169) and (171), we obtain the core mass – halo mass relation

$$\frac{M_c}{(M_h)_{\min}} \sim 0.163 \left[\frac{M_v}{(M_h)_{\min}} \right]^{1/2}. \quad (172)$$

It exhibits the fundamental scaling $M_c \propto M_v^{1/2}$. This theoretical scaling, previously given in the form of Eq. (169) in Appendix H of [65], is consistent with the scaling found numerically by Ruffini *et al.* [73] (they find an exponent equal to 0.52 instead of 1/2).

On the other hand, reversing Eq. (170) following the remark at the end of Sec. V C, we get

$$m = \frac{(4.47)^{5/16}}{(1.76)^{15/16}} \left[\frac{4}{3} \pi \zeta(0) \rho_{m,0} \right]^{5/8} \frac{\hbar^{3/4}}{\Sigma_0^{3/4} G^{3/8}} \frac{1}{B_{3/2}^{15/16}}. \quad (173)$$

Using Eqs. (155) and (156) we obtain

$$m = 3.38 \times 10^4 m_\Lambda^*, \quad (174)$$

where

$$m_\Lambda^* = \left(\frac{\Lambda \hbar^3}{G c^3} \right)^{1/4} = \sqrt{m_\Lambda M_P} = 5.04 \times 10^{-3} \text{ eV/c}^2. \quad (175)$$

To our knowledge, this mass scale has not been introduced before. It is the geometric mean of the cosmon mass m_Λ given by Eq. (158) and the Planck mass $M_P = (\hbar c/G)^{1/2} = 2.18 \times 10^{-5} \text{ g}$.¹⁷

Remark: Comparing Eqs. (151), (161) and (170), we note that the value of B_n defined by Eq. (148) is relatively insensitive on the value of the polytropic index n for the cases contemplated. This is because the parameters have been chosen so that $(M_h)_{\min}$ typically has a fixed value ($\sim 10^8 M_\odot$).

Remark: Returning to original variables, and using Eqs. (6), (50) and (137), the core mass – halo mass relation of DM halos made of fermions may be written as

$$M_c \sim 3.10 \frac{\hbar^{3/2}}{m^2} \left(\frac{M_h}{G r_h} \right)^{3/4} \sim 3.83 \frac{\hbar^{3/2}}{m^2} \left(\frac{M_h \Sigma_0}{G^2} \right)^{3/8} \quad (176)$$

leading to $M_c \propto M_h^{3/8} \propto M_v^{1/2}$.

D. Semiclassical limit

It is interesting to study how the mass M_c , the radius R_c , the velocity dispersion GM_c/R_c and the energy GM_c^2/R_c in the core behave in the semiclassical

¹⁷ In comparison, using the results of [70], the mass of the electron may be written in terms of the fundamental constants of physics as $m_e = 1.03\alpha(m_\Lambda M_P^2)^{1/3} = 9.11 \times 10^{-28} \text{ g}$ where $\alpha \simeq 1/137$ is the fine structure constant.

limit $\hbar \rightarrow 0$. For noninteracting bosons, using Eq. (159), we find $M_c \sim R_c \sim GM_c^2/R_c \sim \hbar \rightarrow 0$ and $GM_c/R_c \sim 1$. For self-interacting bosons, using Eq. (168), we find $M_c \sim R_c \sim GM_c^2/R_c \sim \hbar \rightarrow 0$ and $GM_c/R_c \sim 1$. For fermions, using Eq. (176), we find $M_c \sim R_c \sim GM_c^2/R_c \sim \hbar^{3/2} \rightarrow 0$ and $GM_c/R_c \sim 1$. Therefore, in the semiclassical limit $\hbar \rightarrow 0$, the mass M_c , the size R_c and the energy GM_c^2/R_c of the quantum core go to zero while the velocity dispersion GM_c/R_c remains finite.

VII. GAUSSIAN ANSATZ

In this section, we obtain the core mass – halo mass relation of DM halos by combining the velocity dispersion tracing relation (137) with the approximate core mass-radius relation of a self-gravitating BEC at $T = 0$ obtained in [6] from a Gaussian ansatz. This allows us to recover the preceding results and to generalize them to the case of a repulsive self-interaction ($a_s > 0$), without making the TF approximation, and to the case of an attractive self-interaction ($a_s < 0$). Throughout this section, we introduce appropriate normalizations in order to clearly see the physical origin of the parameters and be able to refine the numerical applications when more precise data will be available.

A. Core mass-radius relation

Using a Gaussian ansatz, it is found in [6] that the approximate mass-radius relation of a self-gravitating BEC at $T = 0$ (ground state) is given by

$$M_c = \frac{2\sigma}{\nu} \frac{\frac{\hbar^2}{Gm^2 R_c}}{1 - \frac{6\pi\zeta a_s \hbar^2}{\nu Gm^3 R_c^2}} \quad (177)$$

with the coefficients $\sigma = 3/4$, $\zeta = 1/(2\pi)^{3/2}$ and $\nu = 1/\sqrt{2\pi}$. Inversely, the radius can be expressed in terms of the mass as

$$R_c = \frac{\sigma}{\nu} \frac{\hbar^2}{GM_c m^2} \left(1 \pm \sqrt{1 + \frac{6\pi\zeta\nu}{\sigma^2} \frac{GmM_c^2 a_s}{\hbar^2}} \right) \quad (178)$$

with $+$ when $a_s > 0$ and with \pm when $a_s < 0$. The results of [6] describe the “minimum halo” (ground state) or the quantum core of larger halos. For noninteracting BECs ($a_s = 0$), the mass-radius relation (177) reduces to

$$M_c = \frac{2\sigma}{\nu} \frac{\hbar^2}{Gm^2 R_c}. \quad (179)$$

In the repulsive case ($a_s > 0$) the mass-radius relation is monotonic (see Fig. 2 of [6]). There is a minimum radius

$$(R_c)_{\min} = \left(\frac{6\pi\zeta}{\nu} \right)^{1/2} \left(\frac{a_s \hbar^2}{Gm^3} \right)^{1/2} \quad (180)$$

corresponding to $M_c \rightarrow +\infty$ (TF limit). Measuring the DM particle mass in units of $10^{-22} \text{eV}/c^2$ and the scattering length in units of 10^{-62}fm , we get $(R_c)_{\min} = 963 a_s^{1/2} m^{-3/2} \text{pc}$. For $R \gg (R_c)_{\min}$ we are in the noninteracting limit (179). In the attractive case ($a_s < 0$) the mass-radius relation is nonmonotonic (see Fig. 3 of [6]). There is a maximum mass

$$(M_c)_{\max} = \left(\frac{\sigma^2}{6\pi\zeta\nu} \right)^{1/2} \frac{\hbar}{\sqrt{Gm|a_s|}} \quad (181)$$

corresponding to the radius

$$(R_c)_* = \left(\frac{6\pi\zeta}{\nu} \right)^{1/2} \left(\frac{|a_s| \hbar^2}{Gm^3} \right)^{1/2}. \quad (182)$$

Measuring the DM particle mass in units of $10^{-22} \text{eV}/c^2$ and the scattering length in units of 10^{-62}fm , we get $(M_c)_{\max} = 1.67 \times 10^8 m^{-1/2} |a_s|^{-1/2} M_\odot$ and $(R_c)_{\min} = 963 |a_s|^{1/2} m^{-3/2} \text{pc}$.

No equilibrium state exists with a mass $M_c > (M_c)_{\max}$. For $M_c < (M_c)_{\max}$ the branch $R_c > (R_c)_*$ (corresponding to the solutions (178) with the sign $+$) is stable and the branch $R_c < (R_c)_*$ (corresponding to the solutions (178) with the sign $-$) is unstable. For $R \gg (R_c)_*$ we are in the noninteracting limit (179) and for $R \ll (R_c)_*$ we are in the (unstable) nongravitational limit where

$$M_c = \frac{\sigma}{3\pi\zeta} \frac{mR_c}{|a_s|}. \quad (183)$$

B. The minimum halo mass

We first determine the minimum halo mass $(M_h)_{\min}$. As explained previously, the minimum halo corresponds to the ground state ($T = 0$) of the self-gravitating BEC. In our approximate approach we write the surface density as

$$\Sigma_0 = \alpha \frac{M_c}{R_c^2}, \quad (184)$$

where α is a constant of order unity (in the numerical applications we take $\alpha = 1/1.76$ for the reason explained in footnote 17). Eliminating R_c between Eqs. (177) and (184), and treating Σ_0 as a universal constant, we get the minimum halo mass $(M_h)_{\min}$ as a function of m and a_s (we recall that $M_h = M_c$ for the ground state since there is no isothermal atmosphere by definition). For noninteracting BECs ($a_s = 0$) we find that the minimum halo mass is

$$(M_h)_{\min,0} = \frac{2^{2/3} \sigma^{2/3}}{\nu^{2/3} \alpha^{1/3}} \left(\frac{\hbar^4 \Sigma_0}{G^2 m^4} \right)^{1/3}. \quad (185)$$

The prefactor is 2.92. This result can be compared with Eq. (26). Measuring the DM particle mass in units of $10^{-22} \text{eV}/c^2$, we get $(M_h)_{\min,0} = 2.95 \times 10^8 m^{-4/3} M_\odot$. In

the general case, valid for an arbitrary value of a_s , we find that the minimum halo mass $(M_h)_{\min}$ is determined by the equation

$$\frac{a_s}{a_*} = \frac{(M_h)_{\min}}{(M_h)_{\min,0}} - \sqrt{\frac{(M_h)_{\min,0}}{(M_h)_{\min}}}, \quad (186)$$

where we have introduced the appropriate scattering length scale

$$a_* = \frac{2^{2/3} \sigma^{2/3} \alpha^{2/3} \nu^{1/3}}{6\pi\zeta} \left(\frac{Gm^5}{\hbar^2 \Sigma_0^2} \right)^{1/3}. \quad (187)$$

The prefactor is 0.553. Measuring the DM particle mass in units of $10^{-22} \text{eV}/c^2$, we get $a_* = 1.28 \times 10^{-62} m^{5/3} \text{fm}$. For $a_s = 0$ we recover $(M_h)_{\min} = (M_h)_{\min,0}$. More generally, the noninteracting limit is valid for $|a_s| \ll a_*$. The relation $(M_h)_{\min}/(M_h)_{\min,0}$ vs a_s/a_* is plotted in Fig. 11. For a given mass m , we see that $(M_h)_{\min}$ is larger than $(M_h)_{\min,0}$ when $a_s > 0$ and smaller when $a_s < 0$.

In the repulsive case, for $a_s \gg a_*$, we have

$$\frac{(M_h)_{\min}}{(M_h)_{\min,0}} \sim \frac{a_s}{a_*}. \quad (188)$$

This corresponds to the TF limit. Returning to the original variables, we obtain

$$(M_h)_{\min} \sim \frac{6\pi\zeta}{\alpha\nu} \frac{a_s \hbar^2 \Sigma_0}{Gm^3}. \quad (189)$$

The prefactor is 5.28. This result can be compared with Eq. (43). Measuring the DM particle mass in units of $10^{-22} \text{eV}/c^2$ and the scattering length in units of 10^{-62}fm , we get $(M_h)_{\min} = 2.30 \times 10^8 a_s m^{-3} M_\odot$.

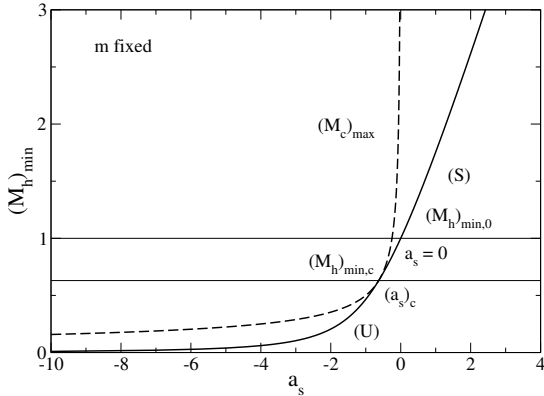


FIG. 11: Minimum halo mass $(M_h)_{\min}$ as a function of the scattering length a_s for a fixed mass m of the DM particle (solid line). We have also plotted the maximum mass $(M_c)_{\max}$ [6] as a function of $a_s < 0$ (dashed line). The intersection between these curves determines the critical minimum halo mass $(M_h)_{\min,c}$. The mass is normalized by $(M_h)_{\min,0}$ and the scattering length by a_* . The stable part of the curve starts at the critical minimum halo point $((a_s)_c, (M_h)_{\min,c})$.

In the attractive case, for $|a_s| \gg a_*$, we have

$$\frac{(M_h)_{\min}}{(M_h)_{\min,0}} \sim \left(\frac{a_*}{a_s} \right)^2. \quad (190)$$

This corresponds to the nongravitational limit in which the configurations are unstable. Returning to the original variables, we obtain

$$(M_h)_{\min} \sim \frac{4\sigma^2 \alpha}{(6\pi\zeta)^2} \frac{m^2}{\Sigma_0 a_s^2}. \quad (191)$$

The prefactor is 0.892. On the other hand, the normalized maximum mass (181) can be written as

$$\frac{(M_c)_{\max}}{(M_h)_{\min,0}} = \frac{1}{2} \left(\frac{a_*}{|a_s|} \right)^{1/2}. \quad (192)$$

We find that the minimum halo is critical (i.e. $(M_h)_{\min} = (M_c)_{\max}$) for

$$\frac{(a_s)_c}{a_*} = -\frac{1}{2^{2/3}}, \quad \frac{(M_h)_{\min,c}}{(M_h)_{\min,0}} = \frac{1}{2^{2/3}}. \quad (193)$$

These relations determine the minimum scattering length $(a_s)_c$ of the DM particle and the minimum mass $(M_h)_{\min,c}$ of the minimum halo. Returning to the original variables, we obtain

$$(a_s)_c = -\frac{\sigma^{2/3} \alpha^{2/3} \nu^{1/3}}{6\pi\zeta} \left(\frac{Gm^5}{\hbar^2 \Sigma_0^2} \right)^{1/3}, \quad (194)$$

$$(M_h)_{\min,c} = \frac{\sigma^{2/3}}{\alpha^{1/3} \nu^{2/3}} \left(\frac{\hbar^4 \Sigma_0}{G^2 m^4} \right)^{1/3}. \quad (195)$$

The prefactors are 0.348 and 1.84. Measuring the DM particle mass in units of $10^{-22} \text{eV}/c^2$, we get $(a_s)_c = -8.06 \times 10^{-63} m^{5/3} \text{fm}$ and $(M_h)_{\min,c} = 1.86 \times 10^8 m^{-4/3} M_\odot$. These relations can be directly obtained by writing $\Sigma_0 = \alpha(M_c)_{\max}/(R_c)_*^2$ and using Eqs. (181) and (182). The minimum halo is stable only for $a_s \geq (a_s)_c$. It has a mass $(M_h)_{\min} \geq (M_h)_{\min,c}$. When $a_s < (a_s)_c$ the minimum halo is unstable (it lies on the branch $R_c < (R_c)_*$ of the mass-radius relation). We note that $(M_h)_{\min,c}$ is relatively close to $(M_h)_{\min,0}$. Therefore, when $(a_s)_c < a_s < 0$, the minimum halo mass $(M_h)_{\min}$ is always of the order of $(M_h)_{\min,0}$ (see the stripe in Fig. 11).

For bosons with an attractive self-interaction, like the axion [11], it is more convenient to express the results in terms of the decay constant (see, e.g., [57])

$$f = \left(\frac{\hbar c^3 m}{32\pi |a_s|} \right)^{1/2}, \quad (196)$$

rather than the scattering length a_s . Measuring the DM particle mass in units of $10^{-22} \text{eV}/c^2$ and the scattering length in units of 10^{-62}fm , we get $f = 1.40 \times 10^{14} m^{1/2} |a_s|^{-1/2} \text{GeV}$. We can write

$$\frac{f}{f_*} = \left(\frac{a_*}{|a_s|} \right)^{1/2} \quad (197)$$

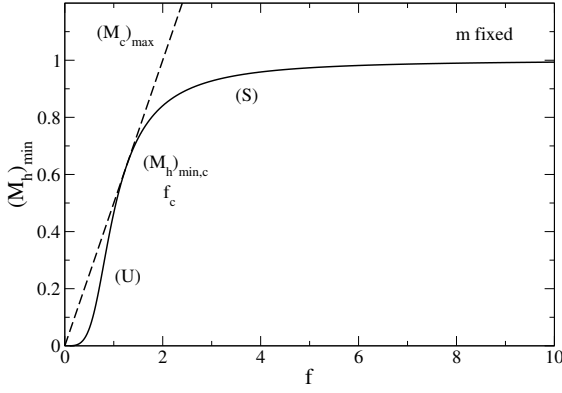


FIG. 12: Minimum halo mass $(M_h)_{\min}$ as a function of the decay constant f for a fixed mass m of the DM particle (solid line). We have also plotted the maximum mass $(M_c)_{\max}$ [6] as a function of f (dashed line). The intersection between these curves determines the critical minimum halo mass $(M_h)_{\min,c}$. The mass is normalized by $(M_h)_{\min,0}$ and the decay constant by f_* . The stable part of the curve starts at the critical minimum halo point $(f_c, (M_h)_{\min,c})$.

with

$$f_* = \frac{(6\pi\zeta)^{1/2}}{(32\pi)^{1/2}2^{1/3}\sigma^{1/3}\alpha^{1/3}\nu^{1/6}} \frac{\hbar^{5/6}\Sigma_0^{1/3}c^{3/2}}{G^{1/6}m^{1/3}}. \quad (198)$$

The prefactor is 0.134. Measuring the DM particle mass in units of $10^{-22}\text{eV}/c^2$, we get $f_* = 1.24 \times 10^{14}m^{-1/3}\text{GeV}$. Eq. (186) can be rewritten as

$$\left(\frac{f_*}{f}\right)^2 = \sqrt{\frac{(M_h)_{\min,0}}{(M_h)_{\min}}} - \frac{(M_h)_{\min}}{(M_h)_{\min,0}}. \quad (199)$$

It determines the minimum halo mass $(M_h)_{\min}$ in terms of m and f . This relation is plotted in Fig. 12. The maximum mass (181) can be written as

$$(M_c)_{\max} = \left(\frac{32\pi\sigma^2}{6\pi\zeta\nu}\right)^{1/2} \left(\frac{\hbar}{Gc^3}\right)^{1/2} \frac{f}{m} \quad (200)$$

or, in normalized form, as

$$\frac{(M_c)_{\max}}{(M_h)_{\min,0}} = \frac{1}{2} \frac{f}{f_*}. \quad (201)$$

Using Eqs. (193) and (197), the minimum decay constant corresponding to the critical minimum halo is

$$\frac{f_c}{f_*} = 2^{1/3}. \quad (202)$$

Returning to the original variables, we find

$$f_c = \frac{(6\pi\zeta)^{1/2}}{(32\pi)^{1/2}\sigma^{1/3}\alpha^{1/3}\nu^{1/6}} \frac{\hbar^{5/6}\Sigma_0^{1/3}c^{3/2}}{G^{1/6}m^{1/3}}. \quad (203)$$

The prefactor is 0.169. Measuring the DM particle mass in units of $10^{-22}\text{eV}/c^2$, we get $f_c = 1.56 \times 10^{14}m^{-1/3}\text{GeV}$. Only the upper part of the curve $(M_h)_{\min}(f)$ starting from the point $(f_c, (M_h)_{\min,c})$ is stable. The noninteracting limit corresponds to $f \gg f_*$.

C. The $m(a_s)$ and $m(f)$ relations

If we consider that the minimum halo mass $(M_h)_{\min}$ is known from the observations, and take $(M_h)_{\min} \sim 10^8 M_\odot$ (Fornax) to fix the ideas, we can use the relation (186) to determine the mass m that the DM particle must have as a function of its scattering length a_s in order to match the value of the minimum halo mass $(M_h)_{\min}$. For $a_s = 0$ we find from Eq. (185) that

$$m_0 = \frac{2^{1/2}\sigma^{1/2}}{\nu^{1/2}\alpha^{1/4}} \frac{\hbar\Sigma_0^{1/4}}{G^{1/2}(M_h)_{\min}^{3/4}}. \quad (204)$$

The prefactor is 2.23. In that case we obtain $m_0 = 2.25 \times 10^{-22}\text{eV}/c^2$ which can be compared to Eq. (24) and Eq. (G17). We can then write

$$\frac{(M_h)_{\min}}{(M_h)_{\min,0}} = \left(\frac{m}{m_0}\right)^{4/3}. \quad (205)$$

On the other hand, we can write

$$\frac{a_s}{a_*} = \frac{a_s}{a'_*} \left(\frac{m_0}{m}\right)^{5/3}, \quad (206)$$

where we have introduced the appropriate scattering length scale

$$a'_* = \frac{2^{3/2}\sigma^{3/2}\alpha^{1/4}}{\nu^{1/2}6\pi\zeta} \frac{\hbar}{G^{1/2}\Sigma_0^{1/4}(M_h)_{\min}^{5/4}}. \quad (207)$$

The prefactor is 2.11. We find $a'_* = 4.95 \times 10^{-62}\text{fm}$. Substituting Eqs. (205) and (206) into Eq. (186), we obtain

$$\frac{a_s}{a'_*} = \left(\frac{m}{m_0}\right)^3 - \frac{m}{m_0}. \quad (208)$$

This relation determines the mass m of the DM particle as a function of its scattering length a_s in order to yield a minimum halo of mass $(M_h)_{\min}$. It is plotted in Fig. 13. For $a_s = 0$, we recover $m = m_0$ which is the mass of a noninteracting boson. More generally, the noninteracting limit corresponds to $|a_s| \ll a'_*$. We see that m is larger than m_0 when $a_s > 0$ and smaller when $a_s < 0$. Therefore, we can increase the DM particle mass by allowing for a repulsive self-interaction between the bosons. As discussed in Appendix D.4 of [14] this could alleviate some tensions with observations of the Lyman- α forest encountered in the noninteracting model [27]. By contrast, an attractive self-interaction implies a (slightly) smaller DM particle mass and may therefore be even more in conflict with observations of the Lyman- α forest. As a result, a repulsive self-interaction ($a_s > 0$) is privileged over an attractive self-interaction ($a_s < 0$). In this respect, we recall that theoretical models of particle physics usually lead to particles with an attractive self-interaction (e.g., the QCD axion). However, some authors [74, 75]

have pointed out the possible existence of particles with a repulsive self-interaction (e.g. the light majoron).

In the repulsive case, for $a_s \gg a'_*$, we have

$$\frac{m}{m_0} \sim \left(\frac{a_s}{a'_*} \right)^{1/3}. \quad (209)$$

This corresponds to the TF limit. Returning to the original variables, we obtain

$$\frac{a_s}{m^3} \sim \frac{\nu\alpha}{6\pi\zeta} \frac{G(M_h)_{\min}}{\hbar^2\Sigma_0}. \quad (210)$$

The prefactor is 0.189. We find $a_s/m^3 = 4.35 \times 10^3 \text{ fm}/(\text{eV}/c^2)^3$ which can be compared with Eq. (39) and Eq. (G21).

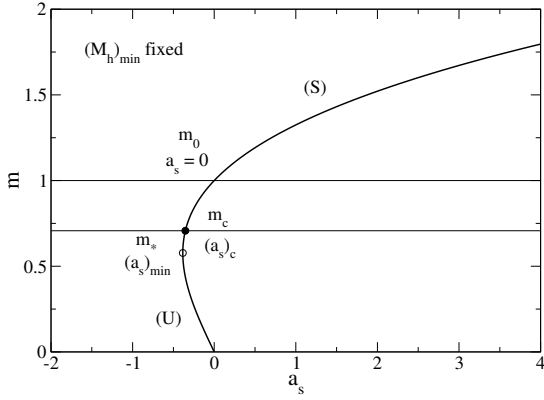


FIG. 13: Mass m of the DM particle as a function of its scattering length a_s for a fixed minimum halo mass $(M_h)_{\min}$ (solid line). The mass is normalized by m_0 and the scattering length by a'_* . The stable part of the curve starts at the critical minimum halo point $((a_s)_c, m_c)$.

In the attractive case, the curve $m(a_s)$ presents a turning point at

$$\frac{(a_s)_{\min}}{a'_*} = -\frac{2}{3\sqrt{3}}, \quad \frac{m_*}{m_0} = \frac{1}{\sqrt{3}}. \quad (211)$$

However, this turning point does *not* correspond to the critical minimum halo for which [see Eqs. (193), (205) and (206)]

$$\frac{(a_s)_c}{a'_*} = -\frac{1}{2^{3/2}}, \quad \frac{m_c}{m_0} = \frac{1}{\sqrt{2}}. \quad (212)$$

Returning to the original variables, we obtain

$$(a_s)_c = -\frac{\sigma^{3/2}\alpha^{1/4}}{6\pi\zeta\nu^{1/2}} \frac{\hbar}{G^{1/2}\Sigma_0^{1/4}(M_h)_{\min}^{5/4}}, \quad (213)$$

$$m_c = \frac{\sigma^{1/2}}{\alpha^{1/4}\nu^{1/2}} \frac{\hbar\Sigma_0^{1/4}}{G^{1/2}(M_h)_{\min}^{3/4}}. \quad (214)$$

The prefactors are 0.746 and 1.58. We find $(a_s)_c = -1.75 \times 10^{-62} \text{ fm}$ and $m_c = 1.59 \times 10^{-22} \text{ eV}/c^2$ which can be compared with Eq. (D19) in Appendix D of [14]. Only the upper part of the curve $m(a_s)$ starting from the point $((a_s)_c, m_c)$ is stable. The existence of a stable minimum halo in the Universe implies that $a_s \geq (a_s)_c$. In that case, the DM particle mass satisfies $m \geq m_c$. We note that m_c is relatively close to m_0 . Therefore, when $(a_s)_c < a_s < 0$, the minimum DM particle mass m is always of the order of m_0 (see the stripe in Fig. 13).

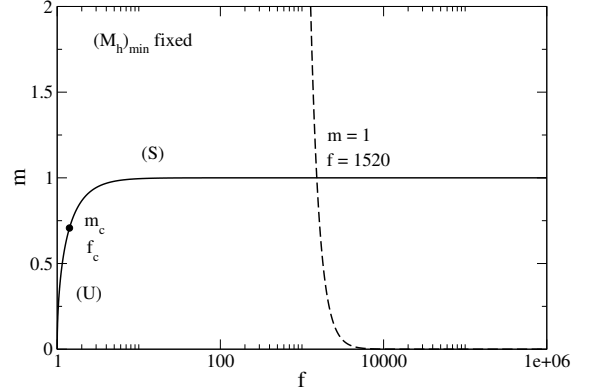


FIG. 14: Mass m of the DM particle as a function of its decay constant f for a fixed minimum halo mass $(M_h)_{\min}$ (solid line). The mass is normalized by m_0 and the decay constant by f'_* . The stable part of the curve starts at the critical minimum halo point (f_c, m_c) . The dashed line corresponds to Eq. (221) predicted by particle physics and cosmology. The intersection between the two curves determines the mass and the decay constant of the DM particle.

For bosons with an attractive self-interaction, like the axion [11], it is more convenient to express the results in terms of the decay constant (196). We can write

$$\frac{f}{f'_*} = \left(\frac{m}{m_0} \right)^{1/2} \left(\frac{a'_*}{|a_s|} \right)^{1/2} \quad (215)$$

with

$$f'_* = \frac{(6\pi\zeta)^{1/2}}{8\pi^{1/2}\sigma^{1/2}\alpha^{1/4}} \hbar^{1/2}\Sigma_0^{1/4}(M_h)_{\min}^{1/4}c^{3/2}. \quad (216)$$

The prefactor is 0.103. We find $f'_* = 9.45 \times 10^{13} \text{ GeV}$. Eq. (208) can be rewritten as

$$\frac{m}{m_0} = \sqrt{1 - \left(\frac{f'_*}{f} \right)^2}. \quad (217)$$

It determines the relation between m and f in order to have a minimum halo (ground state) of mass $(M_h)_{\min}$. This relation is plotted in Fig. 14 (note that $f \geq f'_*$). Using Eqs. (212) and (215), the minimum decay constant corresponding to the critical minimum halo is

$$\frac{f_c}{f'_*} = \sqrt{2}. \quad (218)$$

Returning to the original variables, we obtain

$$f_c = \frac{\sqrt{2}(6\pi\zeta)^{1/2}}{8\pi^{1/2}\sigma^{1/2}\alpha^{1/4}} \hbar^{1/2}\Sigma_0^{1/4}(M_h)_{\min}^{1/4}c^{3/2}. \quad (219)$$

The prefactor is 0.146. We find $f_c = 1.34 \times 10^{14}$ GeV. Only the upper part of the curve $m(f)$ starting from the point (f_c, m_c) is stable. The existence of a stable minimum halo in the Universe implies that $f \geq f_c$. In that case, the DM particle mass satisfies $m \geq m_c$. The noninteracting limit corresponds to $f \gg f'_*$.

There is an interesting by-product of our analysis. Indeed, particle physics and cosmology lead to the following relation between f and m [27]:

$$\Omega_{\text{axion}} \sim 0.1 \left(\frac{f}{10^{17} \text{ GeV}} \right)^2 \left(\frac{m}{10^{-22} \text{ eV}} \right)^{1/2}. \quad (220)$$

Taking $\Omega_{\text{axion}} \sim \Omega_{\text{m},0} = 0.3089$ and $(M_h)_{\min} \sim 10^8 M_\odot$, this relation can be rewritten as

$$\frac{m}{m_0} \sim 5.32 \times 10^{12} \left(\frac{f}{f'_*} \right)^{-4}. \quad (221)$$

This relation is independent from Eq. (217). Equating Eqs. (217) and (221), we obtain $f = 1520 f'_* = 1.44 \times 10^{17}$ GeV and $m = m_0 = 2.25 \times 10^{-22}$ eV/ c^2 . Therefore, we can determine f and m *individually*. We note that m has the same value as in the noninteracting case while f has a finite value $f = 1520 f'_* = 1.44 \times 10^{17}$ GeV. It corresponds to $a_s = -2.14 \times 10^{-68}$ fm. Interestingly, f lies in the range $10^{16} \text{ GeV} \leq f \leq 10^{18} \text{ GeV}$ expected in particle physics [27] (we stress that the value of f has been *deduced* from our model based on the core mass-radius relation (177)). Since $f \gg f'_*$, we are essentially in the noninteracting regime.

Remark: we note that for the critical minimum halo the ratio

$$\frac{(a_s)_c}{m_c^{5/3}} = -\frac{\sigma^{2/3}\alpha^{2/3}\nu^{1/3}}{6\pi\zeta} \left(\frac{G}{\hbar^2\Sigma_0^2} \right)^{1/3} \quad (222)$$

is independent of $(M_h)_{\min}$. The prefactor is 0.348. We find $(a_s)_c/m_c^{5/3} = -3.75 \times 10^{-26}$ fm/(eV/ c^2) $^{5/3}$.

D. The $M_c(M_h)$ relation

To obtain the core mass – halo mass relation $M_c(M_h)$ we use the velocity dispersion tracing relation (137), the core mass-radius relation (178) and the halo-mass radius relation $M_h = 1.76 \Sigma_0 r_h^2$ from Eq. (50). We obtain

$$\frac{M_c}{(M_h)_{\min,0}} = \left(\frac{M_h}{(M_h)_{\min,0}} \right)^{1/4} \sqrt{1 + \frac{a_s}{a_*} \left(\frac{M_h}{(M_h)_{\min,0}} \right)^{1/2}}. \quad (223)$$

For convenience, we have taken $\alpha = 1/1.76$. In this manner, when $M_c = M_h$, we recover the condition (186) determining the minimum halo mass.¹⁸ For $a_s = 0$, we get

$$\frac{M_c}{(M_h)_{\min,0}} = \left(\frac{M_h}{(M_h)_{\min,0}} \right)^{1/4}. \quad (225)$$

This relation is also valid for $|a_s| \ll a_*$ and $M_h/(M_h)_{\min,0} \ll (a_*/a_s)^2$. We recover the scaling from Eq. (150). Returning to the original variables, we get

$$M_c = \frac{2^{1/2}\sigma^{1/2}}{\nu^{1/2}\alpha^{1/4}} \left(\frac{\hbar^4\Sigma_0 M_h}{G^2 m^4} \right)^{1/4}. \quad (226)$$

The prefactor is 2.23. For a DM halo of mass $M_h = 10^{12} M_\odot$ similar to the one that surrounds our Galaxy, we obtain a core mass $M_c = 10^9 M_\odot$ (we have taken $(M_h)_{\min} = 10^8 M_\odot$). The corresponding core radius is $R_c = 63.5$ pc [see Eq. (179)]. The quantum core represents a bulge or a nucleus (it cannot mimic a black hole).

In the repulsive case, for $a_s \gg a_*$ or $M_h/(M_h)_{\min,0} \gg (a_*/a_s)^2$, we have

$$\frac{M_c}{(M_h)_{\min,0}} = \left(\frac{a_s}{a_*} \right)^{1/2} \left(\frac{M_h}{(M_h)_{\min,0}} \right)^{1/2}. \quad (227)$$

This corresponds to the TF limit. Using Eq. (188), we obtain

$$\frac{M_c}{(M_h)_{\min}} = \left(\frac{M_h}{(M_h)_{\min}} \right)^{1/2}. \quad (228)$$

We recover the scaling from Eq. (160). Returning to the original variables, we get

$$M_c = \frac{(6\pi\zeta)^{1/2}}{\nu^{1/2}\alpha^{1/2}} \left(\frac{\hbar^2\Sigma_0 a_s M_h}{G m^3} \right)^{1/2}. \quad (229)$$

The prefactor is 2.30. For a DM halo of mass $M_h = 10^{12} M_\odot$ similar to the one that surrounds our Galaxy, we obtain a core mass $M_c = 10^{10} M_\odot$ (we have taken $(M_h)_{\min} = 10^8 M_\odot$). The core radius is $R_c = 635$ pc [see Eq. (180)]. The quantum core represents a bulge or a nucleus (it cannot mimic a black hole). The core mass – halo mass relation for $a_s > 0$ is plotted in Figs. 15 and 16. These solutions are valid for $M_h > (M_h)_{\min}$.

¹⁸ This can be understood as follows. Combining Eqs. (137) and (50) we get

$$\frac{M_c}{R_c} = \sqrt{1.76 \Sigma_0 M_h}. \quad (224)$$

This equation, that uses the relation $M_h \sim 1.76 \Sigma_0 r_h^2$, is valid only for sufficiently large halos (see Sec. II E). However, if we extrapolate this equation to the minimum halo for which $M_h = M_c$, we get $M_c/R_c^2 = 1.76 \Sigma_0$. Comparing this equation with Eq. (184) we obtain $\alpha = 1/1.76$.

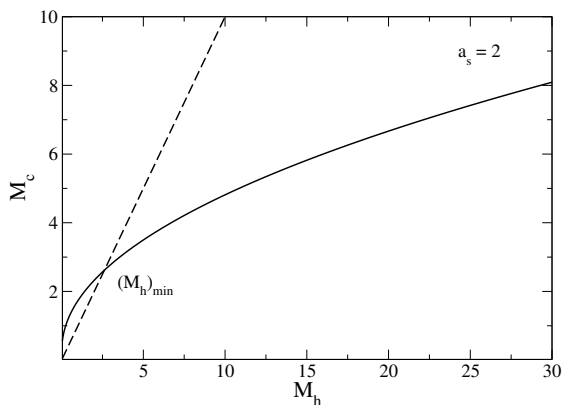


FIG. 15: Core mass M_c as a function of the halo mass M_h for a repulsive self-interaction $a_s > 0$ (solid line). We have also plotted the relation $M_c = M_h$ (dashed line) determining the minimum halo mass $(M_h)_{\min}$. The mass is normalized by $(M_h)_{\min,0}$ and the scattering length by a_* .

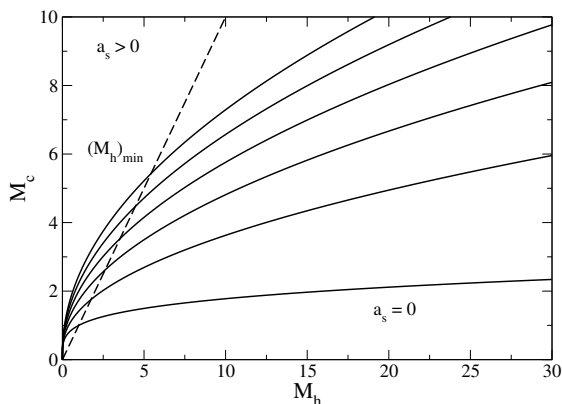


FIG. 16: Core mass M_c as a function of the halo mass M_h for different values of the scattering length $a_s \geq 0$ and a fixed value of the mass m (solid lines). We have plotted the position of the minimum halo mass $(M_h)_{\min}$ (dashed line). The mass is normalized by $(M_h)_{\min,0}$. We have indicated the curve corresponding to the noninteracting case $a_s = 0$.

In the attractive case, the core mass vanishes at

$$\frac{(M_h)_{\max}}{(M_h)_{\min,0}} = \left(\frac{a_*}{a_s}\right)^2. \quad (230)$$

On the other hand the core mass is maximum at

$$\frac{(M_h)_{\max}}{(M_h)_{\min,0}} = \frac{1}{4} \left(\frac{a_*}{a_s}\right)^2 \quad (231)$$

with the value

$$\frac{(M_c)_{\max}}{(M_h)_{\min,0}} = \frac{1}{2} \left(\frac{a_*}{|a_s|}\right)^{1/2}. \quad (232)$$

This corresponds to the maximum core mass given by Eq. (192). The core mass – halo mass relation for

$a_s < 0$ is plotted in Figs. 17 and 18. These solutions are valid for $M_h > (M_h)_{\min}$. On the other hand, the branch $(M_h)_{\max} \leq M_h \leq (M_h)_{\max}$ corresponds to unstable states so that only the branch $(M_h)_{\min} \leq M_h \leq (M_h)_{\max}$, corresponding to stable states, is physical. In summary, when $a_s < (a_s)_c$ there is no halo with a stable quantum core (see Sec. VII B). When $(a_s)_c < a_s < 0$ a stable quantum core exists only in the range $(M_h)_{\min} \leq M_h \leq (M_h)_{\max}$. It has a mass $(M_h)_{\min} \leq M_c \leq (M_c)_{\max}$. Coming back to the original variables, the maximum halo mass is

$$(M_h)_{\max} = \frac{\sigma^2 \alpha}{(6\pi\zeta)^2} \frac{m^2}{a_s^2 \Sigma_0}. \quad (233)$$

The prefactor is 0.223. Measuring the DM particle mass in units of $10^{-22} \text{eV}/c^2$ and the scattering length in units of 10^{-62}fm , we get $(M_h)_{\max} = 1.21 \times 10^8 m^2 |a_s|^{-2} M_\odot$. Note that if we determine the maximum halo mass $(M_h)_{\max}$ approximately by equating Eqs. (225) and (192) [or equivalently Eqs. (226) and (181)], we obtain a value that differs from the real one [Eq. (231) or equivalently (233)] by a factor 1/4.

For bosons with an attractive self-interaction, like the axion [11], it is more convenient to express the results in terms of the decay constant (196). When $f < f_c$ there is no halo with a stable quantum core. When $f > f_c$ a stable quantum core exists only in the range $(M_h)_{\min} \leq M_h \leq (M_h)_{\max}$. The minimum halo mass $(M_h)_{\min}$ is close to $(M_h)_{\min,0}$ given by Eq. (185). The maximum halo mass and the maximum core mass can be written as

$$(M_h)_{\max} = \frac{\sigma^2 \alpha (32\pi)^2}{(6\pi\zeta)^2} \frac{f^4}{\hbar^2 c^6 \Sigma_0}, \quad (234)$$

$$(M_c)_{\max} = \left(\frac{32\pi\sigma^2}{6\pi\zeta\nu}\right)^{1/2} \left(\frac{f^2 \hbar}{c^3 m^2 G}\right)^{1/2}. \quad (235)$$

We note that the maximum halo mass depends only on f while the maximum core mass depends on f and m . The prefactors are 2255 and 10.9. Measuring the DM particle mass in units of $10^{-22} \text{eV}/c^2$ and the decay constant in units of 10^{15}GeV , we get $(M_h)_{\max} = 3.14 \times 10^{11} f^4 M_\odot$ and $(M_c)_{\max} = 1.19 \times 10^9 (f/m) M_\odot$. For $f = 1.44 \times 10^{17} \text{GeV}$ and $m = 2.25 \times 10^{-22} \text{eV}/c^2$ (see Sec. VII C), we find $(M_h)_{\max} = 1.35 \times 10^{20} M_\odot$ and $(M_c)_{\max} = 7.62 \times 10^{10} M_\odot$. Since the largest DM halos observed in the Universe have a mass $M_h \sim 10^{14} M_\odot \ll (M_h)_{\max}$, these results suggest that the effect of an attractive self-interaction is negligible: Everything happens *as if* the bosons were not self-interacting. This favors the consideration of a repulsive self-interaction [7].

In this section, we have expressed the core mass – halo mass relation in terms of M_h . This relation could easily be expressed in terms of M_v by using Eq. (147) with $B = 2.79 \times 10^{-3}$ (we have taken $(M_h)_{\min} = 10^8 M_\odot$).

Remark: We can directly obtain the expression (233) of the maximum halo mass $(M_h)_{\max}$ from the relation

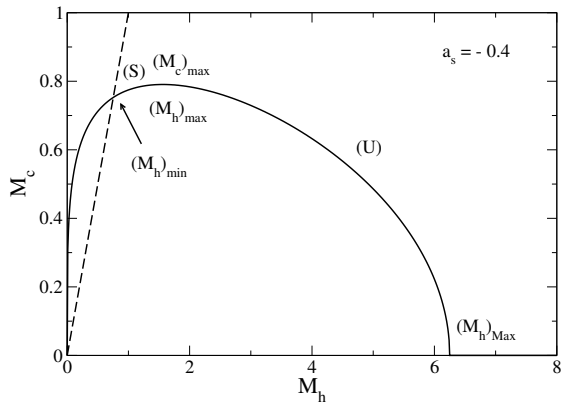


FIG. 17: Core mass M_c as a function of the halo mass M_h for an attractive self-interaction $a_s < 0$ (solid line). We have also plotted the relation $M_c = M_h$ (dashed line) determining the minimum halo mass $(M_h)_{\min}$. The mass is normalized by $(M_h)_{\min,0}$ and the scattering length by a_* .

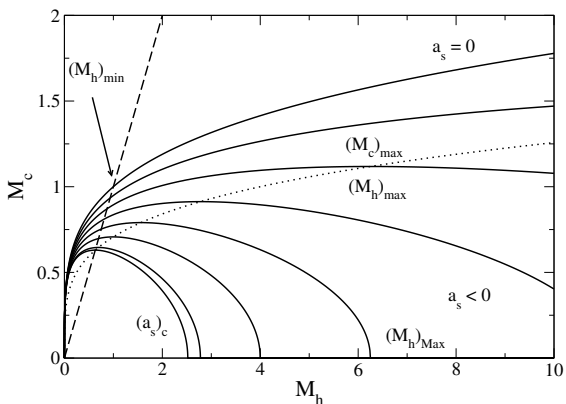


FIG. 18: Core mass M_c as a function of the halo mass M_h for different values of the scattering length $a_s \leq 0$ and a fixed value of the mass m (solid lines). We have plotted the position of the minimum halo mass $(M_h)_{\min}$ (dashed line) and the position of the maximum halo mass $(M_h)_{\max}$ (dotted line). The mass is normalized by $(M_h)_{\min,0}$. We have indicated the curve corresponding to the minimum scattering length $(a_s)_c$ for which $(M_h)_{\min} = (M_h)_{\max}$ (so that the minimum halo is critical) and the curve corresponding to the noninteracting case $a_s = 0$.

[see Eq. (224)]

$$\frac{(M_c)_{\max}}{(R_c)_*} = \sqrt{1.76 \Sigma_0 (M_h)_{\max}} \quad (236)$$

with Eqs. (181) and (182). If we consider a self-gravitating BEC with a central black hole it can be shown that the ratio $(M_c)_{\max}/(R_c)_*$ is independent of the black hole mass [76]. This implies that the expression (233) of the maximum halo mass is unchanged for a fixed central black hole. The case where the black hole mass changes with the halo mass is treated in [77].

E. Summary

In the noninteracting case ($a_s = 0$) the halos with a mass $M_h > (M_h)_{\min,0}$ [see Eq. (185)] contain a quantum core of mass M_c given by Eq. (225). All the configurations are stable.

For a repulsive self-interaction ($a_s > 0$) the halos with a mass $M_h > (M_h)_{\min}$ [see Eq. (186)] contain a quantum core of mass M_c given by Eq. (223). For $a_s \ll a_*$ and M_h not too large ($M_h/(M_h)_{\min,0} \ll (a_*/a_s)^2$), we are in the noninteracting limit discussed previously. For $a_s \gg a_*$ or M_h sufficiently large ($M_h/(M_h)_{\min,0} \gg (a_*/a_s)^2$) we are in the TF limit. In that case, the minimum halo mass $(M_h)_{\min}$ is given by Eq. (189) and the mass M_c of the quantum core is given by Eq. (228). All the configurations are stable.

For an attractive self-interaction ($a_s < 0$) the halos can contain a stable quantum core only if $(a_s)_c < a_s < 0$ [see Eq. (194)] or equivalently if $f > f_c$ [see Eq. (203)]. When this condition is fulfilled the quantum core is stable for $(M_h)_{\min} < M_h < (M_h)_{\max}$. The minimum halo mass $(M_h)_{\min}$ [see Eqs. (186) and (199)] is of the order of $(M_h)_{\min,0}$ [see Eq. (185)]. When we reach the maximum halo mass [see Eqs. (233) and (234)], the core reaches its maximum limit [see Eqs. (181) and (235)] and collapses. The result of the collapse (dense axion star, black hole, bosenova...) is discussed in [51–59].

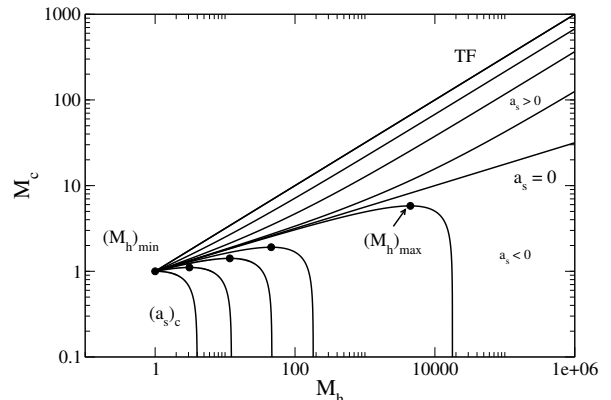


FIG. 19: Core mass M_c as a function of the halo mass M_h for different values of a_s and m (see Table I) so that the minimum halo mass $(M_h)_{\min}$ is fixed (as explained in the text). The mass is normalized by $(M_h)_{\min}$ (typically $(M_h)_{\min} \sim 10^8 M_\odot$). We have plotted the position of the minimum halo mass $(M_h)_{\min}$ (common origin) and the position of the maximum halo mass $(M_h)_{\max}$ (bullets) above which the quantum core becomes unstable when $a_s < 0$. We have indicated the curve corresponding to the minimum scattering length $(a_s)_c/a_* = -1/2^{3/2}$ for which $(M_h)_{\min} = (M_h)_{\max}$ (critical minimum halo), the curve corresponding to the noninteracting case $a_s = 0$ [see Eq. (225)], and the curve corresponding to the TF limit $a_s/a_* \gg 1$ [see Eq. (228)].

These results are summarized in Fig. 19 representing the general core mass – halo mass relation with a nor-

malization such that the minimum halo mass is fixed to a common value obtained from the observations (typically $(M_h)_{\min} \sim 10^8 M_\odot$). The minimum halo mass determines the relation between m and a_s as explained in Sec. VII C. The construction of Fig. 19 is detailed below and the selected values of the DM particle parameters are given in Table I. On this representation, we clearly see that, as compared to the noninteracting case ($a_s = 0$), the core mass M_c increases more rapidly with M_h in the case of a repulsive self-interaction ($a_s > 0$) and less rapidly in the case of an attractive self-interaction ($a_s < 0$). For $a_s \geq 0$, there is a stable core for any halo mass. For $(a_s)_c < a_s < 0$, there is a maximum halo mass $(M_h)_{\max}$ associated with the existence of a maximum core mass $(M_c)_{\max}$. Above that mass, the quantum core collapses.

To make Fig. 19, corresponding to a fixed minimum halo mass $(M_h)_{\min}$, we have proceeded in the following manner. For a given value of a_s/a_* we can obtain m/m_0 from Eq. (208). Then, we get a_s/a_* from Eq. (206) or, equivalently, from

$$\frac{a_s}{a_*} = \left(\frac{m}{m_0}\right)^{4/3} - \left(\frac{m_0}{m}\right)^{2/3}. \quad (237)$$

Finally, we get $(M_h)_{\min}/(M_h)_{\min,0}$ from Eq. (205) or, equivalently, from Eq. (186). We can then plot $M_c/(M_h)_{\min}$ as a function of $M_h/(M_h)_{\min}$ by using Eq. (223). We stress that this procedure yields a “universal” curve for a given value of a_s/a_* . The mass $(M_h)_{\min}$ of the minimum halo then determines the scales m_0 and a'_* according to Eqs. (204) and (207).¹⁹ For convenience, we have proceeded the other way round. We have chosen a value of $(M_h)_{\min}/(M_h)_{\min,0}$, determined a_s/a_* from Eq. (186) and plotted $M_c/(M_h)_{\min}$ as a function of $M_h/(M_h)_{\min}$ by using Eqs. (186) and (223). We have then used Eqs. (205) and (208) to obtain the values of m/m_0 and a_s/a_* corresponding to our choice of $(M_h)_{\min}/(M_h)_{\min,0}$. The selected values of $(M_h)_{\min}/(M_h)_{\min,0}$ and the corresponding DM particle parameters appearing in Fig. 19 are reported in Table I.

In the case of an attractive self-interaction, using Eqs. (205), (206), (215), (231) and (232), the maximum halo mass and the maximum core mass normalized by the minimum halo mass are given by

$$\frac{(M_h)_{\max}}{(M_h)_{\min}} = \frac{1}{4} \left(\frac{a'_*}{a_s}\right)^2 \left(\frac{m}{m_0}\right)^2 = \frac{1}{4} \left(\frac{f}{f'_*}\right)^4 \quad (238)$$

and

$$\frac{(M_c)_{\max}}{(M_h)_{\min}} = \frac{1}{2} \left(\frac{a'_*}{|a_s|}\right)^{1/2} \left(\frac{m_0}{m}\right)^{1/2} = \frac{1}{2} \frac{f}{f'_*} \frac{m_0}{m}, \quad (239)$$

¹⁹ We have assumed that the surface density of the DM halos is universal [see Eq. (1)]. If this were not the case, our general model would remain valid but the problem would depend on M_h and r_h instead of just M_h .

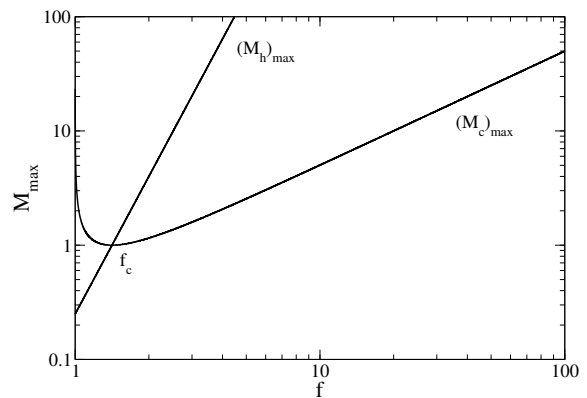


FIG. 20: Maximum halo mass and maximum core mass as a function of the decay constant f in the case of an attractive self-interaction. The mass is normalized by $(M_h)_{\min}$ and the decay constant by f'_* .

where a_s/a'_* , f/f'_* and m/m_0 are related to each other by Eqs. (208) and (217). They are plotted as a function of the decay constant f in Fig. 20. For $f \geq f_c$ (correspondingly $m_c \leq m \leq m_0$ and $(a_s)_c \leq a_s \leq 0$), the maximum halo mass $(M_h)_{\max}$ and the maximum core mass $(M_c)_{\max}$ increase monotonically with f , starting from the value $(M_h)_{\min}$. For $f \gg f'_*$ (i.e. $|a_s| \ll a'_*$) they behave as $(M_h)_{\max}/(M_h)_{\min} \sim (1/4)(f/f'_*)^4 \sim (1/4)(a'_*/a_s)^2$ and $(M_c)_{\max}/(M_h)_{\min} \sim (1/2)(f/f'_*) \sim (1/2)(a'_*/|a_s|)^{1/2}$. As indicated at the end of Sec. VII D, the largest DM halos observed in the Universe have a mass $M_h \sim 10^{14} M_\odot$. Therefore, if $(M_h)_{\max} > 10^{14} M_\odot$ we will never see the effect of an attractive self-interaction (for any DM halo). Taking $(M_h)_{\min} = 10^8 M_\odot$, this condition corresponds to $f > 44.7 f'_* = 4.23 \times 10^{15} \text{ GeV}$. Therefore, for $f > 44.7 f'_* = 4.23 \times 10^{15} \text{ GeV}$ (correspondingly $0.99975 m_0 < m < m_0$ and $-0.0005 a'_* = -2.47 \times 10^{-65} \text{ fm} < a_s \leq 0$) everything happens as if the bosons were noninteracting. This is particularly true for the value $f = 1520 f'_* = 1.44 \times 10^{17} \text{ GeV}$ predicted in Sec. VII C and, more generally, for values of f in the range $10^{16} \text{ GeV} \leq f \leq 10^{18} \text{ GeV}$ expected in particle physics [27].

In the case of a repulsive self-interaction, for a given value of a_s , the transition between the noninteracting limit and the TF limit occurs at a typical halo mass

$$\frac{(M_h)_t}{(M_h)_{\min}} \sim \left(\frac{a'_*}{a_s}\right)^2 \left(\frac{m}{m_0}\right)^2. \quad (240)$$

For $(M_h)_{\min} < M_h \ll (M_h)_t$ we are in the noninteracting limit and for $M_h \gg (M_h)_t$ we are in the TF limit. Using the same argument as above, if $(M_h)_t > 10^{14} M_\odot$ we will not see the effect of a repulsive self-interaction (for any DM halo). Taking $(M_h)_{\min} = 10^8 M_\odot$, this condition corresponds to $0 < a_s < 0.001 a'_* = 4.95 \times 10^{-65} \text{ fm}$. Therefore, for $0 < a_s < 0.001 a'_* = 4.95 \times 10^{-65} \text{ fm}$ (correspondingly $m_0 < m < 1.0005 m_0$) everything happens as if the bosons were noninteracting. To our knowledge, there is

$\frac{(M_h)_{\min}}{(M_h)_{\min,0}}$	$\frac{a_s}{a_*}$	$\frac{m}{m_0}$	$\frac{a_s}{a'_*}$	$\frac{f}{f'_*}$	$\frac{(M_h)_{\max}}{(M_h)_{\min}}$	$\frac{(M_c)_{\max}}{(M_h)_{\min}}$
10^4	10^4	10^3	10^9			
1.6	0.809	1.42	1.46			
1.1	0.1465	1.07	0.165			
1.01	0.015	1.01	0.01515			
1	0	1	0	∞		
0.995	-0.00751	0.996	-0.00746	11.55	4460	5.80
0.95	-0.0760	0.962	-0.0713	3.67	45.6	1.91
0.9	-0.154	0.924	-0.135	2.615	11.7	1.41
0.8	-0.318	0.846	-0.241	1.87	3.09	1.11
0.630	-0.630	0.707	-0.354	1.41	1	1

TABLE I: Values of the DM particle parameters selected in Fig. 19. The scales m_0 , a'_* and f'_* are given by Eqs. (204), (207) and (216). For $(M_h)_{\min} = 10^8 M_\odot$, we obtain $m_0 = 2.25 \times 10^{-22} \text{ eV}/c^2$, $a'_* = 4.95 \times 10^{-62} \text{ fm}$ and $f'_* = 9.45 \times 10^{13} \text{ GeV}$. The noninteracting limit corresponds to $|a_s| \ll a'_*$ (hence $m \sim m_0$). The TF limit corresponds to $a_s \gg a'_*$ (hence $m \gg m_0$). The minimum value of a_s ensuring that the minimum halo is stable is $(a_s)_c = -0.354 a'_*$ (hence $m_c = 0.707 m_0$).

no strong constraint on a repulsive self-interaction (see, however, the Bullet Cluster constraint mentioned in Sec. II C) so that large positive values of a_s ($\gg 0.001 a'_* = 4.95 \times 10^{-65} \text{ fm}$), corresponding to large values of the boson mass m ($\gg 1.0005 m_0 = 2.25 \times 10^{-22} \text{ eV}/c^2$), are possible in principle.

VIII. CONCLUSION

In this paper, we have analytically derived the core mass – halo mass relation of fermionic and bosonic DM halos from an effective thermodynamical approach. We have modeled the DM halos by a quantum core of mass M_c surrounded by an isothermal atmosphere of uniform density. We first determined an analytical expression of the free energy $F(M_c)$ and entropy $S(M_c)$ of the DM halos. The equilibrium core mass M_c is then obtained by extremizing the free energy $F(M_c)$ at fixed mass or by extremizing the entropy $S(M_c)$ at fixed mass and energy. By representing the quantum core by a polytrope of index n we have developed a unified description for fermions ($n = 3/2$), noninteracting bosons ($n = 2$) and self-interacting bosons in the TF approximation ($n = 1$). This allowed us to treat fermionic and bosonic DM halos with the same formalism. In the generic case, the extremization problem determines three solutions corresponding to a gaseous phase (G), a core-halo phase (CH) and a condensed phase (C). The most important solution is the core-halo phase. We showed that this phase is always unstable in the canonical ensemble (maximum of free energy at fixed mass) while it is stable in the micro-canonical ensemble (maximum of entropy at fixed mass and energy) when $M_h < (M_h)_{\text{MCP}}$ (the gaseous and the condensed phases are stable in all statistical ensembles). When $M_h > (M_h)_{\text{MCP}}$ the core-halo phase is unstable in all statistical ensembles. In that case, the quantum core may be replaced by a supermassive black hole [7] resulting from a gravothermal catastrophe [33] followed by a

dynamical instability of general relativistic origin [34].

Our thermodynamical approach leads to the velocity dispersion tracing relation (137) put forward heuristically in [7, 36, 37]. Therefore, this relation can be *justified* by an effective thermodynamical approach (maximum entropy principle). For noninteracting bosons, we obtain the mass-radius relation (153) which is consistent to the one found by Schive *et al.* [26] (see also [67]). For fermions, we obtain the mass-radius relation (172) which is consistent to the one found by Ruffini *et al.* [73]. For bosons with an attractive self-interaction in the TF limit, we predict the mass-radius relation (163) which still has to be confirmed numerically. Combining the velocity dispersion tracing relation [7, 36, 37] with the core mass – core radius relation derived in [6] we have obtained an approximate general core mass – halo mass relation $M_c(M_v)$ [see Eq. (223)] that is valid for bosons with arbitrary repulsive or attractive self-interaction. For an attractive self-interaction, corresponding to axions [11], we have determined the maximum halo mass $(M_v)_{\text{max}}$ [see Eq. (234)] that can harbor a stable quantum core (dilute axion star).

The mass $(M_h)_{\min}$ of the minimum halo (ground state) determines the parameters of the DM particle (depending on the strength of the self-interaction). Observations reveal that $(M_h)_{\min} \sim 10^8 M_\odot$. For fermions, we find $m = 165 \text{ eV}/c^2$ [see Eq. (G12)]. For noninteracting bosons we find $m = 1.44 \times 10^{-22} \text{ eV}/c^2$ [see Eq. (G17)]. For self-interacting bosons in the TF limit we find $a_s/m^3 = 1.76 \times 10^3 \text{ fm}/(\text{eV}/c^2)^3$ [see Eq. (G21)]. We can then use the core mass – halo mass relation to determine the characteristics of the quantum core residing in a given DM halo. Let us consider a DM halo of mass $M_h = 10^{12} M_\odot$ similar to the one that surrounds our Galaxy. For fermions, we find $M_c = 4.74 \times 10^9 M_\odot$ and $R_c = 301 \text{ pc}$ [see Eqs. (6) and (169)]. For noninteracting bosons we find $M_c = 1.84 \times 10^9 M_\odot$ and $R_c = 118 \text{ pc}$ [see Eqs. (E5) and (150)]. For self-interacting bosons in the TF limit we find $M_c = 1.16 \times 10^{10} M_\odot$ and $R_c = 733 \text{ pc}$

[see Eqs. (33) and (160)]. In our model, the quantum core represents a bulge or a nucleus. It cannot mimic a black hole as it has been sometimes suggested.

Finally, we have argued that the mass scale of non-interacting DM bosons is determined in terms of fundamental constants by $m_\Lambda = \hbar\sqrt{\Lambda}/c^2 = 2.08 \times 10^{-33} \text{ eV}/c^2$ while the mass scale of fermions is determined by $m_\Lambda^* = (\Lambda\hbar^3/Gc^3)^{1/4} = \sqrt{m_\Lambda M_P} = 5.04 \times 10^{-3} \text{ eV}/c^2$. We found that the prefactor between the actual DM particle mass and these fundamental mass scales can be very large (11 orders of magnitude for bosons and 4 orders of magnitude for fermions). However, these fundamental mass scales can explain the intrinsic difference of mass between bosonic and fermionic DM particles. Their ratio is $m_\Lambda^*/m_\Lambda = (c^5/G\hbar\Lambda)^{1/4} = 2.42 \times 10^{30}$, corresponding to a difference of 30 orders of magnitude. Finally, in the case of self-interacting bosons, we have found that the fundamental scale of the ratio a_s/m^3 is $r_\Lambda/m_\Lambda^3 = 2Gc^2/\Lambda\hbar^2 = 6.11 \times 10^{17} \text{ fm}(\text{eV}/c^2)^{-3}$.

In the present paper, we have developed an analytical model in which the isothermal atmosphere has a uniform density. This approximation is sufficient to obtain the correct scaling of the core mass – halo mass relation. However, in order to develop more accurate models of fermionic and bosonic DM halos, and in particular to be able to determine their density and circular velocity profiles, we need to solve a generalized Emden equation numerically. The case of self-gravitating BECs with a repulsive self-interaction has been treated in detail in [7]. The case of noninteracting bosons and fermions can be treated with the same method. These models are being presently investigated [78].

It will be important in future works to determine if DM is made of fermions or bosons (either noninteracting, with a repulsive self-interaction, or with an attractive self-interaction). All these models are very interesting from a physical point of view, with fascinating properties, but it is possible that some of them will be ruled out by observations. Alternatively, all these models could be of interest if DM is made of several types of particles (bosons and fermions) as suggested in [7].

It will also be important in future works to go beyond certain approximations made in this paper. For example, we have ignored the influence of baryons. They may have several significant effects on DM halos and, in particular, they can alleviate the cusp problem [79]. It would be interesting to check the validity of our results in the presence of baryons. We have also used a nonrelativistic approach. As we have shown, this nonrelativistic approach is expected to be sufficient in most applications of DM halos. However, in the case of bosons with an attractive self-interaction, if the mass of the quantum core M_c becomes greater than the maximum mass $(M_c)_{\text{max}}$ [6], the core collapses. In that case, relativistic effects can be important and the GPP equations must be replaced by the Klein-Gordon-Einstein (KGE) equations [55–59]. The KGE equations must also be used [84] in order to study boson stars and scalar field configurations in highly

relativistic environments, such as scalar field dark matter laying in the vicinity of compact objects like black holes or neutron stars.

Appendix A: Polytopic spheres

In this Appendix, we recall general results pertaining to self-gravitating polytopic spheres [40, 61]. We apply them to the quantum models of DM halos at $T = 0$ (ground states) discussed in Sec. II.

For classical self-gravitating systems, or for quantum self-gravitating systems in the TF approximation, the condition of hydrostatic equilibrium

$$\nabla P + \rho \nabla \Phi = \mathbf{0} \quad (\text{A1})$$

combined with the Poisson equation

$$\Delta \Phi = 4\pi G \rho \quad (\text{A2})$$

leads to the fundamental differential equation

$$\nabla \cdot \left(\frac{\nabla P}{\rho} \right) = -4\pi G \rho. \quad (\text{A3})$$

For a polytopic equation of state of the form

$$P = K \rho^\gamma, \quad (\text{A4})$$

where K is the polytopic constant and $\gamma = 1 + 1/n$ is the polytopic index, the differential equation (A3) becomes

$$K(n+1)\Delta\rho^{1/n} = -4\pi G\rho. \quad (\text{A5})$$

In the following, we restrict ourselves to spherically symmetric distributions. We also assume $K > 0$ and $6/5 < \gamma < +\infty$ (i.e. $0 \leq n < 5$) for reasons explained below. With the substitution

$$\rho = \rho_0 \theta^n, \quad \xi = \frac{r}{r_0}, \quad (\text{A6})$$

where ρ_0 is the central density and

$$r_0 = \left[\frac{K(n+1)}{4\pi G \rho_0^{1-1/n}} \right]^{1/2} \quad (\text{A7})$$

is the polytopic radius, we obtain the Lane-Emden equation

$$\frac{1}{\xi^2} \frac{d}{d\xi} \left(\xi^2 \frac{d\theta}{d\xi} \right) = -\theta^n \quad (\text{A8})$$

with the boundary conditions

$$\theta(0) = 1, \quad \theta'(0) = 0. \quad (\text{A9})$$

According to the general results of Refs. [40, 61], a polytrope of index n has a compact support provided that $0 \leq n < 5$. In that case, the density falls off to zero at a

finite radius. This characterizes a complete polytrope.²⁰ It is customary to denote by ξ_1 the normalized radius at which the density vanishes: $\theta_1 = 0$. The radius and the mass of a complete polytrope then are

$$R = \xi_1 \left[\frac{K(n+1)}{4\pi G} \right]^{1/2} \frac{1}{\rho_0^{(n-1)/2n}}, \quad (\text{A10})$$

$$M = -4\pi \frac{\theta'_1}{\xi_1} \rho_0 R^3. \quad (\text{A11})$$

Eliminating ρ_0 between these two relations, we find that the mass-radius relation of a complete polytrope of index n is

$$M^{(n-1)/n} R^{(3-n)/n} = \frac{K(1+n)}{G(4\pi)^{1/n}} \omega_n^{(n-1)/n}, \quad (\text{A12})$$

where $\omega_n = -\xi_1^{(n+1)/(n-1)} \theta'_1$ is a constant determined by the Lane-Emden equation (A8). A complete polytrope of index n is dynamically stable with respect to the Euler-Poisson equations if $n < 3$ and linearly unstable if $n > 3$.

For the polytrope $n = 3/2$ (fermion stars), using Eq. (4), we find

$$\xi_1 = 3.65375, \quad \theta'_1 = -0.203302, \quad (\text{A13})$$

$$R = 0.35885 \frac{h}{m^{4/3} G^{1/2} \rho_0^{1/6}}, \quad (\text{A14})$$

$$M = 0.699218 \rho_0 R^3, \quad (\text{A15})$$

$$MR^3 = 0.0014931 \frac{h^6}{G^3 m^8}. \quad (\text{A16})$$

For the polytrope $n = 2$ (noninteracting boson stars), using Eq. (E3), we find

$$\xi_1 = 4.353, \quad \theta'_1 = -0.1272, \quad (\text{A17})$$

$$R = 1.94415 \frac{\hbar^{1/2}}{m^{1/2} G^{1/4} \rho_0^{1/4}}, \quad (\text{A18})$$

$$M = 0.367205 \rho_0 R^3, \quad (\text{A19})$$

$$MR = 5.24594 \frac{\hbar^2}{G m^2}. \quad (\text{A20})$$

For the polytrope $n = 1$ (self-interacting boson stars), using $\theta(\xi) = \sin(\xi)/\xi$ and Eq. (30), we find

$$\xi_1 = \pi, \quad \theta'_1 = -1/\pi, \quad (\text{A21})$$

$$R = \pi \left(\frac{a_s \hbar^2}{G m^3} \right)^{1/2}, \quad (\text{A22})$$

$$M = \frac{4}{\pi} \rho_0 R^3. \quad (\text{A23})$$

Appendix B: Total energy, eigenenergy and virial theorem of a self-gravitating BEC

We consider a self-gravitating BEC described by the GPP equations with a self-interaction corresponding to a power-law potential [38]. In the hydrodynamic representation of the GPP equations, a power-law potential of interaction gives rise to a polytropic equation of state. In that case, the total energy of the BEC is given by

$$E_{\text{tot}} = \Theta_Q + U + W. \quad (\text{B1})$$

This is the sum of the quantum kinetic energy

$$\Theta_Q = \frac{\hbar^2}{8m^2} \int \frac{(\nabla \rho)^2}{\rho} d\mathbf{r} = \frac{\hbar^2}{2m^2} \int (\nabla \sqrt{\rho})^2 d\mathbf{r}, \quad (\text{B2})$$

the internal energy

$$U = \frac{1}{\gamma - 1} \int P d\mathbf{r} = \frac{K}{\gamma - 1} \int \rho^\gamma d\mathbf{r}, \quad (\text{B3})$$

and the gravitational energy

$$W = \frac{1}{2} \int \rho \Phi d\mathbf{r}. \quad (\text{B4})$$

The eigenenergy E satisfies the relation

$$NE = \Theta_Q + \gamma U + 2W. \quad (\text{B5})$$

On the other hand, the equilibrium scalar virial theorem writes

$$2\Theta_Q + 3(\gamma - 1)U + W = 0. \quad (\text{B6})$$

For classical self-gravitating systems, or for self-gravitating BECs in the TF approximation where the quantum potential can be neglected, the foregoing equations reduce to

$$E_{\text{tot}} = U + W, \quad (\text{B7})$$

$$NE = \gamma U + 2W, \quad (\text{B8})$$

$$3(\gamma - 1)U + W = 0. \quad (\text{B9})$$

From these equations, we obtain the relations

$$E_{\text{tot}} = -\frac{3-n}{n} U = \frac{3-n}{3} W = \frac{3-n}{5-n} NE. \quad (\text{B10})$$

²⁰ Polytropes with $n > 5$ have an infinite mass. The polytrope $n = 5$ is unbounded but has a finite mass. For this index, the Lane-Emden equation has a simple analytical expression discovered by Schuster [80]. It was used by Plummer [81] to fit the density profile of globular clusters (Plummer's model).

Appendix C: Betti-Ritter formula

For classical self-gravitating systems, or for self-gravitating BECs in the TF approximation, the condition of hydrostatic equilibrium is given by Eq. (A1). For a polytropic equation of state (A4) we have

$$\frac{\nabla P}{\rho} = (n+1)\nabla\left(\frac{P}{\rho}\right). \quad (\text{C1})$$

As a result, the condition of hydrostatic equilibrium (A1) can be integrated into

$$(n+1)\frac{P}{\rho} + \Phi = \frac{E}{m}, \quad (\text{C2})$$

where E is a constant of integration. For a self-gravitating BEC it represents the eigenenergy [38]. Multiplying Eq. (C2) by ρ and integrating over the whole configuration, we obtain Eq. (B8). Assuming $6/5 < \gamma < +\infty$ (i.e. $0 \leq n < 5$) so that $P/\rho = 0$ on the boundary of the system $r = R$ where the density vanishes, we find from Eq. (C2) that

$$\frac{E}{m} = \Phi(R) = -\frac{GM}{R}. \quad (\text{C3})$$

This equation determines the eigenenergy E . As a result, Eq. (B8) can be rewritten as

$$-\frac{GM^2}{R} = \gamma U + 2W. \quad (\text{C4})$$

Combining this relation with the equilibrium scalar virial theorem (B9) we obtain the Betti-Ritter formula

$$W = -\frac{3}{5-n}\frac{GM^2}{R} \quad (\text{C5})$$

determining the gravitational energy W of a polytropic sphere [40]. From Eqs. (C5) and (B10), we get

$$U = \frac{n}{5-n}\frac{GM^2}{R} \quad (\text{C6})$$

and

$$E_{\text{tot}} = -\frac{3-n}{5-n}\frac{GM^2}{R}. \quad (\text{C7})$$

From the last relation, we can directly conclude that complete polytropes with index $n < 3$, i.e. $\gamma > 4/3$, are stable (because $E_{\text{tot}} < 0$) while complete polytropes with index $n > 3$, i.e. $\gamma < 4/3$, are unstable (because $E_{\text{tot}} < 0$) [40].

Appendix D: Ledoux formula

The complex pulsation of a polytrope of index $0 < n < 5$ is approximately given by the Ledoux formula [82]:²¹

$$\omega^2 = (4 - 3\gamma)\frac{W}{I}, \quad (\text{D1})$$

where $I = \int \rho r^2 d\mathbf{r}$ is the moment of inertia of the system. Using the results of Appendix A it can be written as

$$I = \kappa_n MR^2 \quad \text{with} \quad \kappa_n = \frac{\int_0^{\xi_1} \theta^n \xi^4 d\xi}{\xi_1^2 \int_0^{\xi_1} \theta^n \xi^2 d\xi}. \quad (\text{D2})$$

Combining this equation with the Betti-Ritter formula (C5), we can rewrite Eq. (D1) as

$$\omega^2 = -\frac{3(n-3)}{(5-n)n\kappa_n}\frac{GM}{R^3}. \quad (\text{D3})$$

For $n = 3/2$, we find $\kappa_{3/2} = 0.306899$. For $n = 2$, we find $\kappa_2 = 0.232332$. For $n = 1$, we find $\kappa_1 = 1 - 6/\pi^2 = 0.392073$.

Appendix E: Density profile of a noninteracting self-gravitating BEC with a compact support: polytrope $n = 2$

The fundamental differential equation of quantum hydrostatic equilibrium determining the density profile of a noninteracting self-gravitating BEC is given by Eq. (17). On the other hand, the fundamental differential equation of classical hydrostatic equilibrium determining the density profile of a polytrope of index n is given by Eq. (A5). For $n = 2$ it becomes

$$3K\Delta\sqrt{\rho} = -4\pi G\rho. \quad (\text{E1})$$

Dividing Eq. (E1) by $\sqrt{\rho}$, applying the Laplacian operator, and using Eq. (E1) again, we obtain

$$\Delta\left(\frac{\Delta\sqrt{\rho}}{\sqrt{\rho}}\right) = \left(\frac{4\pi G}{3K}\right)^2 \rho. \quad (\text{E2})$$

Remarkably, this equation coincides with Eq. (17) provided that we make the identification

$$K = \left(\frac{2\pi G\hbar^2}{9m^2}\right)^{1/2}. \quad (\text{E3})$$

As a result, the density profile of a polytrope of index $n = 2$ and polytropic constant given by Eq. (E3) is a

²¹ This formula can also be obtained from a variational principle based on a Gaussian ansatz [38].

particular solution of Eq. (17).²² Using the variables defined in Appendix A, it can be written as

$$\rho(r) = \rho_0 \theta(\xi)^2, \quad \xi = r/r_0, \quad r_0 = \left(\frac{\hbar^2}{8\pi G m^2 \rho_0} \right)^{1/4}, \quad (\text{E4})$$

where $\theta(\xi)$ is the solution of the Lane-Emden equation (A8) of index $n = 2$.

A polytrope of index $n = 2$ has a compact support and is stable. Furthermore, according to Eq. (A12), the mass-radius relation is

$$MR = \frac{1}{2} \omega_2 \frac{\hbar^2}{G m^2} = 5.25 \frac{\hbar^2}{G m^2}, \quad (\text{E5})$$

where we have used $\omega_2 = 10.4950\dots$ Eq. (E5) displays the same scaling as the mass-radius relation from Eq. (18) but the prefactor is different. This is because the density profile given by Eq. (E4) is different from the density profile of the soliton that has been reported previously in the literature [17, 18, 21, 25–27, 42–44] (see Sec. II B). Indeed, the authors of Refs. [17, 18, 21, 25–27, 42–44] have looked for a solution of Eq. (17) corresponding to a density profile that goes to zero at infinity. Actually, there exists another solution of Eq. (17), given by Eq. (E4), corresponding to a density profile with a compact support that vanishes at a finite radius R .²³ The two profiles are plotted in Fig. 2. Apparently, they are both stable. It may therefore be useful to compare their respective energy in order to determine which profile has the lowest energy (ground state).

The quantum kinetic energy of a BEC is given by Eq. (B2). Integrating the second expression by parts, we obtain

$$\Theta_Q = \frac{\hbar^2}{4m^2} \oint \nabla \rho \cdot d\mathbf{S} - \frac{\hbar^2}{2m^2} \int \sqrt{\rho} \Delta \sqrt{\rho} \, d\mathbf{r}. \quad (\text{E6})$$

Since $\rho'(R) \propto \theta_1 \theta_1'$ for a polytrope of index $n = 2$ [see Eq. (E4)] and since $\theta_1 = 0$ and $|\theta_1'| < +\infty$ (see Appendix A), we have $\rho'(R) = 0$. As a result, the surface term vanishes and Eq. (E6) reduces to

$$\Theta_Q = -\frac{\hbar^2}{2m^2} \int \sqrt{\rho} \Delta \sqrt{\rho} \, d\mathbf{r}. \quad (\text{E7})$$

Using Eq. (E1) we then find that

$$\Theta_Q = 3K \int \rho^{3/2} \, d\mathbf{r}. \quad (\text{E8})$$

This result can be compared to the internal energy (B3) of a polytrope of index $n = 2$ which is

$$U = 2K \int \rho^{3/2} \, d\mathbf{r}. \quad (\text{E9})$$

We have the relation

$$\Theta_Q = \frac{3}{2}U. \quad (\text{E10})$$

Therefore, the energy $E_{\text{tot}} = \Theta_Q + W$ of a self-gravitating noninteracting BEC with the density profile (E4) is different from the energy $E_{\text{tot}} = U + W$ of the corresponding $n = 2$ polytrope.

For a self-gravitating noninteracting BEC, we have (see Sec. II B)

$$E_{\text{tot}} = -\Theta_Q = \frac{1}{2}W. \quad (\text{E11})$$

On the other hand, the gravitational energy of a polytrope $n = 2$ is (see Appendix C)

$$W = -\frac{GM^2}{R}. \quad (\text{E12})$$

Combining Eqs. (E11) and (E12) and using the mass-radius relation from Eq. (E5), we find that the energy of a self-gravitating noninteracting BEC with the density profile (E4) is

$$E_{\text{tot}} = -\frac{GM^2}{2R} = -\frac{1}{\omega_2} \frac{G^2 M^3 m^2}{\hbar^2} = -0.0953 \frac{G^2 M^3 m^2}{\hbar^2}. \quad (\text{E13})$$

This energy is lower than the one given by Eq. (22). Therefore, the solution of Eq. (17) that has a compact support [see Eq. (E4)] has a lower energy than the solution of Eq. (17) that extends to infinity (see Sec. II B). The ground state of the self-gravitating noninteracting BEC corresponds therefore to the solution considered in this Appendix, not to the solution that has been considered in Refs. [17, 18, 21, 25–27, 42–44] (see Sec. II B). However, in the case of systems with long-range interactions, we know that a metastable state (i.e. a local but not a global energy minimum) may have a very long lifetime and can be fully relevant. This may be the case of the solution considered in Refs. [17, 18, 21, 25–27, 42–44] which seems to be selected in direct numerical simulations [25, 26].

Remark: the energy of a polytrope of index $n = 2$ can be obtained from the relations (see Appendices B and C):

$$E_{\text{tot}} = U + W, \quad (\text{E14})$$

$$NE = \frac{3}{2}U + 2W, \quad (\text{E15})$$

$$\frac{3}{2}U + W = 0, \quad (\text{E16})$$

²² We note that Eq. (E1) implies Eq. (E2) but the converse is wrong. As a result Eqs. (17) and (E1) are not equivalent.

²³ In Ref. [43] we found a solution of Eq. (17) for which “the program breaks down because the density achieves too small values ($< 10^{-11}$).” This solution corresponds to the density profile (E4) with a compact support.

implying

$$E_{\text{tot}} = -\frac{1}{2}U = \frac{1}{3}W = -\frac{GM^2}{3R}. \quad (\text{E17})$$

It differs from Eq. (E13) by a factor 2/3.

Appendix F: Gravitational energy

The gravitational energy of a spherically symmetric system is given by (see, e.g., Appendix G of [38])

$$W = -\int_0^{+\infty} \rho(r) \frac{GM(r)}{r} 4\pi r^2 dr, \quad (\text{F1})$$

where

$$M(r) = \int_0^r \rho(r) 4\pi r^2 dr \quad (\text{F2})$$

is the mass contained within the sphere of radius r . In our model, the system is made of a core of mass M_c and radius R_c and a uniform atmosphere of density ρ_a and mass $M_a = M - M_c$ contained within the spheres of radius R_c and R . Therefore, we can write

$$W = W_c - 4\pi G \rho_a \int_{R_c}^R M(r) r dr, \quad (\text{F3})$$

where the first term W_c is the gravitational energy of the core and the second term W_a is the gravitational energy of the atmosphere in the presence of the core. For $r \geq R_c$, the cumulated mass is

$$M(r) = M_c + \frac{4}{3}\pi\rho_a(r^3 - R_c^3). \quad (\text{F4})$$

Substituting Eq. (F4) into Eq. (F3) and evaluating the integral we get

$$W = W_c - 4\pi G \rho_a \left[M_c \frac{r^2}{2} + \frac{4}{15}\pi\rho_a r^5 - \frac{2}{3}\pi\rho_a R_c^3 r^2 \right]_{R_c}^R \quad (\text{F5})$$

with

$$\rho_a = \frac{3(M - M_c)}{4\pi(R^3 - R_c^3)}. \quad (\text{F6})$$

These expressions are exact. For our problem, it is a good approximation to assume that $R \gg R_c$. As a result, the foregoing equation simplifies into

$$W = W_c - 4\pi G \rho_a \left(M_c \frac{R^2}{2} + \frac{4}{15}\pi\rho_a R^5 \right) \quad (\text{F7})$$

with

$$\rho_a = \frac{3(M - M_c)}{4\pi R^3}. \quad (\text{F8})$$

We finally obtain

$$W = W_c - \frac{3GM_c(M - M_c)}{2R} - \frac{3G(M - M_c)^2}{5R}. \quad (\text{F9})$$

The first term is the potential energy of the core, the third term is the potential energy of the atmosphere and the second term is the interaction energy. This is as if we had a point mass M_c at the center of a distribution of mass $M - M_c$ [78].

Appendix G: The minimum halo radius, the minimum halo mass and the maximum halo central density

In this Appendix, we determine the radius, the mass and the central density of the ‘‘minimum halo’’ assuming that it corresponds to the ground state ($T = 0$) of a self-gravitating quantum gas. We have seen in Sec. II that it can be represented by a polytropic sphere. For the sake of generality we treat the case of an arbitrary polytropic index n , then consider particular cases corresponding to fermions, noninteracting bosons and self-interacting bosons in the TF limit.

1. General results

The halo radius r_h is defined as the distance at which the central density ρ_0 is divided by 4. Using Eqs. (A6) and (A7), it is given by

$$r_h = \xi_h \left[\frac{K(n+1)}{4\pi G} \right]^{1/2} \frac{1}{\rho_0^{(n-1)/2n}}, \quad (\text{G1})$$

where ξ_h is determined by the equation

$$\theta(\xi_h)^n = \frac{1}{4}. \quad (\text{G2})$$

The value of ξ_h can be obtained by solving the Lane-Emden equation (A8). The halo mass, which is the mass contained within the sphere of radius r_h , is given by

$$M_h = -4\pi \frac{\theta'(\xi_h)}{\xi_h} \rho_0 r_h^3. \quad (\text{G3})$$

Eliminating the central density between Eqs. (G1) and (G3), we obtain the minimum halo mass-radius relation

$$M_h r_h^{(3-n)/(n-1)} = -4\pi \theta'(\xi_h) \xi_h^{(n+1)/(n-1)} \times \left[\frac{K(n+1)}{4\pi G} \right]^{n/(n-1)}, \quad (\text{G4})$$

which is analogous to the mass-radius relation (A12). On the other hand, using Eqs. (G1) and (G3) and introducing the universal surface density of DM halos (1) we find

that the minimum halo radius, the minimum halo mass, and the maximum halo central density are given by

$$(r_h)_{\min} = \xi_h^{2n/(n+1)} \left[\frac{K(n+1)}{4\pi G} \right]^{n/(n+1)} \frac{1}{\Sigma_0^{(n-1)/(n+1)}} \quad (\text{G5})$$

and

$$(M_h)_{\min} = -4\pi\theta'(\xi_h)\xi_h^{(3n-1)/(n+1)} \times \left[\frac{K(n+1)}{4\pi G} \right]^{2n/(n+1)} \Sigma_0^{(3-n)/(n+1)}. \quad (\text{G6})$$

$$(\rho_0)_{\max} = \frac{1}{\xi_h^{2n/(n+1)}} \left[\frac{4\pi G}{K(n+1)} \right]^{n/(n+1)} \Sigma_0^{2n/(n+1)}. \quad (\text{G7})$$

2. Fermions

For the polytrope $n = 3/2$ (fermion stars) using Eq. (4), we have

$$\xi_h = 2.27, \quad \theta'_h = -0.360, \quad (\text{G8})$$

$$r_h = 0.223 \frac{h}{m^{4/3} G^{1/2} \rho_0^{1/6}}, \quad (\text{G9})$$

$$M_h = 1.99 \rho_0 r_h^3, \quad (\text{G10})$$

$$M_h r_h^3 = 2.45 \times 10^{-4} \frac{h^6}{G^3 m^8}. \quad (\text{G11})$$

Using Eq. (1), we obtain Eqs. (13)-(15). Inversely, assuming that the mass $(M_h)_{\min}$ of the minimum halo is known, we obtain the fermion mass

$$m = 1.60 \frac{\hbar^{3/4} \Sigma_0^{3/16}}{G^{3/8} (M_h)_{\min}^{5/16}}. \quad (\text{G12})$$

If we take $(M_h)_{\min} = 10^8 M_\odot$ we obtain $m = 165 \text{ eV}/c^2$.

3. Noninteracting bosons

For the polytrope $n = 2$ (noninteracting boson stars) we have

$$\xi_h = 2.092, \quad \theta'_h = -0.3216, \quad (\text{G13})$$

$$r_h = 0.934333 \frac{\hbar^{1/2}}{m^{1/2} G^{1/4} \rho_0^{1/4}}, \quad (\text{G14})$$

$$M_h = 1.93181 \rho_0 r_h^3, \quad (\text{G15})$$

$$M_h r_h = 1.47221 \frac{\hbar^2}{G m^2}. \quad (\text{G16})$$

Using Eq. (1), we obtain Eqs. (25)-(27). Inversely, assuming that the mass $(M_h)_{\min}$ of the minimum halo is known, we obtain the noninteracting boson mass

$$m = 1.43 \frac{\hbar \Sigma_0^{1/4}}{G^{1/2} (M_h)_{\min}^{3/4}}. \quad (\text{G17})$$

If we take $(M_h)_{\min} = 10^8 M_\odot$ we obtain $m = 1.44 \times 10^{-22} \text{ eV}/c^2$.

4. Self-interacting bosons in the TF limit

For the polytrope $n = 1$ (self-interacting boson stars) we have

$$\xi_h = 2.4746, \quad \theta'_h = -0.41853, \quad (\text{G18})$$

$$r_h = 2.4746 \left(\frac{a_s \hbar^2}{G m^3} \right)^{1/2}, \quad (\text{G19})$$

$$M_h = 2.12535 \rho_0 r_h^3. \quad (\text{G20})$$

Using Eq. (1), we obtain Eqs. (42)-(44). Inversely, assuming that the mass $(M_h)_{\min}$ of the minimum halo is known, we obtain the self-interacting boson parameter (in the TF limit)

$$\frac{a_s}{m^3} = 0.0769 \frac{G (M_h)_{\min}}{\hbar^2 \Sigma_0}. \quad (\text{G21})$$

If we take $(M_h)_{\min} = 10^8 M_\odot$ we obtain $a_s/m^3 = 1.76 \times 10^3 \text{ fm}/(\text{eV}/c^2)^3$.

Appendix H: Results of the quantum Jeans instability theory

In this Appendix, we recapitulate the main results of the quantum Jeans instability theory developed in Refs. [6, 83], restricting ourselves to the nonrelativistic regime. We refer to these papers for details about their derivation and for some generalizations.

1. Fermions

If DM is made of fermions, the Jeans length and the Jeans mass are given by

$$\lambda_J = \frac{1}{2} \left(\frac{\pi}{3} \right)^{1/6} \frac{h}{G^{1/2} m^{4/3} \rho^{1/6}}, \quad (\text{H1})$$

$$M_J = \frac{4}{3}\pi\rho\left(\frac{\lambda_J}{2}\right)^3 = \frac{1}{16}\left(\frac{\pi}{3}\right)^{3/2}\frac{\hbar^3\rho^{1/2}}{G^{3/2}m^4}. \quad (\text{H2})$$

Eliminating the density between these expressions, we get the Jeans mass-radius relation

$$M_J\lambda_J^3 = \frac{\pi^2}{1152}\frac{\hbar^6}{G^3m^8}. \quad (\text{H3})$$

We can also define a Jeans surface density

$$\Sigma_J = \rho\frac{\lambda_J}{2} = \frac{1}{4}\left(\frac{\pi}{3}\right)^{1/6}\frac{\hbar\rho^{5/6}}{G^{1/2}m^{4/3}}. \quad (\text{H4})$$

These equations display the same scalings as Eqs. (G9)-(G11) and (15) for DM halos.

2. Noninteracting bosons

If DM is made of noninteracting bosons, the Jeans length and the Jeans mass are given by

$$\lambda_J = 2\pi\left(\frac{\hbar^2}{16\pi G\rho m^2}\right)^{1/4}, \quad (\text{H5})$$

$$M_J = \frac{4}{3}\pi\rho\left(\frac{\lambda_J}{2}\right)^3 = \frac{\pi}{6}\left(\frac{\pi^3\hbar^2\rho^{1/3}}{Gm^2}\right)^{3/4}. \quad (\text{H6})$$

Eliminating the density between these expressions, we get the Jeans mass-radius relation

$$M_J\lambda_J = \frac{\pi^4}{6}\frac{\hbar^2}{Gm^2}. \quad (\text{H7})$$

The Jeans surface density is

$$\Sigma_J = \rho\frac{\lambda_J}{2} = \pi\left(\frac{\hbar^2\rho^3}{16\pi Gm^2}\right)^{1/4}. \quad (\text{H8})$$

These equations display the same scalings as Eqs. (G14)-(G16) and (27) for DM halos.

3. Self-interacting bosons in the TF limit

If DM is made of self-interacting bosons in the TF limit, the Jeans length and the Jeans mass are given by

$$\lambda_J = 2\pi\left(\frac{a_s\hbar^2}{Gm^3}\right)^{1/2}, \quad (\text{H9})$$

$$M_J = \frac{4}{3}\pi\rho\left(\frac{\lambda_J}{2}\right)^3 = \frac{\pi}{6}\rho\left(\frac{4\pi^2a_s\hbar^2}{Gm^3}\right)^{3/2}. \quad (\text{H10})$$

The Jeans surface density is

$$\Sigma_J = \rho\frac{\lambda_J}{2} = \pi\rho\left(\frac{a_s\hbar^2}{Gm^3}\right)^{1/2}. \quad (\text{H11})$$

These equations display the same scalings as Eqs. (G19), (G20) and (44) for DM halos.

Appendix I: The mass of the DM particle

In this Appendix, we relate the mass m of the DM particle to the cosmological constant Λ and to the other fundamental constants of physics.

1. Fermions

We have seen in Sec. II A that the minimum mass of DM halos made of fermions is given by

$$(M_h)_{\min} = 4.47\left(\frac{\hbar^{12}\Sigma_0^3}{G^6m^{16}}\right)^{1/5}. \quad (\text{I1})$$

It is obtained by requiring that the smallest DM halo in the Universe corresponds to the ground state of the self-gravitating Fermi gas.

On the other hand, the minimum mass of DM halos may be obtained from a quantum Jeans instability theory (see, e.g., Refs. [6, 83]) leading to the Jeans mass (H2). Let us compute the Jeans mass at the present epoch where $\rho_{m,0} = 2.66 \times 10^{-24} \text{ g m}^{-3}$. For a fermion mass $m = 170 \text{ eV}/c^2$, the Jeans mass is $M_J = 1.10 \times 10^5 M_\odot$ [83]. It is 3 orders of magnitude smaller than the minimum mass $(M_h)_{\min} \sim 10^8 M_\odot$ of observed DM halos. Actually, we cannot expect to have a perfect agreement between the Jeans mass computed at the present epoch and the observed minimum mass of DM halos because the linear Jeans instability took place at an earlier epoch (see Appendix I 4) and the present DM halos result from a nonlinear evolution. Therefore, we write $(M_h)_{\min} = \chi_F M_J$, where χ_F is a dimensionless factor that is difficult to predict theoretically (for fermions the previous estimate gives $\chi_F \sim 10^3$). Using Eq. (H2), we obtain

$$(M_h)_{\min} = 16.6\chi_F\frac{\hbar^3\rho_{m,0}^{1/2}}{G^{3/2}m^4}. \quad (\text{I2})$$

Comparing (I1) and (I2) we get

$$m = 5.16\chi_F^{5/4}\frac{\hbar^{3/4}\rho_{m,0}^{5/8}}{\Sigma_0^{3/4}G^{3/8}}. \quad (\text{I3})$$

This relation gives the surface density Σ_0 of the smallest DM halo if we know the fermion mass m . Inversely, since Σ_0 appears to have a universal value (see Eq. (1)), we can use Eq. (I3) to obtain the fermion mass m . More precisely, since $\rho_{m,0}$ and Σ_0 can be expressed in terms of the cosmological constant Λ by Eqs. (155) and (156), we find that the mass of the fermionic particle is given by

$$m = 7.62\chi_F^{5/4}\left(\frac{\Lambda\hbar^3}{Gc^3}\right)^{1/4}. \quad (\text{I4})$$

It is equal to the mass scale $m_\Lambda^* = 5.04 \times 10^{-3} \text{ eV}/c^2$ given by Eq. (175) multiplied by a large numerical factor of

order 4×10^4 (for $\chi_F \sim 10^3$). This gives $m \sim 200 \text{ eV}/c^2$ which is the correct order of magnitude of the fermion mass usually advocated in DM models (see Appendix D of [14]). We note that, up to the dimensionless factor χ_F , this mass scale has been predicted in terms of the fundamental constants of physics independently from the observations.

Remark: We can obtain these results (without the prefactor) directly from the Jeans scales of Appendix H 1. From Eq. (H4), we have

$$\Sigma \sim \frac{\hbar \rho^{5/6}}{m^{4/3} G^{1/2}} \quad \text{i.e.} \quad m \sim \frac{\hbar^{3/4} \rho^{5/8}}{\Sigma^{3/4} G^{3/8}}. \quad (15)$$

If we take $\rho \sim \rho_{m,0} \sim \Lambda/G$ and $\Sigma \sim c\sqrt{\Lambda}/G$ (see Eqs. (155) and (156)), we get

$$m \sim \left(\frac{\Lambda \hbar^3}{G c^3} \right)^{1/4} \sim m_\Lambda^*. \quad (16)$$

Inversely, if we assume that $\rho \sim \rho_{m,0} \sim \Lambda/G$ and $m \sim m_\Lambda^*$ we find that $\Sigma \sim c\sqrt{\Lambda}/G$. We also note that $\lambda \sim \Sigma/\rho \sim c/\sqrt{\Lambda}$ and $M \sim \rho \lambda^3 \sim c^3/G\sqrt{\Lambda}$ are the cosmological scales corresponding to the size and to the mass of the Universe [70].

2. Noninteracting bosons

We have seen in Sec. II B that the minimum mass of DM halos made of noninteracting bosons is given by

$$(M_h)_{\min} = 1.61 \left(\frac{\hbar^4 \Sigma_0}{G^2 m^4} \right)^{1/3}. \quad (17)$$

On the other hand, the quantum Jeans instability theory [6, 83] leads to the Jeans mass (H6). For a boson mass $m = 2.92 \times 10^{-22} \text{ eV}/c^2$, the Jeans mass computed at the present epoch where $\rho_{m,0} = 2.66 \times 10^{-24} \text{ g m}^{-3}$ is $M_J = 3.07 \times 10^6 M_\odot$ [83]. It is 1 order of magnitude smaller than the minimum mass $(M_h)_{\min} \sim 10^8 M_\odot$ of observed DM halos. Writing $(M_h)_{\min} = \chi_B M_J$ with $\chi_B \sim 10$, we obtain

$$(M_h)_{\min} = 6.88 \chi_B \frac{\hbar^{3/2} \rho_{m,0}^{1/4}}{G^{3/4} m^{3/2}}. \quad (18)$$

Comparing Eqs. (17) and (18) we get

$$m = 6089 \chi_B^6 \frac{\hbar \rho_{m,0}^{3/2}}{\Sigma_0^2 G^{1/2}}. \quad (19)$$

Using Eqs. (155) and (156), we find that the mass of the bosonic particle (in the noninteracting case) is given by

$$m = 33748 \chi_B^6 \frac{\hbar \sqrt{\Lambda}}{c^2}. \quad (110)$$

It is equal to the mass scale $m_\Lambda = 2.08 \times 10^{-33} \text{ eV}/c^2$ given by Eq. (158) multiplied by a huge numerical factor

of order 3×10^{10} (for $\chi_B \sim 10$). This is because χ_B is raised in Eq. (I10) to the power 6. This gives $m \sim 10^{-22} \text{ eV}/c^2$ which is the correct order of magnitude of the mass of ultralight axions usually advocated in DM models (see Appendix D of [14]).

Remark: We can obtain these results (without the prefactor) directly from the Jeans scales of Appendix H 2. From Eq. (H8), we have

$$\Sigma \sim \left(\frac{\hbar^2 \rho^3}{G m^2} \right)^{1/4} \quad \text{i.e.} \quad m \sim \left(\frac{\hbar^2 \rho^3}{G \Sigma^4} \right)^{1/2}. \quad (111)$$

If we take $\rho \sim \rho_{m,0} \sim \Lambda/G$ and $\Sigma \sim c\sqrt{\Lambda}/G$ (see Eqs. (155) and (156)), we get

$$m \sim \frac{\hbar \sqrt{\Lambda}}{c^2} \sim m_\Lambda. \quad (112)$$

Inversely, if we assume that $\rho \sim \rho_{m,0} \sim \Lambda/G$ and $m \sim m_\Lambda$ we find that $\Sigma \sim c\sqrt{\Lambda}/G$.

3. Self-interacting bosons in the TF limit

We have seen in Sec. II C that the minimum mass of DM halos made of self-interacting bosons in the TF limit is given by

$$(M_h)_{\min} = 13.0 \frac{a_s \hbar^2 \Sigma_0}{G m^3}. \quad (113)$$

On the other hand, the quantum Jeans instability theory [6, 83] leads to the Jeans mass (H10). For a ratio $a_s/m^3 = 3.28 \times 10^3 \text{ fm} (\text{eV}/c^2)^{-3}$, the Jeans mass computed at the present epoch where $\rho_{m,0} = 2.66 \times 10^{-24} \text{ g m}^{-3}$ is $M_J = 165 M_\odot$ [83]. It is 6 order of magnitude smaller than the minimum mass $(M_h)_{\min} \sim 10^8 M_\odot$ of observed DM halos. Writing $(M_h)_{\min} = \chi_{\text{TF}} M_J$ with $\chi_{\text{TF}} \sim 10^6$, we obtain

$$(M_h)_{\min} = 130 \chi_{\text{TF}} \rho_{m,0} \left(\frac{a_s \hbar^2}{G m^3} \right)^{3/2}. \quad (114)$$

Comparing (I13) and (I14) we get

$$\frac{a_s}{m^3} = \frac{0.01}{\chi_{\text{TF}}^2} \frac{G \Sigma_0^2}{\hbar^2 \rho_{m,0}^2}. \quad (115)$$

Using Eqs. (155) and (156), we find that the ratio a_s/m^3 is given by

$$\frac{a_s}{m^3} = \frac{0.0135}{\chi_{\text{TF}}^2} \frac{G c^2}{\Lambda \hbar^2}. \quad (116)$$

It is equal to the scale $r_\Lambda/m_\Lambda^3 = 2Gc^2/\Lambda\hbar^2 = 6.11 \times 10^{17} \text{ fm} (\text{eV}/c^2)^{-3}$ given by Eq. (166) multiplied by a very small numerical factor of order 10^{-14} (for $\chi_{\text{TF}} \sim 10^6$). This gives $a_s/m^3 \sim 10^3 \text{ fm} (\text{eV}/c^2)^{-3}$ which is the correct order of magnitude of the parameter a_s/m^3 of

self-interacting bosons usually advocated in DM models (see Appendix D of [14]).

Remark: We can obtain these results (without the prefactor) directly from the Jeans scales of Appendix H3. From Eq. (H11), we have

$$\Sigma \sim \rho \left(\frac{a_s \hbar^2}{Gm^3} \right)^{1/2} \quad \text{i.e.} \quad \frac{a_s}{m^3} \sim \frac{G\Sigma^2}{\hbar^2 \rho^2}. \quad (\text{I17})$$

If we take $\rho \sim \rho_{m,0} \sim \Lambda/G$ and $\Sigma \sim c\sqrt{\Lambda}/G$ (see Eqs. (155) and (156)), we get

$$\frac{a_s}{m^3} \sim \frac{Gc^2}{\Lambda \hbar^2} \sim \frac{r_\Lambda}{m_\Lambda^3}. \quad (\text{I18})$$

Inversely, if we assume that $\rho \sim \rho_{m,0} \sim \Lambda/G$ and $a_s/m^3 \sim r_\Lambda/m_\Lambda^3$ we find that $\Sigma \sim c\sqrt{\Lambda}/G$.

4. The epoch where we can apply the Jeans instability theory

Let us consider how the minimum halo mass $(M_h)_{\min}$ depends on the density ρ_m and on the dimensionless constant χ in Eqs. (I2), (I8) and (I14). For

fermions, they appear in the combination $\chi_{\text{F}} \rho_{m,0}^{1/2} = (\chi_{\text{F}}^2 \rho_{m,0})^{1/2} = (10^6 \rho_{m,0})^{1/2}$. For noninteracting bosons, we have $\chi_{\text{B}} \rho_{m,0}^{1/4} = (\chi_{\text{B}}^4 \rho_{m,0})^{1/4} = (10^4 \rho_{m,0})^{1/4}$. For self-interacting bosons in the TF limit, we have $\chi_{\text{TF}} \rho_{m,0} = 10^6 \rho_{m,0}$. Remarkably, the last terms in these equalities involve the *same* typical number $\sim 10^5 \rho_{m,0}$. These relations suggest that $(M_h)_{\min}$ is not equal to the present Jeans length but rather to the Jeans length at the epoch where the density of the Universe is $\sim 10^5 \rho_{m,0}$. Indeed, if we calculate the Jeans mass at the epoch where the density of the Universe is $10^5 \rho_{m,0}$, we find in the three cases considered above that $M_J \sim (M_h)_{\min}$. Using $\rho_m = \rho_{m,0}/a^3$ and $z+1 = 1/a$ (redshift), this epoch corresponds to

$$\rho_m = 2.66 \times 10^{-19} \text{ g m}^{-3}, \quad a = 0.0215, \quad z = 45.5. \quad (\text{I19})$$

It is intermediate between the epoch of radiation-matter equality ($\rho_{\text{eq}} = 8.77 \times 10^{-14} \text{ g m}^{-3}$, $a_{\text{eq}} = 2.95 \times 10^{-4}$, $z_{\text{eq}} = 3389$) and the present epoch ($\rho_{m,0} = 2.66 \times 10^{-24} \text{ g m}^{-3}$, $a_0 = 1$, $z_0 = 0$). It may correspond to the epoch where we can apply the linear Jeans instability theory to predict the typical mass of DM halos.

-
- [1] Planck Collaboration, *Astron. Astrophys.* **571**, 66 (2014)
 - [2] Planck Collaboration, *Astron. Astrophys.* **594**, A13 (2016)
 - [3] J.F. Navarro, C.S. Frenk, S.D.M. White, *Astrophys. J.* **462**, 563 (1996)
 - [4] A. Burkert, *Astrophys. J.* **447**, L25 (1995)
 - [5] G. Kauffmann, S.D.M. White, B. Guiderdoni, *Mon. Not. R. astr. Soc.* **264**, 201 (1993); A. Klypin, A.V. Kravtsov, O. Valenzuela, *Astrophys. J.* **522**, 82 (1999); M. Kamionkowski, A.R. Liddle, *Phys. Rev. Lett.* **84**, 4525 (2000)
 - [6] P.H. Chavanis, *Phys. Rev. D* **84**, 043531 (2011)
 - [7] P.H. Chavanis, arXiv:1810.08948
 - [8] A. Suárez, V.H. Robles, T. Matos, *Astrophys. Space Sci. Proc.* **38**, 107 (2014)
 - [9] T. Rindler-Daller, P.R. Shapiro, *Astrophys. Space Sci. Proc.* **38**, 163 (2014)
 - [10] P.H. Chavanis, *Self-gravitating Bose-Einstein condensates*, in *Quantum Aspects of Black Holes*, edited by X. Calmet (Springer, 2015)
 - [11] D. Marsh, *Phys. Rep.* **643**, 1 (2016)
 - [12] J.W. Lee, *EPJ Web of Conferences* **168**, 06005 (2018)
 - [13] E. Braaten, H. Zhang, arXiv:1810.11473
 - [14] A. Suárez, P.H. Chavanis, *Phys. Rev. D* **95**, 063515 (2017)
 - [15] D. Lynden-Bell, *Mon. Not. R. Astron. Soc.* **136**, 101 (1967)
 - [16] E. Seidel, W.M. Suen, *Phys. Rev. Lett.* **72**, 2516 (1994)
 - [17] F.S. Guzmán, L.A. Ureña-López, *Phys. Rev. D* **69**, 124033 (2004)
 - [18] F.S. Guzmán, L.A. Ureña-López, *Astrophys. J.* **645**, 814 (2006)
 - [19] J.R. Oppenheimer, G.M. Volkoff, *Phys. Rev.* **55**, 374 (1939)
 - [20] D.J. Kaup, *Phys. Rev.* **172**, 1331 (1968)
 - [21] R. Ruffini, S. Bonazzola, *Phys. Rev.* **187**, 1767 (1969)
 - [22] M. Colpi, S.L. Shapiro, I. Wasserman, *Phys. Rev. Lett.* **57**, 2485 (1986)
 - [23] I.I. Tkachev, *Sov. Astron. Lett.* **12**, 305 (1986)
 - [24] P.H. Chavanis, T. Harko, *Phys. Rev. D* **86**, 064011 (2012)
 - [25] H.Y. Schive, T. Chiueh, T. Broadhurst, *Nature Physics* **10**, 496 (2014)
 - [26] H.Y. Schive *et al.*, *Phys. Rev. Lett.* **113**, 261302 (2014)
 - [27] L. Hui, J. Ostriker, S. Tremaine, E. Witten, *Phys. Rev. D* **95**, 043541 (2017)
 - [28] B. Bar-Or, J.B. Fouvry, S. Tremaine, *Astrophys. J.* **871**, 28 (2019)
 - [29] J. Binney, S. Tremaine, *Galactic Dynamics* (Princeton, NJ: Princeton University Press, 1987)
 - [30] J. Kormendy, K.C. Freeman, in S.D. Ryder, D.J. Pisano, M.A. Walker, K.C. Freeman, eds., *Proc. IAU Symp. 220, Dark Matter in Galaxies*. *Astron. Soc. Pac.*, San Francisco, p. 377 (2004)
 - [31] M. Spano, M. Marcellin, P. Amram, C. Carignan, B. Epinat, O. Hernandez, *Mon. Not. R. Astron. Soc.* **383**, 297 (2008)
 - [32] F. Donato *et al.*, *Mon. Not. R. Astron. Soc.* **397**, 1169 (2009)
 - [33] D. Lynden-Bell, R. Wood, *Mon. Not. R. Astron. Soc.* **138**, 495 (1968)
 - [34] S. Balberg, S.L. Shapiro, S. Inagaki, *Astrophys. J.* **568**, 475 (2002)
 - [35] P.H. Chavanis, *Phys. Rev. E* **65**, 056123 (2002)
 - [36] P. Mocz *et al.*, *Mon. Not. R. Astron. Soc.* **471**, 4559

- (2017)
- [37] N. Bar, D. Blas, K. Blum, S. Sibiryakov, Phys. Rev. D **98**, 083027 (2018)
- [38] P.H. Chavanis, Eur. Phys. J. Plus **132**, 248 (2017)
- [39] P.H. Chavanis, Phys. Dark Univ. **22**, 80 (2018)
- [40] S. Chandrasekhar, *An Introduction to the Theory of Stellar Structure* (Dover, 1942)
- [41] E. Madelung, Zeit. F. Phys. **40**, 322 (1927)
- [42] M. Membrado, A.F. Pacheco, J. Sanudo, Phys. Rev. A **39**, 4207 (1989)
- [43] P.H. Chavanis, L. Delfini, Phys. Rev. D **84**, 043532 (2011)
- [44] D. Marsh, A.R. Pop, Monthly Not. Roy. Astron. **451**, 2479 (2015)
- [45] M. Membrado, J. Abad, A.F. Pacheco, J. Sañudo, Phys. Rev. D **40**, 2736 (1989)
- [46] J.W. Lee, I. Koh, Phys. Rev. D **53**, 2236 (1996)
- [47] J. Goodman, New Astronomy **5**, 103 (2000)
- [48] A. Arbey, J. Lesgourgues, P. Salati, Phys. Rev. D **68**, 023511 (2003)
- [49] C.G. Böhrer, T. Harko, J. Cosmol. Astropart. Phys. **06**, 025 (2007)
- [50] S.W. Randall, M. Markevitch, D. Clowe, A.H. Gonzalez, M. Bradac, Astrophys. J. **679**, 1173 (2008)
- [51] E. Braaten, A. Mohapatra, H. Zhang, Phy. Rev. Lett. **117**, 121801 (2016)
- [52] E. Cotner, Phys. Rev. D **94**, 063503 (2016)
- [53] P.H. Chavanis, Phys. Rev. D **94**, 083007 (2016)
- [54] J. Eby *et al.*, JHEP **12**, 066 (2016)
- [55] D.G. Levkov, A.G. Panin, I.I. Tkachev, Phys. Rev. Lett. **118**, 011301 (2017)
- [56] T. Helfer *et al.*, JCAP **03**, 055 (2017)
- [57] P.H. Chavanis, Phys. Rev. D **98**, 023009 (2018)
- [58] L. Visinelli, S. Baum, J. Redondo, K. Freese, F. Wilczek, Phys. Lett. B **777**, 64 (2018)
- [59] F. Michel, I.G. Moss, Phys. Lett. B **785**, 9 (2018)
- [60] P.H. Chavanis, Int. J. Mod. Phys. B **20**, 3113 (2006)
- [61] R. Emden, *Gaskugeln* (Teubner Verlag, Leipzig, 1907)
- [62] P.H. Chavanis, Astron. Astrophys. **381**, 340 (2002)
- [63] P.H. Chavanis, Astron. Astrophys. **432**, 117 (2005)
- [64] G. Alberti, P.H. Chavanis, arXiv:1808.01007
- [65] P.H. Chavanis, M. Lemou, F. Méhats, Phys. Rev. D **92**, 123527 (2015)
- [66] P.H. Chavanis, Y. Pomeau, M. Le Berre and B. Denet, arXiv
- [67] J. Veltmaat, J.C. Niemeyer, B. Schwabe, Phys. Rev. D **98**, 043509 (2018)
- [68] P.H. Chavanis, Eur. Phys. J. Plus **130**, 130 (2015)
- [69] P.H. Chavanis, Phys. Lett. B **758**, 59 (2016)
- [70] P.H. Chavanis, Phys. Dark Univ. **24**, 100271 (2019)
- [71] A. Arvanitaki, S. Dimopoulos, S. Dubovsky, N. Kaloper, J. March-Russell, Phys. Rev. D **81**, 123530 (2010)
- [72] A.S. Goldhaber, M.M. Nieto, Rev. Mod. Phys. **82**, 939 (2010)
- [73] R. Ruffini, C.R. Argüelles, J.A. Rueda, Mon. Not. R. Astron. Soc. **451**, 622 (2015)
- [74] J. Fan, Phys. Dark Univ. **14**, 84 (2016)
- [75] M. Reig, J.W.F. Valle, M. Yamada, arXiv:1905.01287
- [76] P.H. Chavanis, Eur. Phys. J. Plus **134**, 352 (2019)
- [77] P.H. Chavanis, preprint
- [78] P.H. Chavanis, preprint
- [79] E. Romano-Díaz, I. Shlosman, Y. Hoffman, C. Heller, Astrophys. J. **685**, L105 (2008); A. Pontzen, F. Governato, Nature **506**, 171 (2014); J. Oñorbe *et al.* Mon. Not. R. astr. Soc. **454**, 2092 (2015)
- [80] A. Schuster, Brit. Assoc. Rept., P. 427 (1883)
- [81] H.C. Plummer, Mon. Not. R. Astron. Soc. **71**, 460 (1911)
- [82] P. Ledoux, C.L. Pekeris, Astrophys. J. **94**, 124 (1941)
- [83] A. Suárez, P.H. Chavanis, Phys. Rev. D **98**, 083529 (2018)
- [84] T. Matos, A. Avilez, T. Bernal, P.H. Chavanis, arXiv:1608.03945